DOE/NASA/1028-77/14
NASA TM-73868

WAKE CHARACTERISTICS OF AN EIGHT-LEG TOWER FOR A MOD-0 TYPE WIND TURBINE

Joseph M. Savino, Lee H. Wagner, and Donald M. Sinclair
National Aeronautics and Space Administration
Lewis Research Center
Cleveland, Ohio 44135

December 1977

Prepared for
DEPARTMENT OF ENERGY
Division of Solar Energy
Federal Wind Energy Program
Under Interagency Agreement E(49-26)-1028

NOTICE

1 Report No	2 Government Accession No	3 Recipient's Catalog No
NASA TM-73868		

4 Title and Subtitle	5 Report Date
WAKE CHARACTERISTICS OF AN EIGHT-LEG TOWER FOR A MOD-0 TYPE WIND TURBINE	December 1977
	6 Performing Organization Code
7 Author(s)	8 Performing Organization Report No
Joseph M. Savino, Lee H Wagner, and Donald M. Sinclair	E-9463
	10 Work Unit No
9 Performing Organization Name and Address	
National Aeronautics and Space Administration Lewis Research Center Cleveland, Ohio 44135	11 Contract or Grant No
	13 Type of Report and Period Covered
12 Sponsoring Agency Name and Address	Technical Memorandum
Department of Energy Division of Solar Energy Washington, D. C. 20545	14 Sponsoring Agency Code Report No. DOE/NASA/1028-77/14

15 Supplementary Notes

Prepared under Interagency Agreement E(49-26)-1028.

16 Abstract

Low-speed wind tunnel tests were conducted to determine the flow characteristics of the wake downwind of a 1/25th-scale, all-tubular eight-leg tower concept suitable for application to the DOE-NASA MOD-0 wind power turbine Measurements were made of wind speed profiles, and from these were determined the wake local minimum velocity, average velocity, and width for several wind approach angles. These data are presented herein along with tower shadow photographs and comparisons with data from an earlier lattice-type, four-leg tower model constructed of tubular members. Values of average wake velocity defect ratio and average ratio of wake width to blade radius for the eight-leg model were estimated to be around 0. 17 and 0. 30, respectively, at the plane of the rotor blade. These characteristics suggest that the tower wake of the eight-leg concept is slightly less than that of the four-leg design.

17 Key Words (Suggested by Author(s))	18 Distribution Statement
Tower shadow Tower wake flow Wind turbine	Unclassified - unlimited STAR Category 44 DOE Category UC-60

19 Security Classif (of this report)	20 Security Classif (of this page)	21 No of Pages	22 Price*
Unclassified	Unclassified		

* For sale by the National Technical Information Service, Springfield, Virginia 22161

WAKE CHARACTERISTICS OF AN EIGHT-LEG TOWER FOR A MOD-0 TYPE WIND TURBINE*

by Joseph M. Savino, Lee H. Wagner, and Donald M. Sinclair

Lewis Research Center

E-9463

SUMMARY

Low-speed wind tunnel tests were conducted to measure the characteristics of the wake in a plane downwind of an eight-leg tower concept suitable for application to the DOE-NASA MOD-0 wind power turbine. The 1/25th-scale tower model was composed of tubular members and circular stiffening rings. Data for wake wind-speed profiles and the local values of the minimum velocity, average velocity and width are presented for several wind approach angles from 0° to 45°. At the measuring station, the average value of the ratios of local minimum velocity to free-stream velocity was 0.76, while the average value of the ratios of local average velocity to free-stream velocity was 0.88. Ratio of wake width to projected tower width varied from about 1.7 at the top of the tower, to about 1.4 at the elevation corresponding to the tip of the blade. In the plane of the rotor blade, the ratio of wake average velocity defect to free-stream velocity was estimated to be about 0.17, and the average ratio of wake width to blade radius was around 0.30

Comparisons with similar data for a conventional four-leg model (also with circular members) showed that the eight-leg tower concept produces a modest improvement in wake properties. At the plane of the blade, the average velocity ratio was 0.83 compared to 0.81, and the average ratio of wake width to blade radius was 0.30 compared to 0.33. Shadow photographs of the tower models are included.

INTRODUCTION

A major element in the DOE (formerly ERDA) Wind Energy Program is the development of large propeller type (horizontal axis) wind turbines (ref. 1). A first step in this program was the construction of an experimental 100-kilowatt wind turbine, commonly referred to as the MOD-0 design. This effort is being managed for DOE by the NASA-Lewis Research Center (ref. 2). In this type of turbine design, the rotor operates downwind of the support tower (ref. 3), as shown in figure 1.

*Mr. Seymour Lieblein of Technical Report Services assisted in the preparation of the report text and analysis.

The DOE-NASA 100-kilowatt wind turbine consists of a two-bladed 125-foot-diameter rotor and a nacelle containing the rotor turbine and gearbox. The nacelle assembly is mounted on a 93-foot-high steel truss tower. This tower, called the MOD-0 configuration herein, is constructed of pipe legs, horizontal channels, diagonal back-to-back angles and gusset-plate attachments. The original tower also contained a service personnel stairway and rails for an equipment elevator (fig. 2(a)).

Early operating experience with the MOD-0 wind turbine showed sizeable unwanted fluctuations in rotor torque and blade root stresses (ref. 4). These fluctuations were attributed to the effects of the reduced wind speed in the wake downwind of the tower (the so-called "tower shadow"). These early results indicated a need for investigating ways of reducing the tower shadow effect, that is, increasing the wind flow through the tower structure.

Scale models of the MOD-0 tower were built and their wake characteristics were measured in a low-speed wind tunnel (ref. 5). Two tower models of the MOD-0 basic design were tested: a 1/25th-scale configuration; and a 1/48th-scale configuration. In the 1/25th-scale model, circular rods were used for the legs, and square bars were used to simulate the horizontal channel members and the diagonal angle members. This model was tested with and without models of the stairs and elevator rails. The 1/48th-scale model was made of all tubular members without gusset plates and without the stairway and rails.

Test results of these MOD-0 tower models, presented in reference 5, showed that the stairs and rails were a major source of wind flow blockage. Consequently, these components were removed from the 100-kilowatt experimental wind turbine (fig. 2(b)) and from subsequent tower designs. The removal of these components in the full-scale tower resulted in a substantial reduction in blade dynamic stresses (ref. 6). The test results also indicated that further small improvements in tower wake flow could be obtained from the use of all tubular members both with and without gusset plates.

For wind turbine applications, support tower design must meet the major requirements of low cost, aesthetic appeal, and, as demonstrated by recent experience, low wind blockage. The conventional approach to support tower design is to use standard structural members such as I-beams, channels, and angles. This leads to the so-called four-leg lattice or truss type tower. The older style electric transmission tower is one of the most familiar example of this kind of design. The MOD-0 tower design was based on this approach.

In general, the technology of conventional lattice tower design is well developed. However, as indicated by the MOD-0 tests, such configurations may not be acceptable from tower wake considerations. Therefore, there exists an incentive to explore other tower design concepts that have a better potential for producing a small tower shadow while at the same time meeting the major design and cost requirements.

An eight-leg tower concept is currently under study. This construction uses all-tubular members without cross-bars, gussets or stairs, and relies on circular rings at several heights for stiffness. (An actual full-size tower would probably have straight pipe members connecting the legs instead of rings.) The concept was designed to meet the structural requirements of the MOD-0 tower, and, in addition, was judged to have a gracefulness that is pleasing to the eye.

A 1/25th-scale model of the eight-leg tubular tower concept was constructed for testing in a low-speed wind tunnel, as was done for the previous tower models described in reference 5. The objective of these tests was to determine the wake characteristics of the eight-leg tower concept at various elevations behind the upper sections of the tower model over a range of wind approach angles, and to compare the results with those of the previous four-leg tower designs of reference 5.

This report contains a description of the tower concept, an outline of the test installation and procedure, the test results, and a comparison of these results with those of the all-tubular four-leg tower. Wake characteristics are presented in dimensionless form. These results include some typical plots of the wind speed profiles and plots of the vertical distribution of wake local minimum velocity, average velocity, and width. The dimensionless average velocities and the average of these local averages were used as the basis for comparison to determine whether the wake of the eight-leg tower is less than that of the four-leg tower.

APPARATUS AND TEST PROCEDURE

A scale model installed in a low-speed wind tunnel was selected as the test vehicle for determining the wake characteristics of the eight-leg tower concept because of the simplicity and low cost with which the test could be conducted. Wind tunnel tests with scale models is a standard method for determining flow characteristics in the wake of various objects and is used to identify the principal factors affecting wake form and flow variations. The results of wind tunnel model tests are applicable to larger size configurations provided the model is properly scaled geometrically and dynamically, and the wake characteristics are similar.

It is recognized that a wind tunnel test cannot simulate the atmospheric wind flow patterns around a full-size tower. In addition to having a wind speed gradient close to the ground, natural wind flow generally has a different turbulence intensity and scale than tunnel air flow. (The free-stream turbulence level in the wind tunnel used for these tests is considerably greater than in other low-speed tunnels.) Also, the boundary conditions in the model case (no nacelle on top and no infinite ground plane at the base) can produce pressure fields and three-dimensional wake effects in the end regions of the tower that are different than in the full-scale situation. Nevertheless, the wind tunnel tests are very useful for making relative comparisons of different tower concepts and design changes, and for acquiring detailed wind speed profiles in the wake that are reasonably accurate representations of the profiles in the wake of the full-scale tower.

Model

A photograph of a 1/25th-scale model of the eight-leg tower concept is shown in figure 3. The top section is square in form (4 by 4 in.), and the circumscribed square of the base (dashed line) measures 14.4 by 14.4 inches. The distance of each leg from the corner of the square of the base is 2.82 inches. Circular rings are spaced along the height for stiffness. The height of the rings above the base and their diameters are listed in table I. Overall tower height is 44.40 inches.

All members are circular in cross section. The diameter of the vertical legs is 0.25 inch, and the diameter of the circular rings is 0.156 inch. In a full-scale design, the corresponding dimensions would be around 6 and 4 inches for the vertical and horizontal members, respectively. This compares to 8 and 10 inches, respectively, for the original four-leg tower. The reduced cross-sectional dimensions of the members of the eight-leg tower, in conjunction with the elimination of cross supports and gussets, provides a potential for a reduced wake formation.

The problem of wake formation downwind of such a tower in actual operation is illustrated in figure 4. In figure 4(a) is sketched a planview of the tower and a qualitative approximation of the outer limits of the region of wake flows generated by the members of the tower structure for the example cases of wind approaching at 0° and 45°. Also indicated is the interception of the wake by the plane of rotation of the rotor which is usually oriented to follow the wind direction. The vertical view of figure 4(b) shows the area of the wake region, $A_\delta = \delta_{av} R_b$ compared to the area swept by the rotating blades $A_b = \pi R_b^2$. It can be seen that a significant portion of the blade travel is immersed in a re-

duced velocity field; that is, $A_\delta/A_b \sim \delta_{av}/R_b$. This suggests that the ratio δ/R_b is one of the important parameters to be determined.

The detailed form of the wake downwind of the tower will depend on the individual wakes that are formed behind each structural member of the tower, how they progress downstream of each member, and how they interact in the plane of the rotor (or measuring probe). Thus, the specific orientation of the tower members as projected on a downwind plane perpendicular to the wind direction can provide some insight into the wake-producing potential of a particular structural configuration. Such projections are obtained from shadow photographs of the tower structure over a range of wind approach angles. Shadow photographs of the eight-leg tower concept model are shown for wind approach angles θ of 0°, 15°, 30°, and 45° in figures 5(a) through (d), respectively.

Installation

The eight-leg tower model was installed in the test section of a 6- by 9-foot low-speed wind tunnel, as had been done in the previous investigation (ref. 5). A photograph of the wind tunnel installation (with the 1/48th-scale model of the four-leg tower of ref. 5 with stairs included) is shown in figure 6. The base of the tower model was elevated off the floor of the tunnel in order to clear the ancillary equipment. The model could be rotated up to 90° with respect to the tunnel axis (approaching wind).

The wind speed profiles in the wake of the model were determined from measurements from a Pitot tube that was mounted on a remotely-controlled traveling carriage. Vertical and horizontal probe movement was provided. The total pressure sensed by the Pitot tube was referenced to a static pressure measured by a tap on the tunnel wall. Earlier surveys had indicated a sufficiently uniform static pressure at the measuring plane to allow wake velocity determination based on a fixed static pressure value. The velocity head (total minus static pressure) was sensed by a differential pressure gage of the variable-inductance type. A separate probe (shown in fig. 6) was used to determine the free-stream wind speed V_0.

All wake profile measurements were made in a plane $15\frac{9}{16}$ inches downstream of the vertical centerline of the tower model. This distance is 1.5 times the diameter of the second ring above the base of the tower. This distance ratio was selected to be consistent with the tests of the earlier models of reference 5, where the measuring plane was chosen to be 1.5 times the width of the tower at a reference level close to the lowest elevation that the tips of the blades achieve during operation. However, the reference tower width of the eight-leg tower was chosen to be the diameter of the second

ring, rather than the true width of the tower vertical legs (which is less than the ring diameter) at that height. Because of this, the measuring plane in these tests was located relatively farther back from the tower than in the previous tests. Hence, the measuring station location for the eight-leg model was actually 2.09 times the reference tower width (7.45 in.).

Pertinent properties and dimensions for the model installation and measurement are given in figure 7. Geometric parameters in the vertical plane are shown to scale in figure 7(a), and the important wake flow parameters are identified in figure 7(b). These are the local values of: minimum velocity V_{min}; the average velocity V_{av}; the average velocity defect $\Delta V_{av} = V_0 - V_{av}$; and the wake width δ. Values of the parameters X_ℓ, X_b, and W, which vary with tower elevation, are tabulated in table I. Symbols are defined in appendix A. Values of the tower projected width W were determined from measurements off the shadow photographs of figure 5. The specific variations with elevation for each wind angle are given in figure 8.

Inasmuch as the measuring station is a short distance downwind of the rotor plane of rotation, the wake properties determined in the tests are not exactly the same as those in the plane of the rotor. However, because of the short distance involved, the wake flow properties at the measuring station are not expected to vary substantially from those in the plane of rotation. Fluid speed deficits in the wakes behind blunt objects are persistent and require long distances to be dissipated.

Test Procedure

Horizontal wind speed profiles behind the tower were determined at vertical intervals of 1/2 or 1 inch over the upper three sections of the tower (fig. 7(a)). This was done by positioning the probe at the desired elevation in the free stream. Then the probe was made to slowly travel horizontally from the free stream on one side to the free stream on the other. This procedure resulted in a continuous recording of the local flow profile at each elevation. A complete set of profiles was measured for each wind approach angle θ of 0°, 15°, 30°, and 45°. The tests were run in two series: the first covered elevations from about 22 to 44 inches, and the second from 16 to 24 inches.

All measurements were made at a nominal wind speed of 100 mph and at ambient temperature and pressure (close to atmospheric). For these tunnel air flow conditions, the Reynolds number for the tower model based on the diameter of the legs of 0.25 inch is 1.83×10^4. The MOD-0 Wind Turbine Generator usually operates in

winds from 10 to 40 mph and in air temperatures from about 0° to 100° F. The range of Reynolds number for these conditions is from 5.4×10^4 to about 3.5×10^5. For flow over a smooth slender cylinder, the drag coefficient is essentially constant for Reynolds numbers from about 10^3 to 4×10^5. From momentum and similarity considerations, the constancy of the drag coefficient implies that the dimensionless velocity profiles downstream of the cylinder are identical for values of Reynolds numbers within this range. Since the tower model is made of all tubular members, there should be no difference, due to Reynolds number effects, in the dimensionless wind speed profiles in the wake of a full scale tower compared to those of the model.

The survey probe and wall tap signals were converted to local velocity ratio V/V_0 by means of an analog module and plotted as a continuous on-line trace to show the wake profile. Damping was provided in the output circuit to reduce local turbulent fluctuations in the wake. However, even with the damping, the printed velocity ratio trace contained high-frequency fluctuations as large as several percent. A precise determination of the mean value of the velocity variation was consequently extremely difficult to obtain. For simplicity, each profile trace was smoothed to a single faired variation according to best judgment. The faired profile was then digitized and processed to establish the minimum velocity ratio V_{min}/V_0 and the integrated average velocity ratio V_{av}/V_0. Velocity ratio values for the faired profiles were calculated and presented herein to three significant figures, with the values of V_{min}/V_0 rounded off to the nearest 0.005. However, it is recognized that such presentation implies a higher degree of precision than exists in reality for the wake mean velocity.

For the determination of wake width, the edges of the wake were selected from the faired curves to be the points where the local velocity ratio V/V_0 increased to a value of around 0.995. Clearly, from the manner in which the profiles gradually approach the free-stream value, a precise measure of the wake width was difficult to determine.

RESULTS AND DISCUSSION

Wake Flow Characteristics

The presentation of wake characteristic data obtained from the tunnel surveys will include illustrations of the wake velocity profiles and the variations with tower elevation and wind direction of the properties of local wake average velocity ratio, minimum velocity ratio, and width. A complete tabulation of these data parameters is given in table II.

Velocity profiles. - Representative measured wind speed profiles from the continuous trace output are shown in figures 9 through 12. These profiles are typical, and were selected to illustrate some of the local characteristics of the wake for several wind approach angles. Several elevations covering the upper sections of the tower are included for each wind angle. Each figure contains the value of V_{min}/V_0, V_{av}/V_0, and δ for the wake profile. Also included as an insert in each figure is a shadow photograph of the local section of the tower as viewed from the downwind side, and the elevation at which the profile was measured is indicated by a dot-dash line. The turbulent nature of the local wake flow is clearly indicated in all traces.

An inspection of the wind speed profiles and the shadow photo inserts clearly indicates that each profile shape is complex and is determined by the number of members and their relation and proximity to each other. The local wind speed distribution immediately downwind of a round member may be close to that of an isolated cylinder. However, the velocity reduction in the wake of a member is generally reduced further when there are other tower members close to it, intersecting with it, or upwind from it. Conversely, when the separation between members is increased, the velocity defects are smaller and flow through the tower is increased. Thus, the shape of the wake at some distance down stream of a tower at any given elevation is a superposition and a coalescence of the wakes of the individual members.

Average and minimum velocities. - Results for the vertical variation of minimum velocity ratio V_{min}/V_0 and the averaged velocity ratio V_{av}/V_0 for each test profile are shown in figure 13. Figures 13(a) through (d) present the vertical variations of V_{av}/V_0 and V_{min}/V_0 for $\theta = 0°$, 15°, 30°, and 45°, respectively. Also shown on each figure are the locations of the tower rings and the calculated average value of all the local values of V_{av}/V_0 for the upper three sections of the tower ($H \geq H_b$).

An inspection of figure 13 reveals rather large variations of V_{min}/V_0 with elevation especially for $\theta = 0°$ and 45°. These variations in V_{min}/V_0 with elevation are not surprising because of the complex interactions of the wakes of the individual members, as was discussed in the previous sections. In other words, the value of minimum velocity ratio is a manifestation of the different ways in which the individual wakes from the tower structural members superimpose and coalesce at the location of the measuring plane. The arithmetic average value of V_{min}/V_0 for all data points in the upper three sections of the tower ($H \geq H_b$) is 0.76.

The variations of V_{av}/V_0 with elevation are smaller than for the minimum velocity ratio. The arithmetic average values of V_{av}/V_0

for each wind approach angle (dashed lines in fig. 13) were found to be within about ±1.2 percent of the overall average value of 0.88 obtained from all of the data points for $H \geq H_b$. This strongly suggests that the flow through the eight-leg tower is relatively insensitive to the wind approach angle and to the tower section solidity. However, the lowest of the three upper sections does have a consistently higher average velocity ratio (from 1 percent at $\theta = 0°$, to 3 percent at $\theta = 45°$). This higher wake flow reflects the effect of the lower solidity of this section, and is an advantage because the outer radial regions of the wind turbine rotor blades would then be exposed to smaller impulse loads.

Width. - Since the principal determinant of the overall width of the tower wake is the projected width of the tower onto a plane normal to the wind approach angle, the measured wake width δ was expressed as a ratio of the local tower width W (fig. 8). Plots of the ratio δ/W are given in figure 14 for the four wind approach angles. Also shown on each figure is the elevation of the tower stiffening rings.

According to figure 14, there is a definite tendency for the wake width ratio to increase with tower elevation (except for the upper section at $\theta = 45°$ where the projected width of tower decreases with height). There are also peak values for each angle that appear to correspond to the presence of the horizontal rings. This increase in wake thickness at the elevation of the rings is expected, inasmuch as the rings are wider than the projected width of the tower legs (fig. 5) which forms the basis for the value of W. Furthermore, in many cases, an intersection of the tower legs occurs at the location of the horizontal rings, as can be seen in figure 5. Such intersections (at low included angle) substantially increase the effective projected width of the members with a subsequent increase in local wake width. This interaction effect is especially pronounced for ring 2 at $\theta = 0°$ in figure 14(a) and ring 4 at 45° in figure 14(d) (see shadow photographs of figs. 5(a) and (d)). However, there does not appear to be any relationship between the locations of peak δ/W and minimum velocity ratio V_{min}/V_0 (fig. 13).

For practical purposes, it can be taken that the wake thickness ratio for the eight-leg tower concept is roughly independent of wind direction. Furthermore, a single representative variation can be adopted with a linear variation of δ/W from 1.4 at ring 2 to 1.7 at ring 4 and constant at 1.7 to the top of the tower.

Comparison of Eight- and Four-Leg Tower Wakes

Inasmuch as the eight-leg tower concept was intended to be applicable to the MOD-0 class of wind power turbines, it is necessary

to compare its wake characteristics with the best of those obtained for the earlier four-leg MOD-0 tower models reported in reference 5. The best wake performance was measured with the 1/48th-scale model with tubular members and without stairs, rails or gusset plates. An attempt is also necessary in the comparisons to compensate for the differences in relative location of the measuring station between the eight-leg model ($X_m/R_b = 0.519$) and the four-leg model ($X_m/R_b = 0.360$).

In general, the rate at which a wake expands depends on the downstream distance and also on the obstacle shape and solidity. In the case of wakes generated by isolated long slender solid rods with any type of cross-section (circular, square, elliptical, etc.) the wake width far downstream (over 40 rod diam) has been found to vary as the square root of the distance. At distances less than about 40 rod diameters, the wake width dependence on distance is more complicated and not as well defined. The spreading of a wake close to porous three-dimensional obstacles such as towers is even more complex than behind slender solid rods. This makes it difficult to accurately correct the eight-leg tower data for V_{min}/V_0, V_{av}/V_0, and δ/W to another station so as to facilitate exact comparison with the four-leg tower data.

Models. - A photographic comparison between the two tower models is presented in figure 15. The eight-leg model has no cross members and a fewer number of horizontal members than the four-leg design. Furthermore, to the same scale as the eight-leg model, the four-leg configuration would have vertical members of 0.36-inch-diameter (compared to 0.25 in.), and horizontal members of 0.18 inch (compared to 0.156 in.). It is a question, therefore, whether these favorable differences would offset the larger number of legs for the eight-leg concept.

A further comparison of the two models is provided by the shadow photographs shown in figure 16. A pairing is presented for several wind approach angles. It is not readily apparent from observation of these images what the differences in blockage between the two structures would be. The eight-leg tower appears to be more open (lower solidity) than the four-leg tower. Therefore, it would be easy to conjecture that the flow through the eight-leg tower would be higher and the wake width narrower than for the four-leg tower.

For the comparison of wake characteristics, data for the eight-leg model are those given in table II. The wake data for the four-leg model are taken from the revised values (not included in ref. 5) presented in appendix B.

Wake velocity ratios. - Composite plots of the measured values of the minimum velocity ratio and the average velocity ratio against elevation for all wind angles for the two tower models are shown in figure 17. A comparison of the as-measured data, that is, uncorrected for different measuring locations, shows higher values of V_{min}/V_0 and V_{av}/V_0 for the eight-leg concept compared to the four-leg design. Average minimum velocity ratio $(V_{min}/V_0)_{av}$ for all data points for $H \geq H_b$ is 0.76 for the eight-leg model, and 0.66 for the four-leg model. The corresponding overall value $(V_{av}/V_0)_{av}$ for the eight-leg concept is 0.88 compared to 0.84 for the four-leg design, suggesting that the eight-leg tower allows a higher wind flow through it than the four-leg tower. But, this advantage may be more apparent than real because the eight-leg data were recorded at a station relatively further downstream than for the four-leg model.

Another important feature of the data is that there is basically little variation in V_{av}/V_0 with either tower section or wind approach angle for both models, as shown in figure 18. Also shown on figure 18(b) is the value of average velocity ratio produced by the original MOD-0 configuration (ref. 5).

In order to make a direct comparison between the eight- and four-leg towers, the $(V_{av}/V_0)_{av}$ and $(V_{min}/V_0)_{av}$ data from the eight-leg model were corrected to the same relative location as the four-leg model. As implied earlier, such corrections were of necessity based on some gross simplifying assumptions. The basic assumptions are that the overall wake development of the tower is largely determined by the wake development of slender isolated circular cylinders (as represented by the tower legs), and that changes in tower wake characteristics can be adequately described by changes in classical cylinder wake behavior with downstream distance.

Based on the diameter of the tower leg (0.25 in.), the measuring station distance downwind of the tower centerline is $X_m/d_t = 62.25$ (for $X_m/R_b = 0.519$), and the value that corresponds to the relative location of the four-leg measuring station is $X_m/d_t = 43.2$ (for $X_m/R_b = 0.360$). Since these values are relatively high, it is assumed that the classical variation for fully-developed wake flow for downstream of a cylinder (e.g., ref. 7) is applicable to the tower wake, that is,

$$\left(1 - \frac{V_{min}}{V_0}\right) \sim \left(\frac{X}{d_t}\right)^{-1/2} \qquad (1)$$

A further useful assumption is that the averages of the minimum and average velocity ratios are related by the expression,

$$b = \frac{1 - \left(\frac{V_{av}}{V_0}\right)_{av}}{1 - \left(\frac{V_{min}}{V_0}\right)_{av}} \tag{2}$$

which is essentially constant for the range of X values covered. This assumption is correct for fully developed wake flow with similar profiles (ref. 7).

The relations for velocity ratios at the two station locations in the same wake, designated by stations 4 and 8, are then

$$\frac{1 - \left(\frac{V_{min}}{V_0}\right)_{av,4}}{1 - \left(\frac{V_{min}}{V_0}\right)_{av,8}} = \sqrt{\frac{\left(\frac{X_m}{d_t}\right)_8}{\left(\frac{X_m}{d_t}\right)_4}} \tag{3}$$

and

$$\frac{1 - \left(\frac{V_{av}}{V_0}\right)_{av,4}}{1 - \left(\frac{V_{av}}{V_0}\right)_{av,8}} = \sqrt{\frac{\left(\frac{X_m}{d_t}\right)_8}{\left(\frac{X_m}{d_t}\right)_4}} \tag{4}$$

For the values $(X_m/d_t)_8 = 62.25$ and $(X_m/d_t)_4 = 43.2$, the value of the right side of equations (3) and (4) is 1.20.

Equations (3) and (4) were used to correct the $(V_{av}/V_0)_{av}$ and $(V_{min}/V_0)_{av}$ values for the eight-leg model to the relative measuring station location of the four-leg model ($X_m/d_t = 43.2$). Results are given in table III together with the measured values for both tower models. It is seen that even with the calculated adjustment for differences in relative measuring station location, the average velocity ratios of the eight-leg tower concept are slightly larger than for the four-leg tower: 0.85 against 0.84 for $(V_{av}/V_0)_{av}$; and 0.72 against 0.66 for $(V_{min}/V_0)_{av}$. The corresponding values of average velocity defect are 0.15 against 0.16.

Wake width. - During normal operation, each rotor blade is totally immersed in the wake for a short period of time which depends on the wake width and the rotor rpm. Because of the importance of wake width in determining the impulse forces that the wake average velocity deficit imposed on the blade, it was decided to compare the wake widths of the four- and eight-leg models using the MOD-0 rotor blade radius R_b as the reference dimension. The width data from both models were nondimensionalized by the blade radius R_b (a fixed value) and plotted in figure 19 against the ratio of local elevation H to the elevation of the rotor axis H_a (fig. 7) for several wind angle groupings. Also shown in the figure are the locations of the horizontal members of the towers and the variation of nondimensional tower projected width W/R_b for both models. Inasmuch as the tower width W is the principal determinant of the width of the wake from the tower, the variation of δ/R_b should be similar to the variation of W/R_b (decreases with increasing elevation).

For low values of θ (figs. 19(a) and (b)), the nondimensional wake widths for both the eight- and four-leg models are practically identical, with a variation that is essentially parallel to the variation of the tower width ratio. For the wind angles from 30° to 45° (figs. 19(c) and (d)), there is a deviation in the data from the two configurations in the upper part of the tower, as a result of the difference in tower width variation. For these angles, the eight-leg wake width is less than that for the four-leg model. Values of δ/R_b tend to increase with increasing wind approach angle. This is a reflection of the increase in projected tower width as θ is increased from 0°. Average values of wake width ratio $(\delta/R_b)_{av}$, for all the data in the upper sections of the towers are 0.33 and 0.35, respectively, for the eight- and four-leg towers.

An approximate correction was also made for the effect on wake thickness of the difference in relative measuring-stating location between the two test models. The correction was based on the simplifying assumption that the width of the tower wake can be modeled as the outer limits of the wakes generated by two identical circular cylinders with $d_t = 0.25$ inch and with centerline separation distance equal to $(W - d_t)$, where W, representing the width of the tower, is the overall projected width of the tube pair. Thus, if the wake of the individual cylinder is denoted by δ_t, then the overall (tower) wake at any elevation is given by

$$\delta = (W - d_t) + \delta_t \tag{5}$$

or

$$\frac{\delta}{d_t} = \left(\frac{W}{d_t} - 1\right) + \frac{\delta_t}{d_t} \tag{6}$$

For classical fully-developed wake flow,

$$\frac{\delta_t}{d_t} \sim \sqrt{\frac{X}{d_t}} \tag{7}$$

Thus, for the two measuring station locations in the same wake

$$\frac{\left(\frac{\delta}{d_t}\right)_{av,4} - \left(\frac{W}{d_t} - 1\right)}{\left(\frac{\delta}{d_t}\right)_{av,8} - \left(\frac{W}{d_t} - 1\right)} = \sqrt{\frac{\left(\frac{X_m}{d_t}\right)_4}{\left(\frac{X_m}{d_t}\right)_8}} \tag{8}$$

Substitution of appropriate values in equation (8) then showed that the value of $(\delta/R_b)_{av}$ for the eight-leg model was reduced from 0.33 at the measuring station to 0.31 at the relative location of the four-leg tests. These values are compared to the measured value of $(\delta/R_b)_{av} = 0.35$ for the four-leg data in table III. It is thus seen that the eight-leg tower model produces a more favorable wake than the four-leg tower model in that wake width is decreased and velocity ratios are increased.

Correction to plane of blade. - Calculation procedures for the effect of the tower wake on rotor blade bending stress require inputs of wake width δ and velocity defect $(V_0 - V_{av})$. The calculation of reference 6, for example, uses wake width and average velocity defect at the 3/4-radius elevation as representative of the outer half of the blade. These properties in the plane of the blade are not precisely available from the eight- and four-leg model test results because the measuring station in both cases was located downstream of the plane of the blade (e.g., fig. 7(a)). However, these measured values can be corrected to the plane of rotation of each tower model by using the simplified wake model discussed previously in the comparison of wake velocities and width. This correction was made to the arithmetic average of the measured values of δ/R_b, V_{av}/V_0, and V_{min}/V_0 for all the upper sections of each tower $(H \geq H_b)$ for all wind approach directions. These corrected average values were then used for the comparison.

Average wake characteristics for both towers were calculated at an axial position corresponding to the three-quarter radius point

on the blade (X/R_b = 0.268). At this blade location, X/d_t = 32.16 for the eight-leg model (compared to 62.25 at its measuring station), and X/d_t = 22.33 for the four-leg model (compared to 30.0 at its measuring station). Equations similar to (4) and (8) were then used to obtain wake property values at the blade. Results are shown in table IV, where it is seen that the average wind speed in the wake of the eight-leg model at the blade location (0.83) is higher by a few percent than that in the wake of the four-leg tower (0.81). For the eight-leg model, this amounts to an average velocity defect ratio of 0.17 with a wake width ratio of 0.30, as compared to a defect ratio of 0.19 and a wake width ratio of 0.33 for the four-leg tower. These results suggest that the eight-leg tower offers slightly less resistance to the wind flow than does the comparable four-leg tower.

SUMMARY OF RESULTS

Based on the data and analysis contained herein, the all-tubular eight-leg tower concept produced a slight improvement in tower wake characteristics compared to an earlier four-leg lattice-type design (MOD-0), also constructed with tubular members. The ultimate desirability of the eight-leg concept will then depend on nonaerodynamic factors such as the cost of fabrication and assembly, and aesthetic appeal.

APPENDIX A

SYMBOLS

Most of the symbols used herein are denoted in figure 7.

A	area, $in.^2$
b	ratio of defect in average velocity to defect in minimum velocity
d_t	diameter of leg of tower, in.
H	local tower elevation (height) above the base, in.
H_a	elevation of horizontal axis of rotor blades, in.
H_b	minimum height of rotor blade tip above the base of the tower, in.
R_b	radius of the tip of the rotor blade, in.
V	local wind speed in wake, mph
V_{av}	arithmetic average wind speed in wake at any local elevation, H, mph
V_{min}	minimum wind speed in wake at any local elevation, H, mph
V_0	approaching free-stream wind speed, mph
ΔV_{av}	defect in the average velocity, $V_0 - V_{av}$, mph
W	local projected width of tower in plane normal to approaching angle, in.
W_{ref}	projected width of the tower legs at the elevation of the blade tip for the 0° wind direction orientation, in.
X	local distance downstream from the vertical centerline of tower, in.
X_b	local distance between the vertical centerline of the tower and the plane of the centerline of the blade, in.
X_ℓ	local distance between the measuring station and the most downwind leg of the tower ($X_m - X_t$), in.

X_m distance between the vertical centerline of the tower and the measuring plane, in.

X_t local distance between the vertical centerline of the tower and the most downwind leg of the tower, in.

δ local horizontal width of the wake downstream of the tower, in.

δ_t width of wake from individual tower leg, in.

θ angle between the approaching wind direction and a normal to the front side of the square top of the tower, deg

APPENDIX B

WAKE DATA FOR FOUR-LEG TOWER MODEL

The original data of the all-tubular four-leg MOD-0 tower model reported in reference 5 were reexamined with a more precise fairing and averaging procedure. Revised values were determined for wake local average velocity ratio, minimum velocity ratio, and width. The velocity ratio V_{av}/V_0 for each wake profile was calculated from digitized values of V/V_0 obtained from a fairing of the profile trace. Minimum velocity ratio V_{min}/V_0 was obtained from inspection. Values of wake width δ were also obtained from inspection. Fairing lines were drawn through the traces at the edges of the wake, and values were marked off at around $V/V_0 = 0.995$.

The revised wake characteristics for the four-leg tower model are tabulated in table V for wind approach angles of 0°, 10°, 35°, and 40°. Complete vertical coverage was not obtained at all angles. As in the case of table II, the data are presented as calculated to three significant figures even though the accuracy does not warrant more than two.

The arithmetic average values of all data points in the upper three sections of the tower (elevations corresponding to the blade, $H \geq H_b$) are:

$$\left(\frac{V_{min}}{V_0}\right)_{av} = 0.655$$

$$\left(\frac{V_{av}}{V_0}\right)_{av} = 0.836$$

$$\left(\frac{\delta}{R_b}\right)_{av} = 0.345$$

Pertinent geometric data for the four-leg tower model are:

Vertical leg diameter, $d_t = 0.1875$ in.
Blade radius, $R_b = 15.625$ in.
Measuring location, $X_m = 5.625$ in.
Projected tower width, for $H \geq H_b = 9.625$ in.,
$W = (4.9862 - 0.02844\ H)(\sin\theta + \cos\theta)$, in.

REFERENCES

1. Summary Report, Federal Wind Energy Program, January 1, 1977. ERDA-77-32, Energy Research and Development Administration, 1977.

2. Thomas, Ronald L.: Large Experimental Wind Turbines - Where Are We Now. NASA TM X-71890, 1976.

3. Puthoff, Richard L.: Fabrication and Assembly of the ERDA/NASA 100-Kilowatt Experimental Wind Turbine. NASA TM X-3390, 1976.

4. Glasgow, John C.; and Linscott, Bradford S.: Early Operation Experience on the ERDA/NASA 100-kW Wind Turbine. NASA TM X-71601, 1976.

5. Savino, Joseph M.; and Wagner, Lee H.: Wind Tunnel Measurements of the Tower Shadow on Models of the ERDA/NASA 100-kW Wind Turbine Tower. NASA TM X-73548, 1976.

6. Spera, D. A.; Janetzke, D. C.; and Richards, T. R.: Dynamic Blade Loading in the ERDA-NASA 100-kW and 200-kW Wind Turbines. NASA TM X-73711, 1977.

7. Schichting, Hermann (J. Kestin, transl.): Boundary Layer Theory. McGraw-Hill Book Co., Inc., 1955, p. 494.

TABLE I. - MODEL TOWER AND MEASURING PLANE DIMENSIONS

[All dimensions in in.]

Location	Elevation, H	Dimensions	Projected width, W				Measurement distance, X_ℓ		Blade distance, X_b
			$\theta = 0°$	15°	30°	45°	$\theta = 0°$	45°	
Top	44.40	4 x 4	3.94	4.61	5.00	5.66	13.59	12.88	5.78
Ring 4	35.70	$5\frac{3}{4}$ diam	5.42	5.23	4.71	3.94	12.85	13.59	6.82
Ring 3	27.10	$7\frac{5}{8}$ diam	6.53	6.97	7.19	6.93	12.30	12.10	7.88
Ring 2	18.25	$10\frac{3}{8}$ diam	7.44	8.81	9.78	10.08	11.84	10.52	8.96
Ring 1	9.10	$13\frac{3}{4}$ diam	----	----	----	----	----	----	----
Base	0	$14\frac{3}{8}$ by $14\frac{3}{8}$	----	----	----	----	----	----	----

TABLE II. - SUMMARY OF WAKE CHARACTERISTICS FOR EIGHT-LEG TOWER MODEL[a]

(a) Wind approach angle, $\theta = 0°$

Elevation, H, in.	Average velocity, V_{av}/V_0	Minimum velocity, V_{min}/V_0	Width, δ, in.	Elevation, H, in.	Average velocity, V_{av}/V_0	Minimum velocity, V_{min}/V_0	Width, δ, in.
44.0	0.920	0.845	7.4	24.0	0.863	0.705	10.1
43.0	.865	.740	7.7	23.5	.863	.695	10.1
42.0	.838	.760	8.2	23.0	.867	.680	10.5
41.0	.832	.755	8.0	22.5	.874	.680	10.4
40.0	.845	.770	8.1	22.0	.894	.720	10.5
39.0	.841	.695	8.5	21.5	.908	.745	10.7
38.0	.892	.770	8.3	21.0	.921	.775	11.7
37.5	.901	.775	8.7	20.5	.921	.785	11.9
37.0	.879	.765	9.0	20.0	.914	.780	11.9
36.5	.866	.755	9.3	19.5	.895	.755	11.9
36.0	.877	.775	9.1	19.0	.866	.755	11.7
35.0	.914	.790	8.9	18.5	.841	.770	11.1
34.0	.882	.745	8.2	18.25	.855	.795	10.8
33.0	.857	.710	8.9	18.0	.882	.830	10.3
32.0	.869	.780	9.1	17.5	.954	.905	10.0
31.0	.870	.790	9.4	17.0	.971	.880	10.3
30.0	.871	.795	9.4	16.5	.960	.850	10.5
29.0	.876	.790	9.3	16.0	.951	.820	10.7
28.5	.872	.790	9.4				
28.0	.860	.795	9.2				
27.5	.846	.785	9.4				
27.0	.857	.780	10.1				
26.5	.871	.770	10.3				
26.0	.863	.755	10.2				
25.0	.860	.730	10.2				
24.0	.858	.700	10.2				
23.5	.858	.670	10.1				
23.0	.886	.685	10.6				
22.5	.885	.710	10.8				
22.0	.902	.745	10.4				
21.5	.927	.775	[b]11.8				

[a]The values of V_{av}/V_0 and V_{min}/V_0 listed in the tables are one significant figure more than is justified by the accuracy.

[b]Estimated - velocity trace incomplete at edge.

TABLE II. - Continued.

(b) Wind approach angle, $\theta = 15°$

Elevation, H, in.	Average velocity, V_{av}/V_0	Minimum velocity, V_{min}/V_0	Width, δ, in.	Elevation, H, in.	Average velocity, V_{av}/V_0	Minimum velocity, V_{min}/V_0	Width, δ, in.
44.0	0.886	0.800	8.0	24.0	0.874	0.785	11.1
43.0	.830	.725	8.1	23.5	.875	.790	11.1
42.0	.834	.740	8.0	23.0	.879	.800	11.3
41.0	.839	.745	8.4	22.5	.880	.800	11.2
40.0	.836	.735	8.4	22.0	.887	.800	11.2
39.0	.837	.750	7.9	21.5	.900	.780	11.3
38.0	.842	.710	7.6	21.0	.911	.780	11.9
37.0	.874	.745	8.7	20.5	.916	.805	12.5
36.5	.869	.735	8.9	20.0	.914	.830	12.5
36.0	.878	.745	8.5	19.5	.903	.815	12.7
35.0	.888	.795	8.2	19.0	.880	.785	12.4
34.0	.871	.750	8.4	18.5	.865	.780	12.5
33.0	.857	.785	8.9	18.25	.866	.800	12.0
32.0	.860	.785	9.2	18.0	.891	.820	11.7
31.0	.853	.780	9.3	17.5	.942	.870	11.2
30.0	.864	.760	9.3	17.0	.960	.905	11.2
29.0	.864	.755	9.4	16.5	.965	.905	11.3
28.5	.864	.750	9.3	16.0	.961	.905	11.7
28.0	.849	.745	9.3				
27.5	.848	.750	9.7				
27.0	.863	.740	10.5				
26.0	.873	.735	10.6				
25.0	.870	.755	10.7				
24.0	.872	.755	10.8				
23.0	.871	.750	11.0				
22.0	.889	.750	11.1				

TABLE II. - Continued.

(c) Wind approach angle, $\theta = 30°$

Elevation, H, in.	Average velocity, V_{av}/V_0	Minimum velocity, V_{min}/V_0	Width, δ, in.	Elevation, H, in.	Average velocity, V_{av}/V_0	Minimum velocity, V_{min}/V_0	Width, δ, in.
44.0	0.900	0.810	8.1	24.0	0.881	0.785	11.3
43.0	.845	.720	8.7	23.5	.880	.795	11.3
42.0	.842	.760	8.6	23.0	.886	.800	11.5
41.0	.845	.745	8.6	22.5	.894	.810	11.3
40.0	.856	.775	8.3	22.0	.904	.800	11.5
39.0	.848	.760	7.6	21.5	.912	.775	11.6
38.0	.861	.735	7.7	21.0	.917	.785	12.0
37.0	.879	.780	8.0	20.5	.927	.820	13.1
36.5	.878	.760	7.9	20.0	.923	.835	13.6
36.0	.866	.760	7.4	19.5	.913	.830	13.6
35.5	.878	.770	7.3	19.0	.892	.800	13.7
35.0	.882	.770	7.7	18.5	.872	.775	13.6
34.0	.851	.740	8.4	18.25	.878	.770	13.6
33.0	.863	.755	8.9	18.0	.894	.780	13.5
32.0	.865	.770	8.9	17.5	.928	.800	13.2
31.0	.864	.765	9.4	17.0	.956	.885	12.4
30.0	.858	.770	10.0	16.5	.968	.905	12.3
29.0	.862	.765	9.9	16.0	.960	.890	12.8
28.5	.856	.785	9.7				
28.0	.878	.775	10.0				
27.0	.880	.800	10.5				
26.5	.923	.805	10.8				
26.0	.881	.795	[a]11.1				
25.0	.877	.785	[a]11.2				
24.0	.904	.800	[a]11.4				
23.0	.892	.805	[a]11.4				
22.0	.906	.765	[a]11.3				
21.5	.918	.800	[a]11.3				

[a]Estimated - velocity trace incomplete at edge.

TABLE II. - Concluded.

(d) Wind approach angle, $\theta = 45°$

Elevation, H, in.	Average velocity, V_{av}/V_0	Minimum velocity, V_{min}/V_0	Width, δ, in.	Elevation, H, in.	Average velocity, V_{av}/V_0	Minimum velocity, V_{min}/V_0	Width, δ, in.
44.0	0.908	0.850	8.5	24.0	0.889	0.735	11.1
43.0	.854	.720	8.3	23.5	.893	.715	11.3
42.0	.845	.705	8.4	23.0	.898	.700	11.3
41.0	.854	.775	8.1	22.5	.910	.695	11.3
40.0	.846	.730	8.2	22.0	.924	.700	11.6
39.0	.838	.705	7.9	21.5	.931	.720	11.7
38.0	.891	.770	7.6	21.0	.938	.750	12.1
37.0	.903	.810	8.1	20.5	.940	.775	12.8
36.0	.881	.810	7.8	20.0	.937	.795	13.3
35.5	.893	.810	7.1	19.5	.925	.795	13.9
35.0	.899	.805	7.3	19.0	.894	.775	14.1
34.0	.882	.750	8.0	18.5	.874	.745	14.3
33.0	.841	.685	8.5	18.25	.877	.740	14.4
32.0	.849	.730	8.8	18.0	.888	.740	14.5
31.0	.868	.785	9.2	17.5	.921	.775	14.1
30.0	.875	.790	9.5	17.0	.939	.805	13.7
29.5	.875	.780	9.8	16.5	.948	.785	13.6
29.0	.919	.765	9.6	16.0	.954	.765	13.6
28.0	.860	.750	9.5				
27.5	.879	.780	10.1				
27.0	.890	.785	10.5				
26.5	.882	.770	11.0				
26.0	.883	.775	11.3				
25.5	.881	.750	11.1				
25.0	.890	.750	[a]11.5				
24.0	.890	.690	[a]11.6				
23.0	.913	.690	[a]11.1				
22.0	.929	.755	(a)				

[a]Estimated - velocity trace incomplete at edge.

TABLE III. - COMPARISON OF WAKE CHARACTERISTICS OF EIGHT- AND FOUR-LEG TOWER MODELS

Characteristic	Eight-leg model		Four-leg model
	Measured, eight-leg location	Calculated, four-leg location	Measured, four-leg location
Location, X_m/R_b	0.519	0.360	0.360
$\left(V_{min}/V_0\right)_{av}$	.76	.72	.66
$\left(V_{av}/V_0\right)_{av}$	.88	.85	.84
$\left(\Delta V_{av}/V_0\right)_{av}$	.12	.15	.16
$\left(\delta/R_b\right)_{av}$	.33	.31	.35

TABLE IV. - COMPARISON OF WAKE CHARACTERISTICS AT THE PLANE OF ROTATION

Characteristic	Eight-leg model		Four-leg model	
	Measured	Calculated at blade	Measured	Calculated at blade
Location, X/R_b	0.519	0.268	0.360	0.268
$\left(V_{min}/V_0\right)_{av}$	.76	.67	.66	.60
$\left(V_{av}/V_0\right)_{av}$	.88	.83	.84	.81
$\left(\Delta V_{av}/V_0\right)_{av}$	.12	.17	.16	.19
$\left(\delta/R_b\right)_{av}$	.33	.30	.35	.33

TABLE V. - SUMMARY OF WAKE CHARACTERISTICS FOR FOUR-LEG TOWER MODEL[a]

(a) Wind approach angle, $\theta = 0°$

Elevation, H, in.	Average velocity, V_{av}/V_0	Minimum velocity, V_{min}/V_0	Width, δ, in.	Elevation, H, in.	Average velocity, V_{av}/V_0	Minimum velocity, V_{min}/V_0	Width, δ, in.
8.40	0.830	0.695	6.0	13.00	0.834	0.625	5.0
8.70	.824	.675	6.0	13.25	.822	.650	4.8
8.80	.830	.640	6.1	13.40	.800	.615	4.4
8.90	.810	.605	6.0	13.50	.802	.650	4.6
9.00	.805	.615	5.9	13.70	.806	.650	4.8
9.10	.801	.605	6.1	13.80	.813	.680	4.6
9.20	.791	.630	6.0	14.00	.828	.650	4.5
9.30	.783	.645	5.9	14.25	.865	.660	4.8
9.40	.791	.670	6.1	14.50	.855	.695	4.8
9.50	.778	.650	5.4	14.75	.847	.710	5.0
9.60	.798	.630	5.4	15.25	.870	.710	5.1
9.80	.825	.605	5.6	15.50	.879	.695	5.0
9.90	.834	.630	5.2	15.75	.850	.695	4.9
10.00	.830	.610	5.4	16.00	.836	.680	6.0
10.10	.850	.615	5.3	16.50	.833	.630	4.8
10.20	.863	.615	5.4	16.75	.810	.650	4.4
10.30	.862	.620	5.4	17.00	.805	.640	4.3
10.40	.854	.625	5.2	17.50	.830	.670	4.2
10.50	.836	.650	5.3	18.00	.836	.705	4.3
10.60	.832	.650	5.3	18.50	.838	.725	4.6
10.70	.834	.665	5.4	19.00	.852	.700	4.5
11.00	.854	.685	5.7	19.50	.808	.670	4.5
11.50	.879	.680	5.6	20.00	.821	.665	4.0
11.60	.881	.685	5.4	20.50	.815	.680	4.0
11.70	.889	.690	5.4	21.00	.842	.660	3.9
11.90	.872	.685	5.5	21.50	.811	.720	4.2
12.00	.870	.680	5.4	22.50	.819	.690	4.1
12.25	.859	.690	5.3	23.00	.868	.700	4.0
12.75	.828	.665	5.4				

[a]The values of V_{av}/V_0 and V_{min}/V_0, listed in the tables contain one significant figure more than is justified by the accuracy.

TABLE V. - Continued.

(b) Wind approach angle, $\theta = 10°$

Elevation, H, in.	Average velocity, V_{av}/V_0	Minimum velocity, V_{min}/V_0	Width, δ, in.	Elevation, H, in.	Average velocity, V_{av}/V_0	Minimum velocity, V_{min}/V_0	Width, δ, in.
8.50	0.815	0.640	6.4	13.65	0.793	0.615	5.0
8.75	.814	.620	6.2	13.75	.788	.625	5.1
9.00	.794	.605	6.2	13.85	.794	.635	5.1
9.25	.767	.625	5.9	14.00	.800	.630	5.2
9.50	.762	.620	5.6	14.25	.849	.680	5.0
9.75	.794	.595	5.8	14.50	.858	.695	5.0
9.95	.802	.590	5.8	14.75	.838	.660	5.1
10.05	.816	.605	5.8	15.00	.827	.650	5.0
10.15	.828	.610	5.8	15.25	.834	.640	5.0
10.25	.841	.650	5.9	15.50	.837	.630	5.0
10.30	.849	.660	5.9	15.75	.824	.640	5.0
10.40	.861	.665	5.8	16.00	.825	.655	5.0
10.50	.858	.680	5.8	16.25	.822	.675	4.8
10.75	.860	.675	5.7	16.50	.823	.665	4.8
11.00	.840	.670	5.6	16.75	.816	.620	4.8
11.25	.843	.665	5.5	17.00	.798	.600	4.7
11.50	.852	.650	5.6	17.15	.800	.605	4.7
11.75	.861	.665	5.8	17.25	.802	.610	4.7
12.00	.843	.660	5.6	17.40	.802	.620	4.8
12.25	.843	.675	5.6	17.50	.868	.635	4.6
12.50	.839	.685	5.5	17.75	.837	.660	4.6
12.75	.847	.675	5.5	18.00	.838	.680	4.4
13.00	.836	.665	5.4	18.25	.824	.645	4.6
13.25	.804	.620	5.0				
13.50	.808	.595	5.3				

TABLE V. - Continued.

(c) Wind approach angle, $\theta = 35°$

Elevation, H, in.	Average velocity, V_{av}/V_0	Minimum velocity, V_{min}/V_0	Width, δ, in.	Elevation, H, in.	Average velocity, V_{av}/V_0	Minimum velocity, V_{min}/V_0	Width, δ, in.
8.70	0.809	0.620	7.6	12.25	0.863	0.755	6.5
8.80	.808	.590	7.5	12.50	.849	.750	6.4
8.90	.811	.595	7.5	12.75	.861	.690	6.2
9.00	.810	.555	7.3	13.00	.857	.625	6.1
9.10	.814	.555	7.3	13.25	.842	.590	5.6
9.20	.802	.550	6.8	13.40	.827	.585	5.6
9.30	.807	.570	6.7	13.50	.805	.590	5.7
9.40	.806	.565	6.8	13.70	.802	.585	5.6
9.50	.807	.590	6.6	13.80	.821	.590	5.6
9.60	.821	.600	6.8	14.00	.833	.595	5.5
9.70	.816	.605	6.6	14.25	.856	.615	5.4
9.80	.824	.610	6.7	14.50	.851	.650	5.5
9.90	.830	.615	6.7	14.75	.842	.700	5.8
10.00	.837	.610	6.5	15.25	.845	.685	5.9
10.10	.846	.595	6.5	15.50	.849	.710	5.8
10.20	.851	.610	6.4	15.75	.846	.715	5.7
10.30	.855	.620	6.3	16.00	.843	.735	5.8
10.40	.861	.635	6.5	16.50	.842	.640	5.5
10.50	.851	.645	6.2	16.75	.839	.590	5.1
10.60	.850	.650	6.3	17.00	.821	.585	5.1
10.70	.845	.660	6.2	17.50	.829	.600	5.2
10.80	.852	.665	6.3	18.00	.831	.645	5.2
11.00	.858	.670	6.6	18.50	.880	.705	5.4
11.50	.864	.690	6.3	19.00	.828	.695	5.2
11.60	.859	.665	6.3	19.50	.812	.635	5.1
11.70	.865	.695	6.4	20.00	.805	.600	4.5
11.80	.863	.690	6.3	20.50	.804	.600	4.9
11.90	.871	.685	6.4	21.00	.799	.650	4.6
12.00	.867	.710	6.4				

TABLE V. - Concluded.

(d) Wind approach angle, $\theta = 40°$

Elevation, H, in.	Average velocity, V_{av}/V_0	Minimum velocity, V_{min}/V_0	Width, δ, in.
15.50	0.873	0.675	6.5
15.75	.854	.670	5.9
16.00	.832	.675	5.8
16.50	.846	.580	5.5
16.75	.854	.595	5.4
17.00	.815	.600	5.1
17.50	.818	.595	5.2
18.25	.789	.620	5.4
18.50	.824	.660	5.4
19.50	.814	.590	5.2
20.00	.828	.630	4.8
20.50	.812	.615	4.8
21.00	.802	.600	4.8

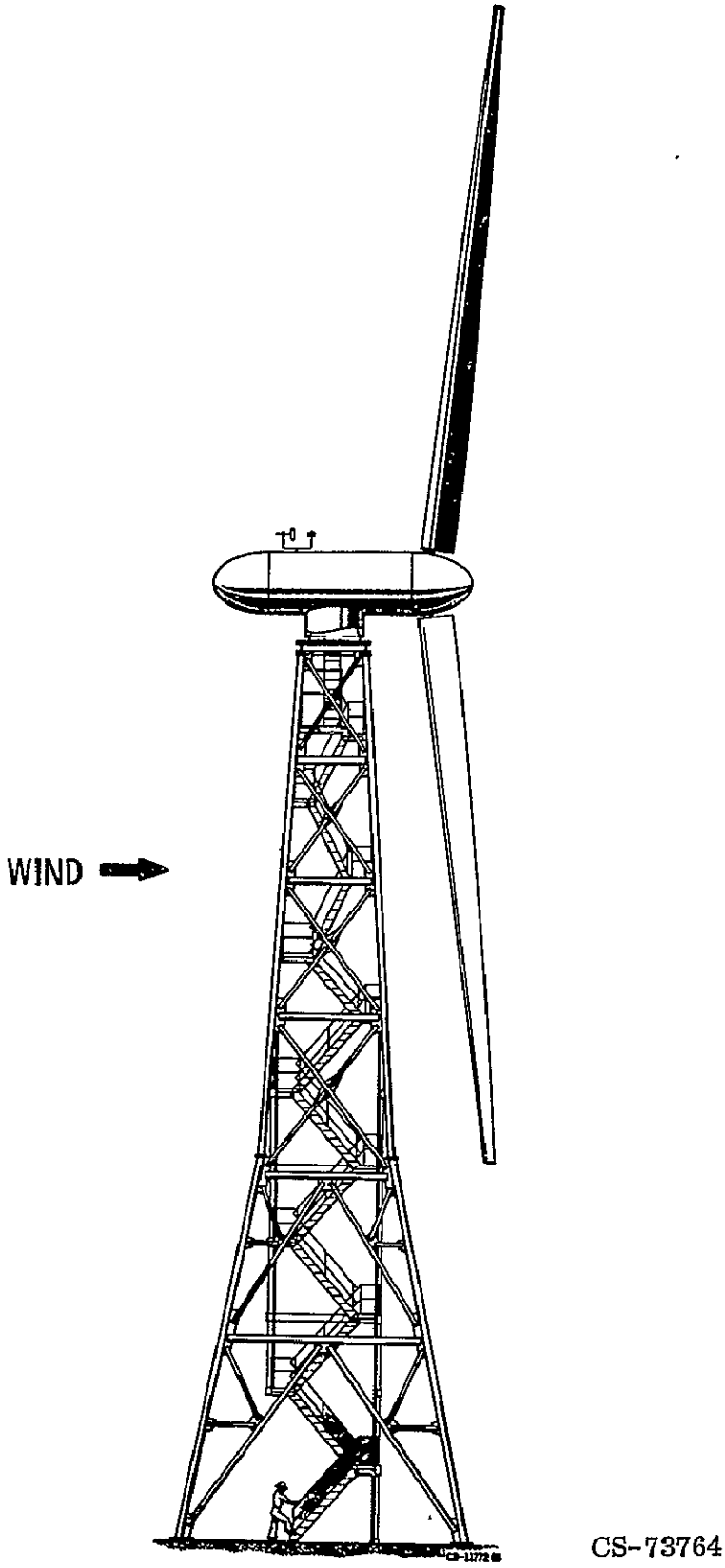

Figure 1. - ERDA-NASA 100-kilowatt experimental wind turbine.

NASA
C-75-2799

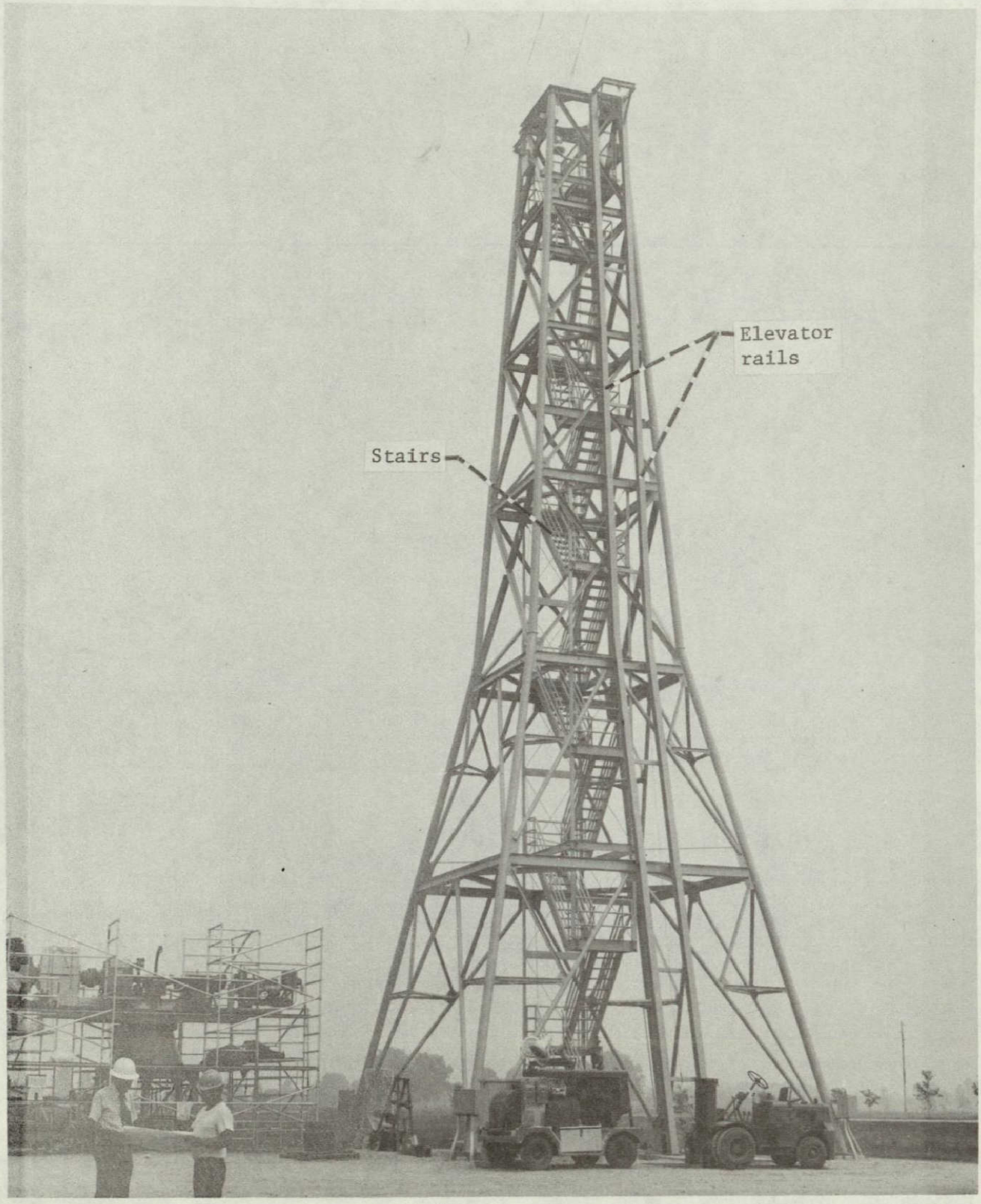

(a) Original design.

Figure 2. - ERDA-NASA 100-kilowatt wind turbine tower installation (MOD-0).

NASA
C-76-3261

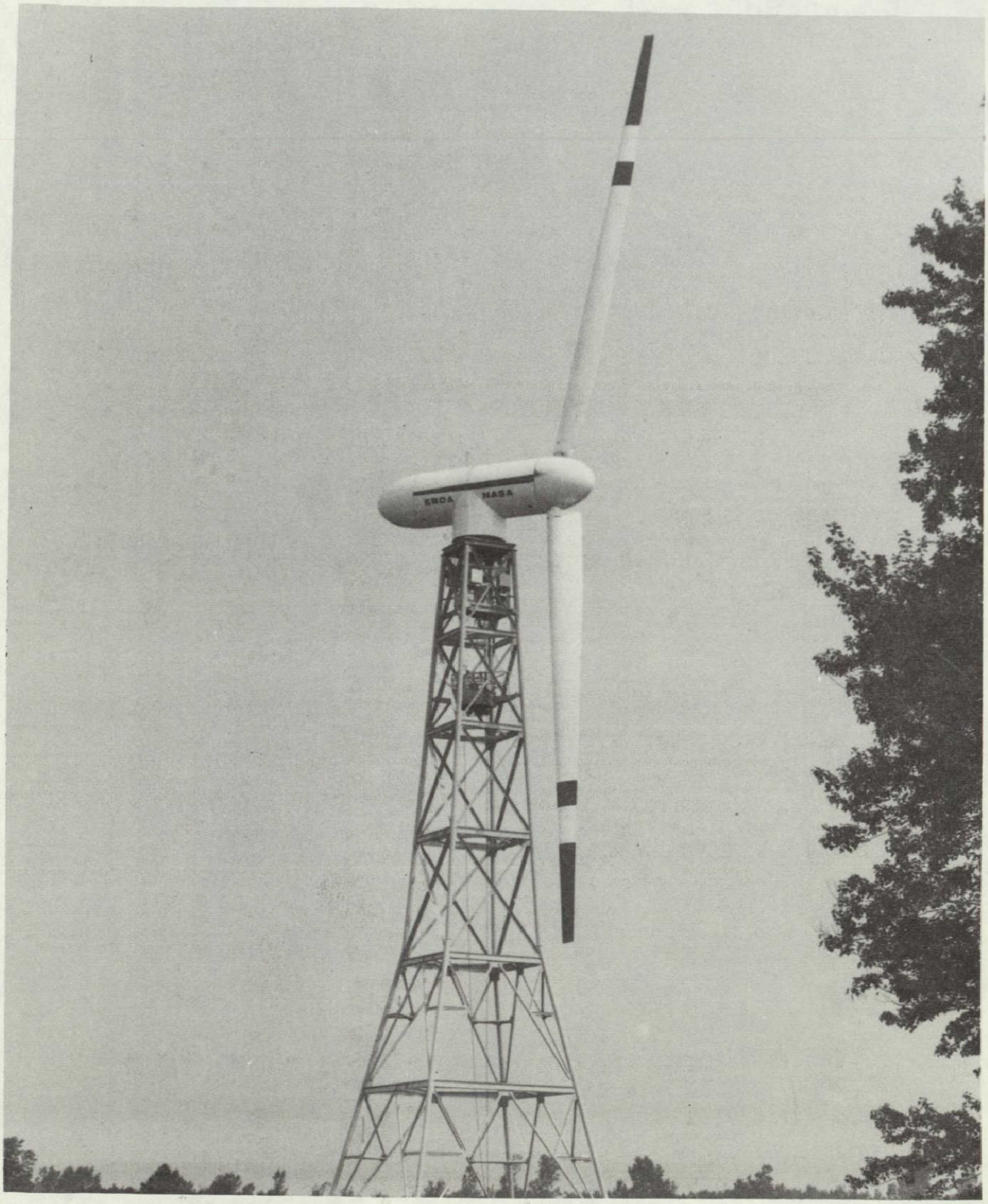

(b) After removal of stairs and rails.

Figure 2. - Concluded.

NASA
C-76-3291

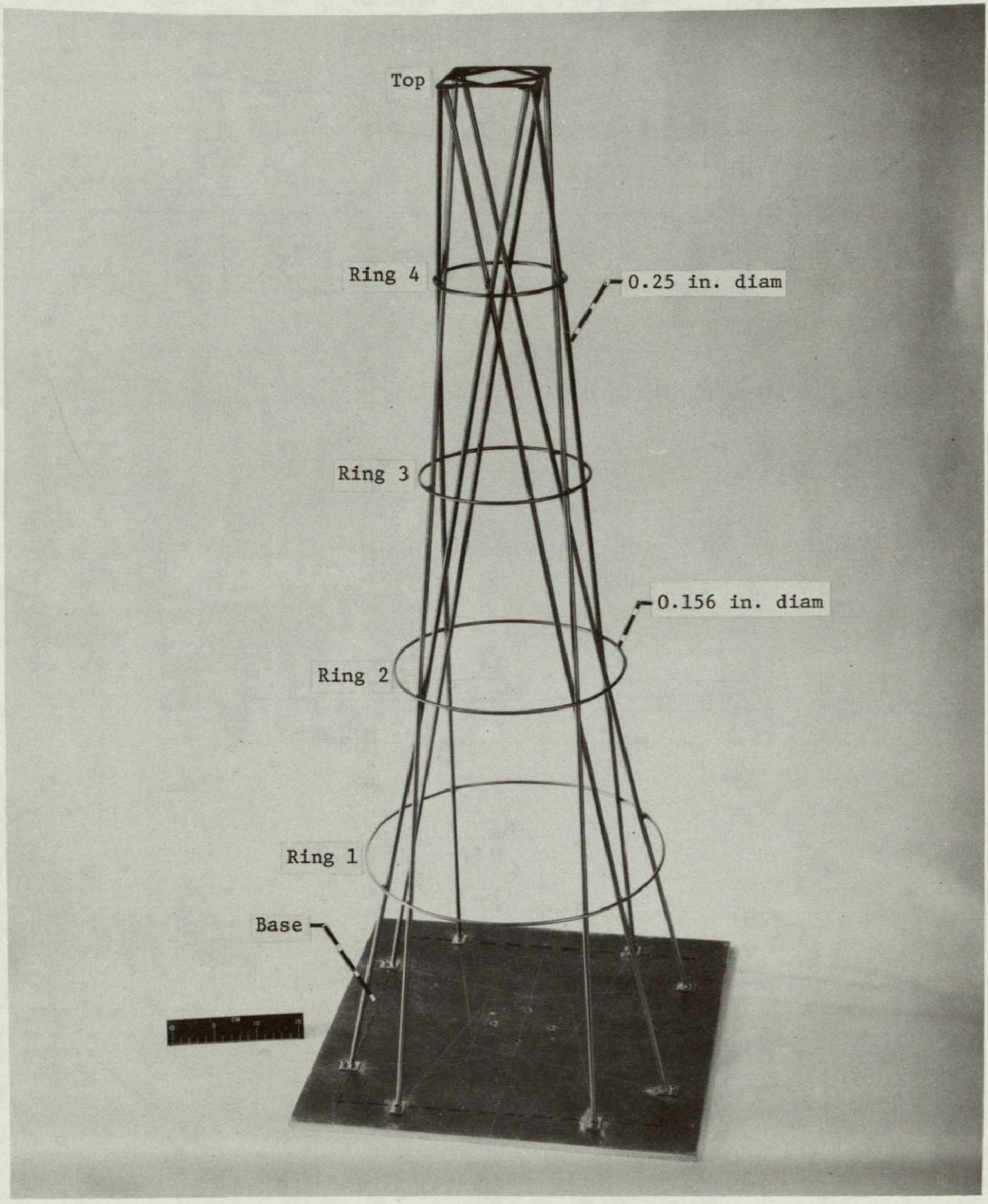

Figure 3. - 1/25th-Scale model of 8-leg tower concept for the MOD-0 wind turbine.

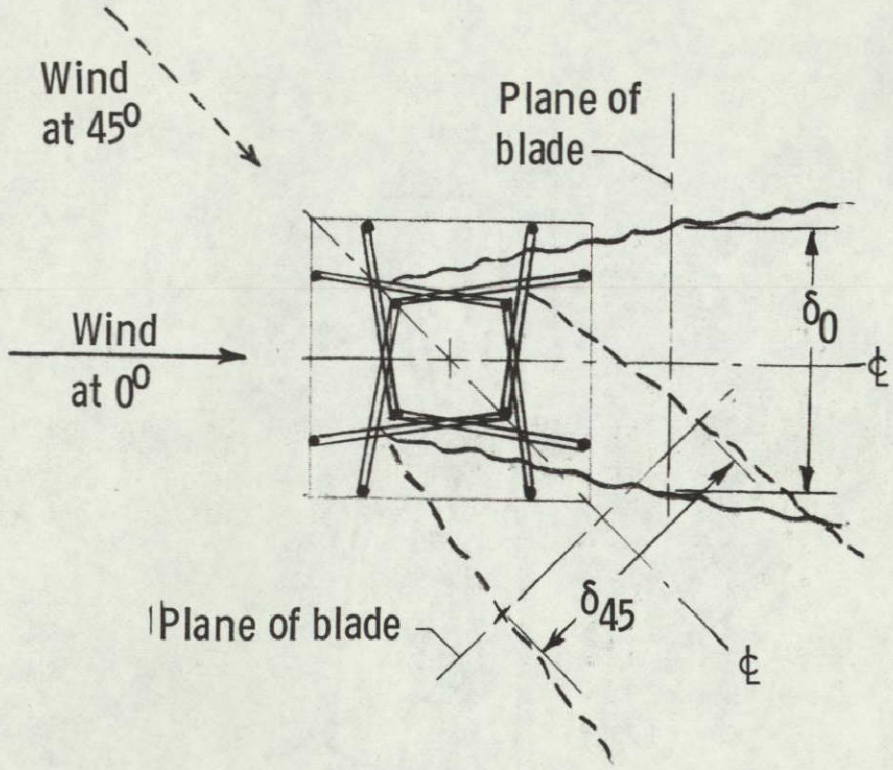

(a) Wake development.

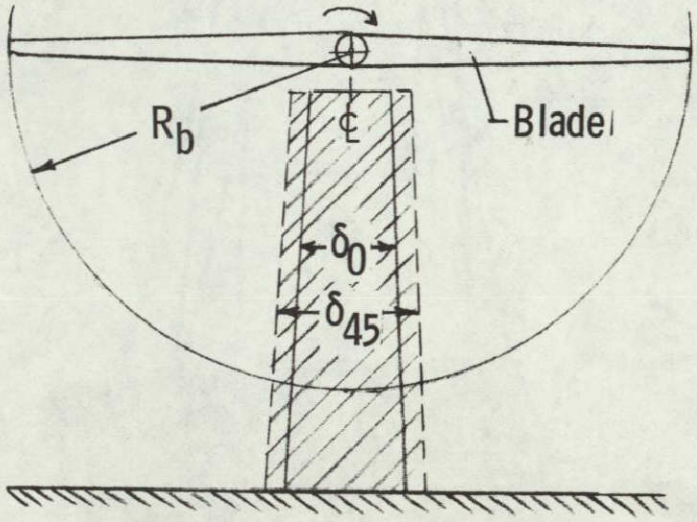

(b) Shadow areas in plane of blade.

Figure 4. - Wake shadow of wind turbine tower. Illustrated for approach angles of 0° and 45°.

NASA
C-77-2369

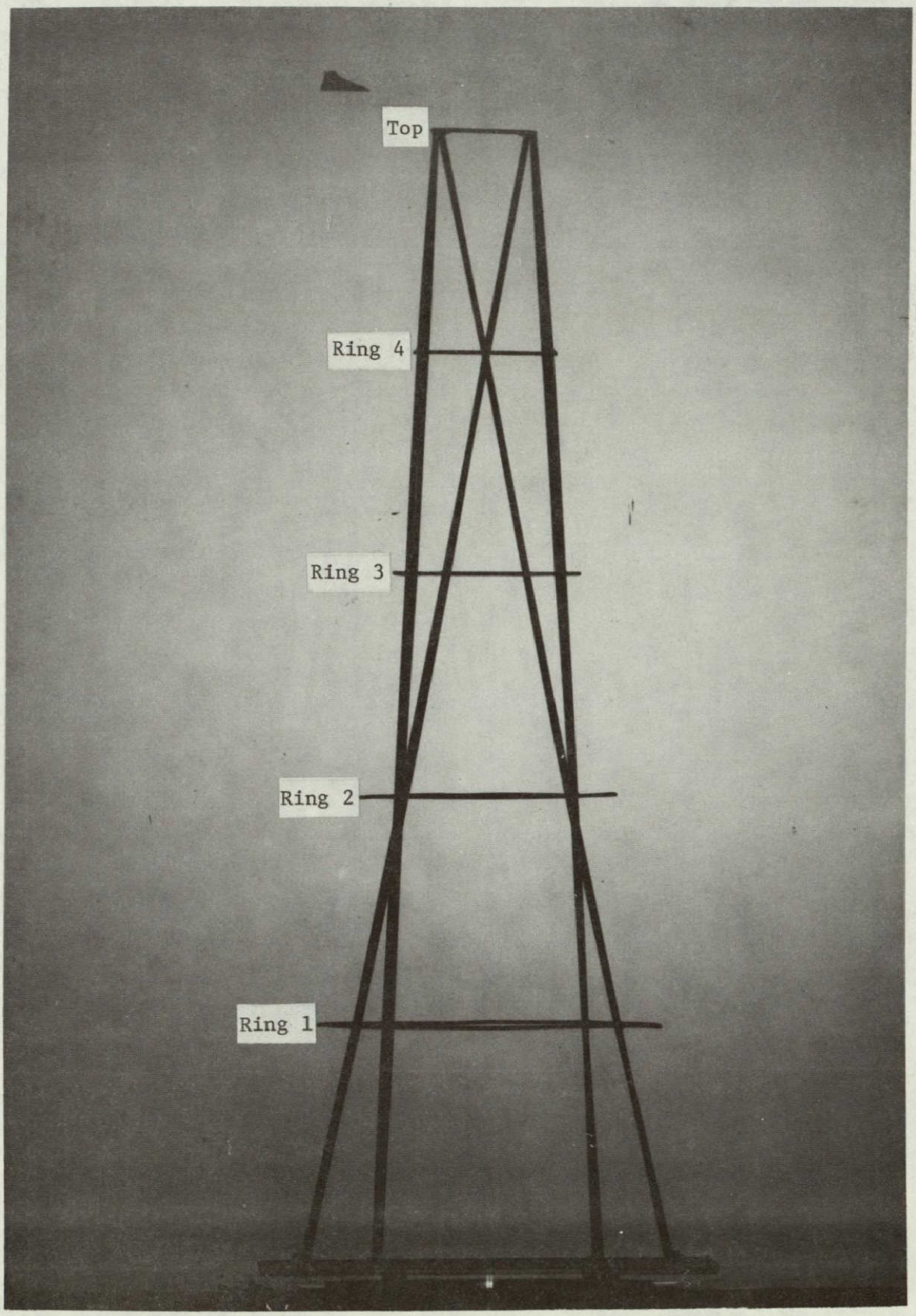

(a) Wind approach angle, $\theta = 0°$.

Figure 5. - Shadow photographs of 8-leg tower concept model.

NASA
C-77-2370

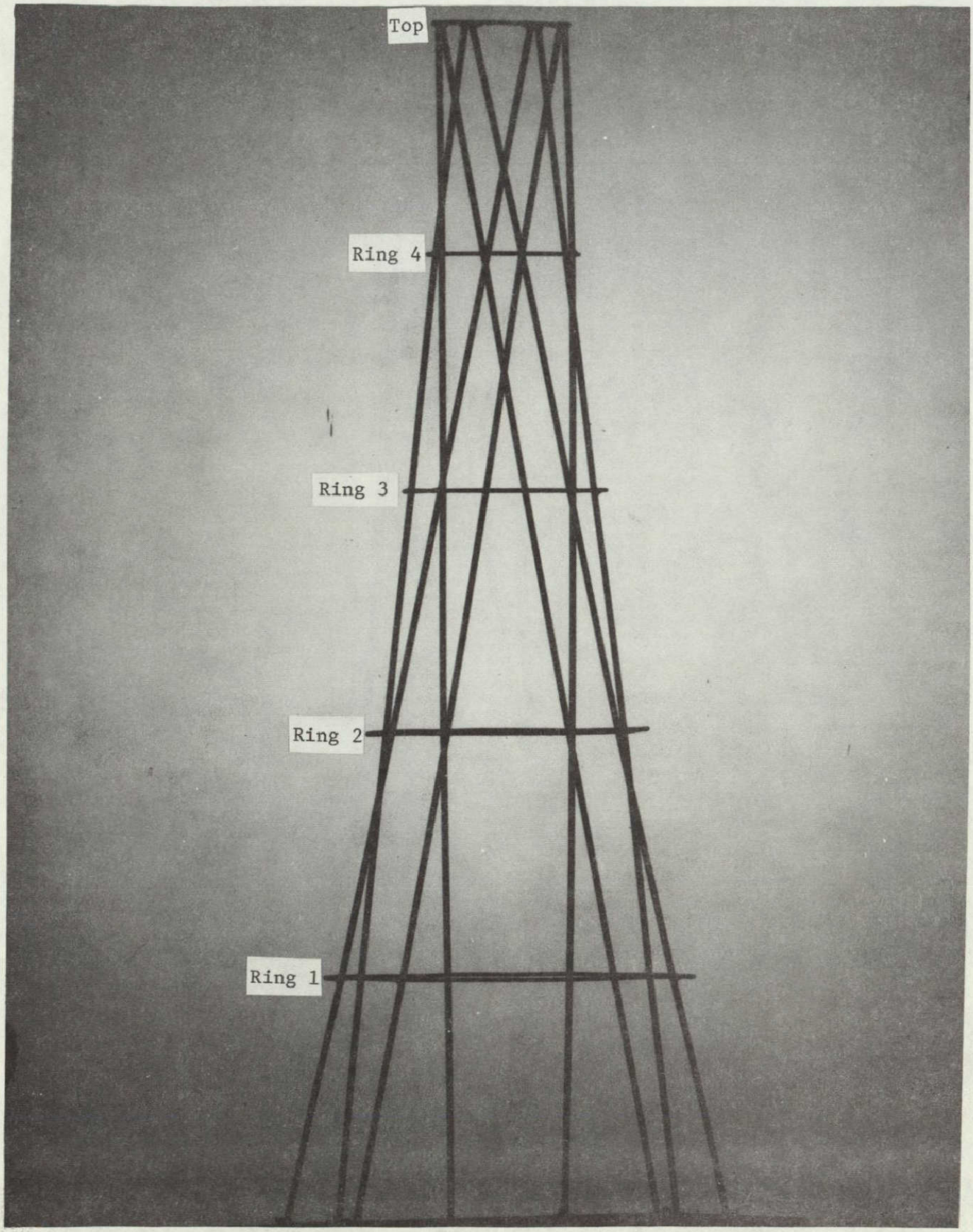

(b) Wind approach angle, $\theta = 15°$.

Figure 5. - Continued.

NASA
C-77-2371

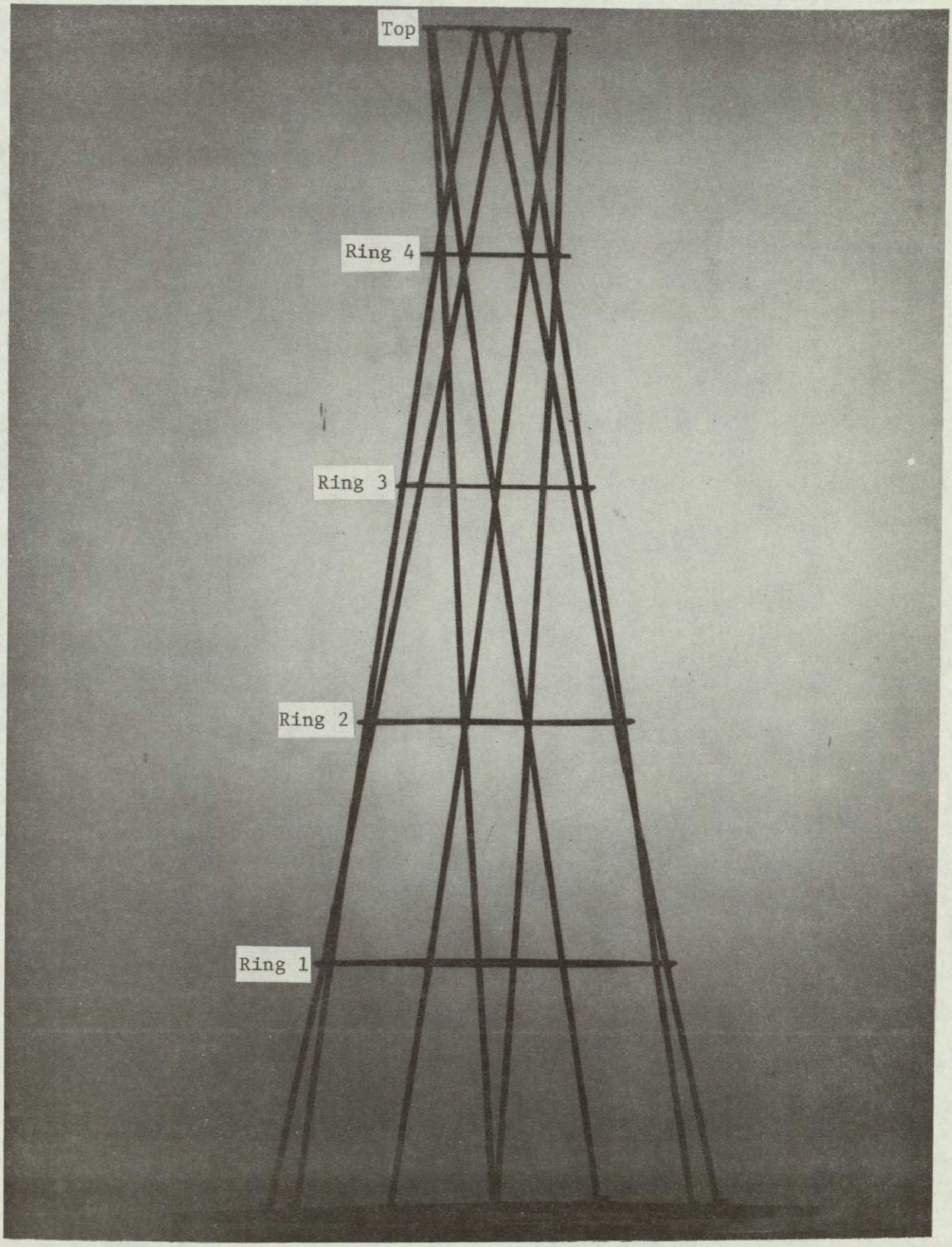

(c) Wind approach angle, $\theta = 30°$.

Figure 5. - Continued.

NASA
C-77-2372

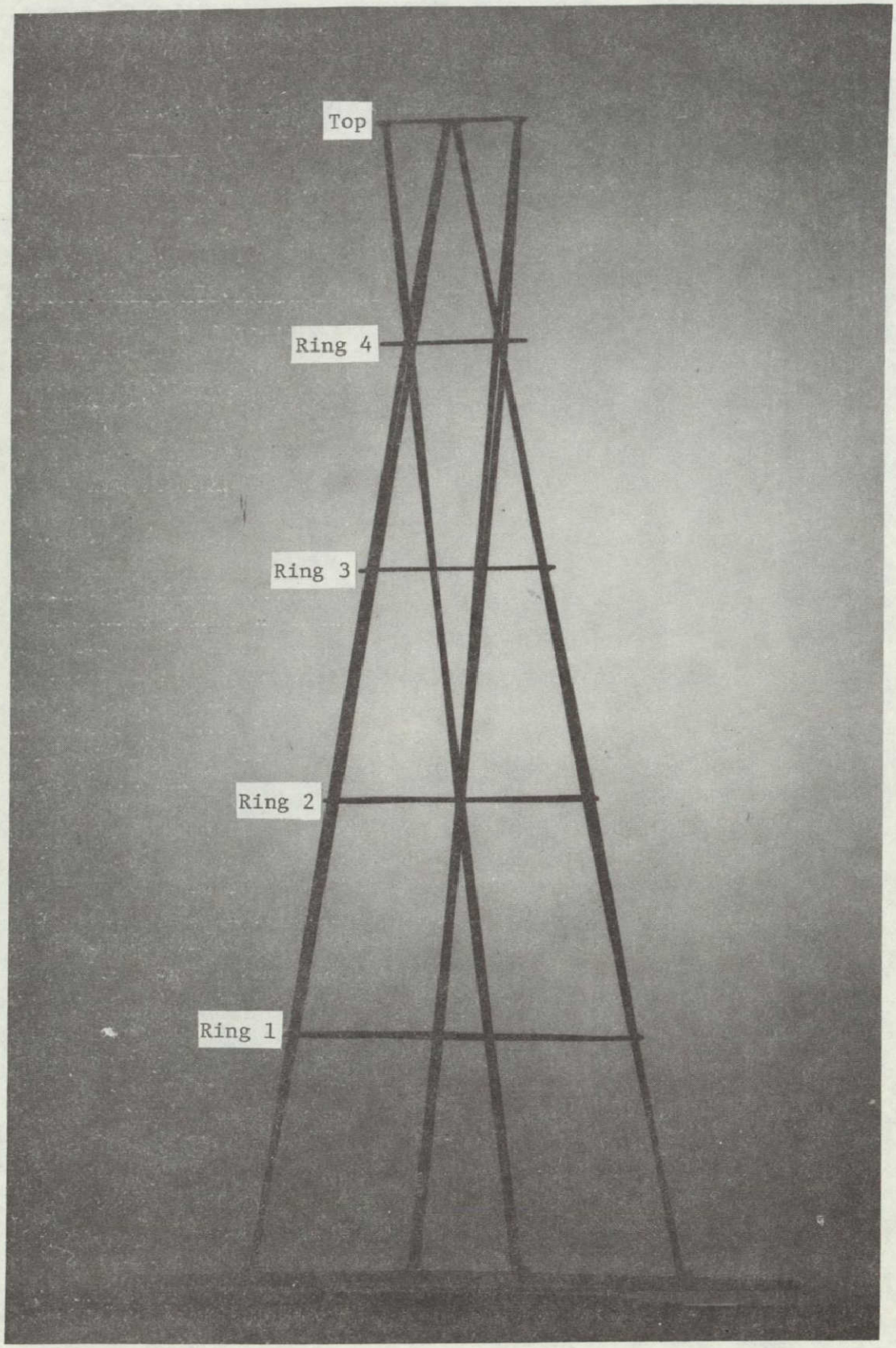

(d) Wind approach angle, $\theta = 45°$.

Figure 5. - Concluded.

NASA
C-76-1005

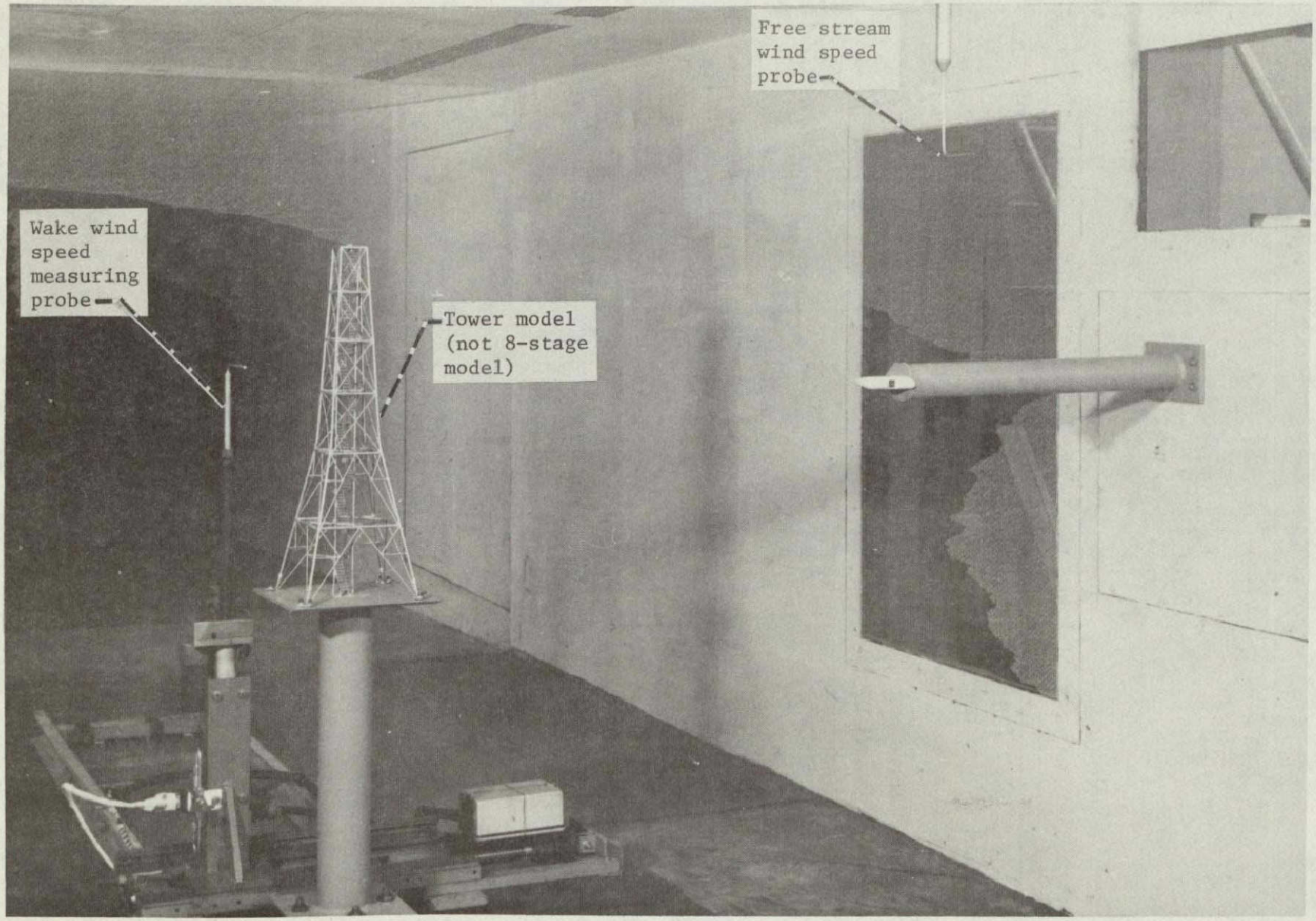

Figure 6. - Scale model test installation. (The tower shown is the 1/48th-scale model of the all-tubular 4-leg tower with a stairway inside.)

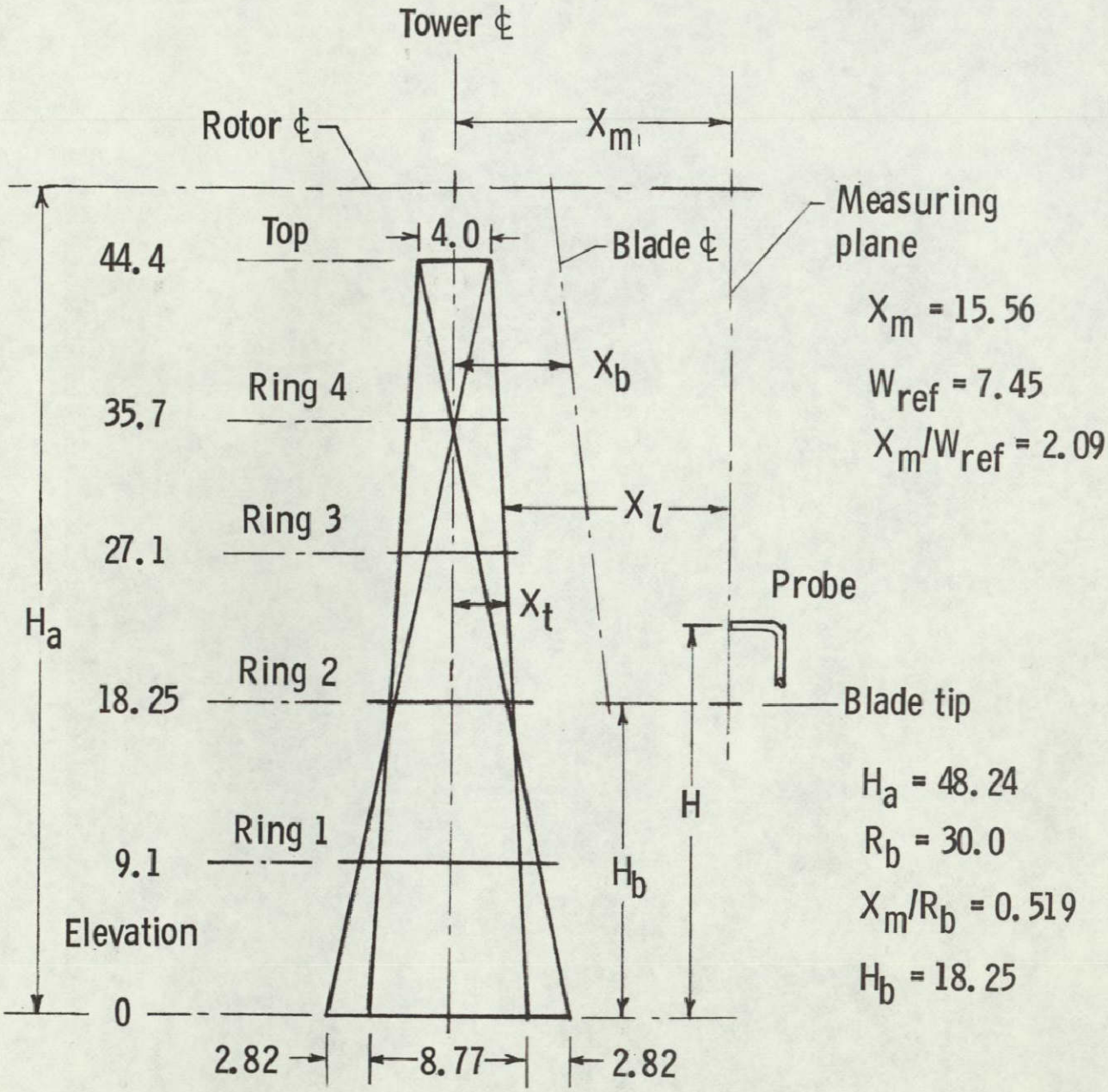

(a) Vertical plane.

Figure 7. - Model and measurement properties. All dimensions in inches.

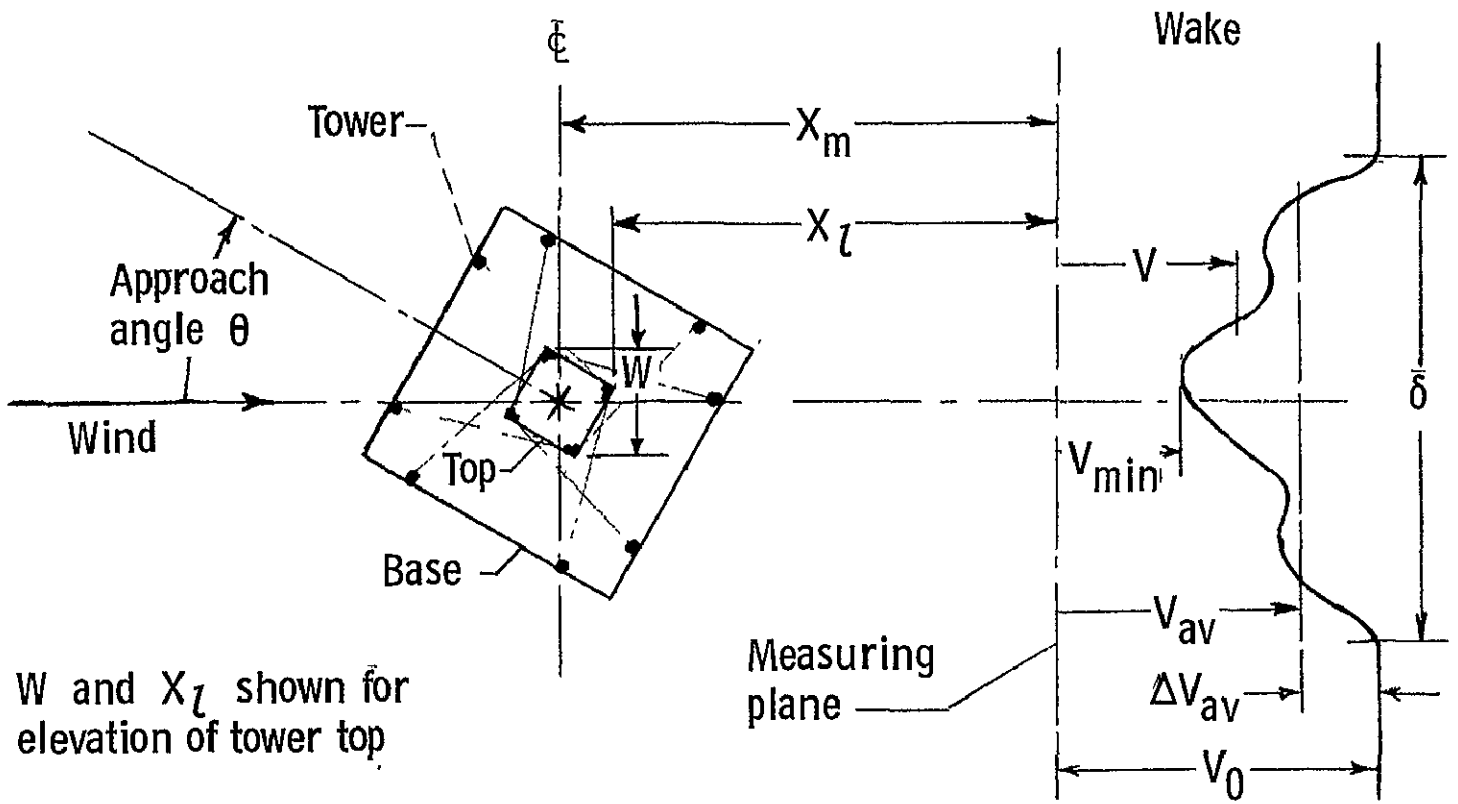

(b) Horizontal plane.

Figure 7. - Concluded.

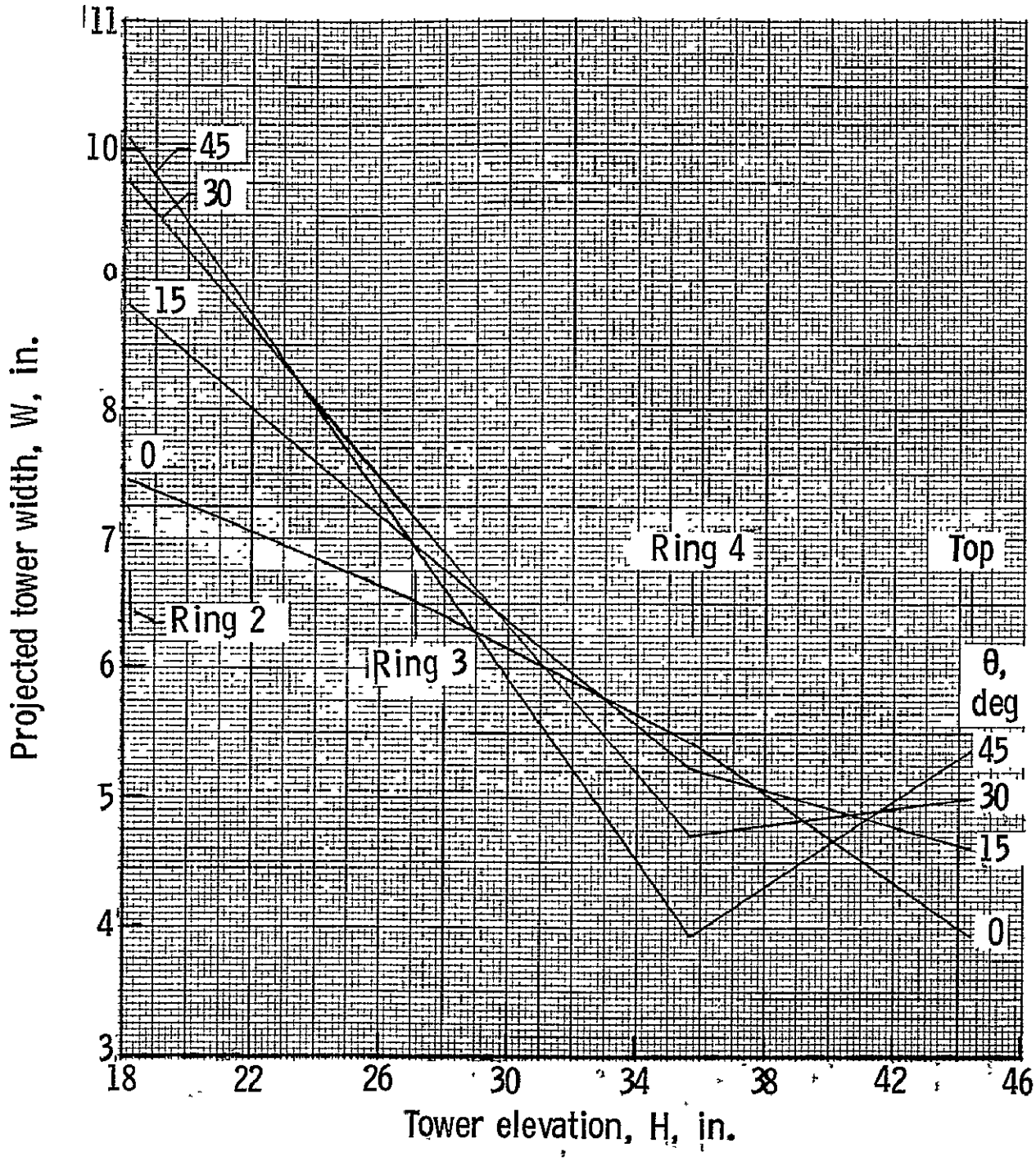

Figure 8. - Variation of projected tower width with height for 1/25-scale 8-leg tower concept.

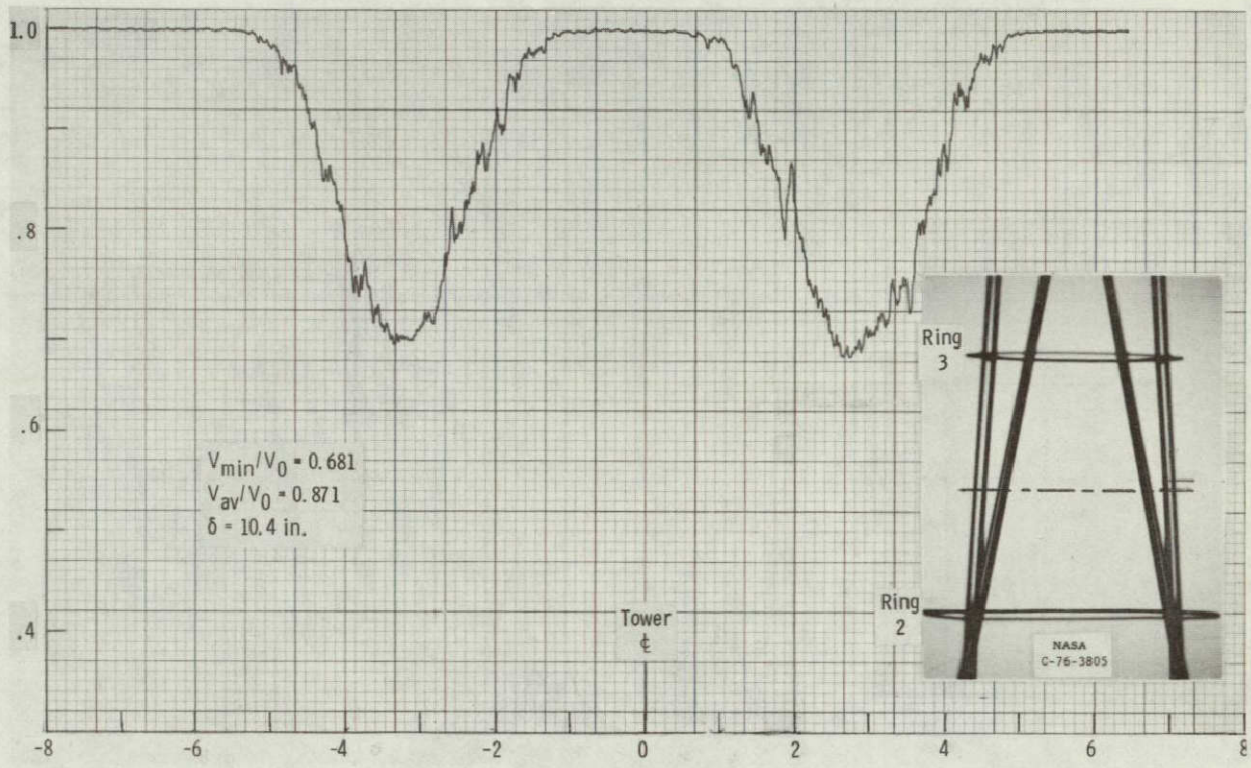

(a) Elevation, H = 22.5 in.

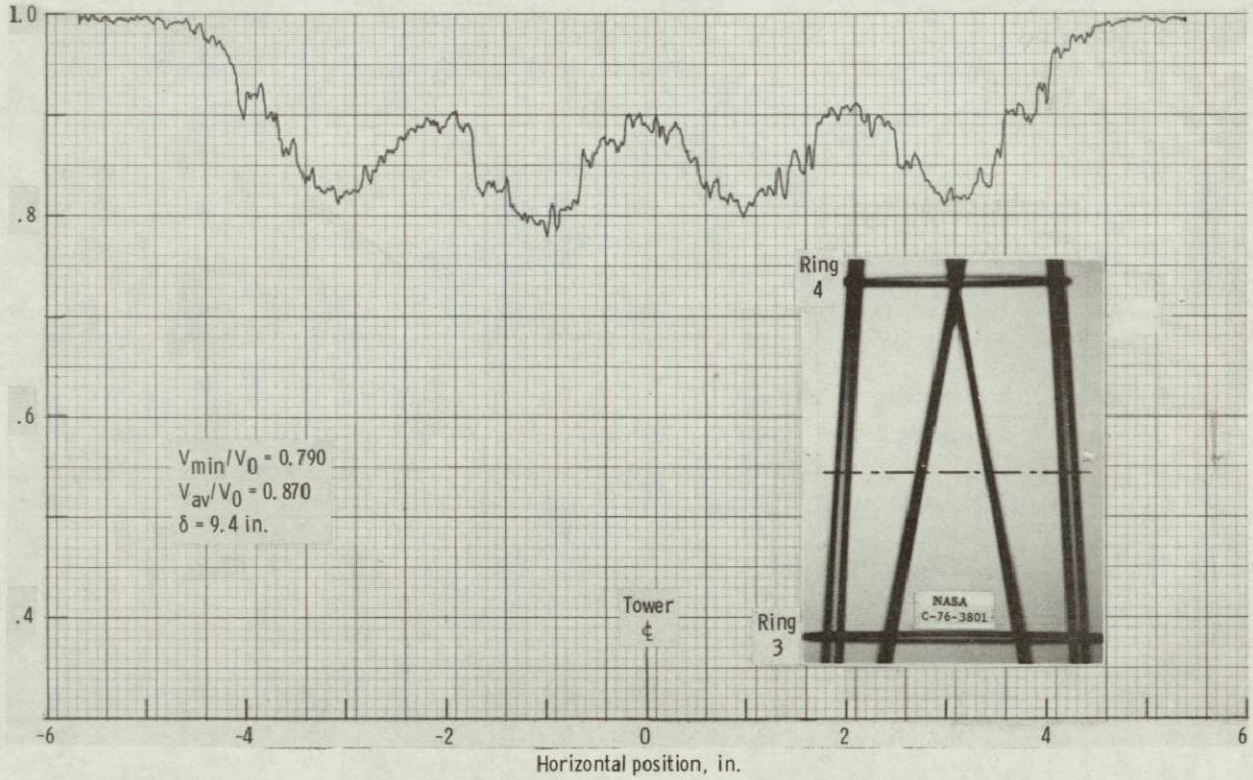

Velocity ratio, V/V_0

Horizontal position, in.

(b) Elevation, H = 31.0 in.

Figure 9. - Wind speed profiles in the wake of the tower model. Wind approach angle, $\theta = 0^0$.

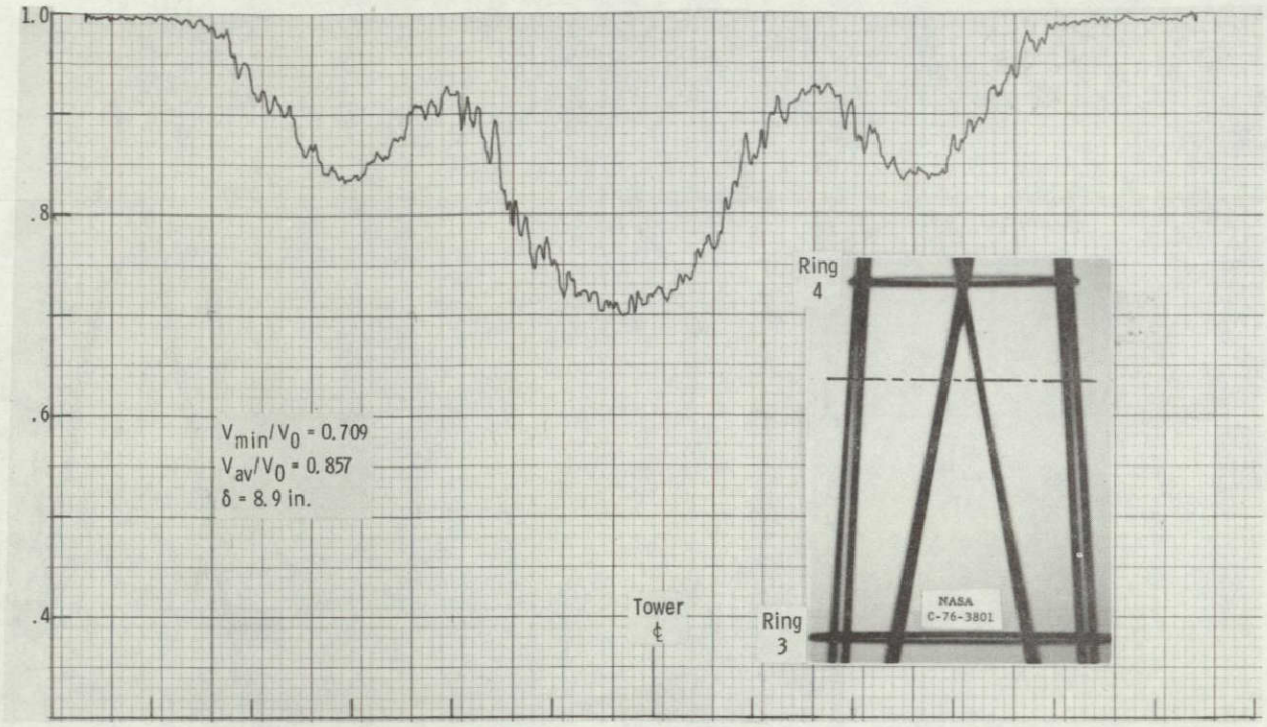

(c) Elevation, H = 33.0 in.

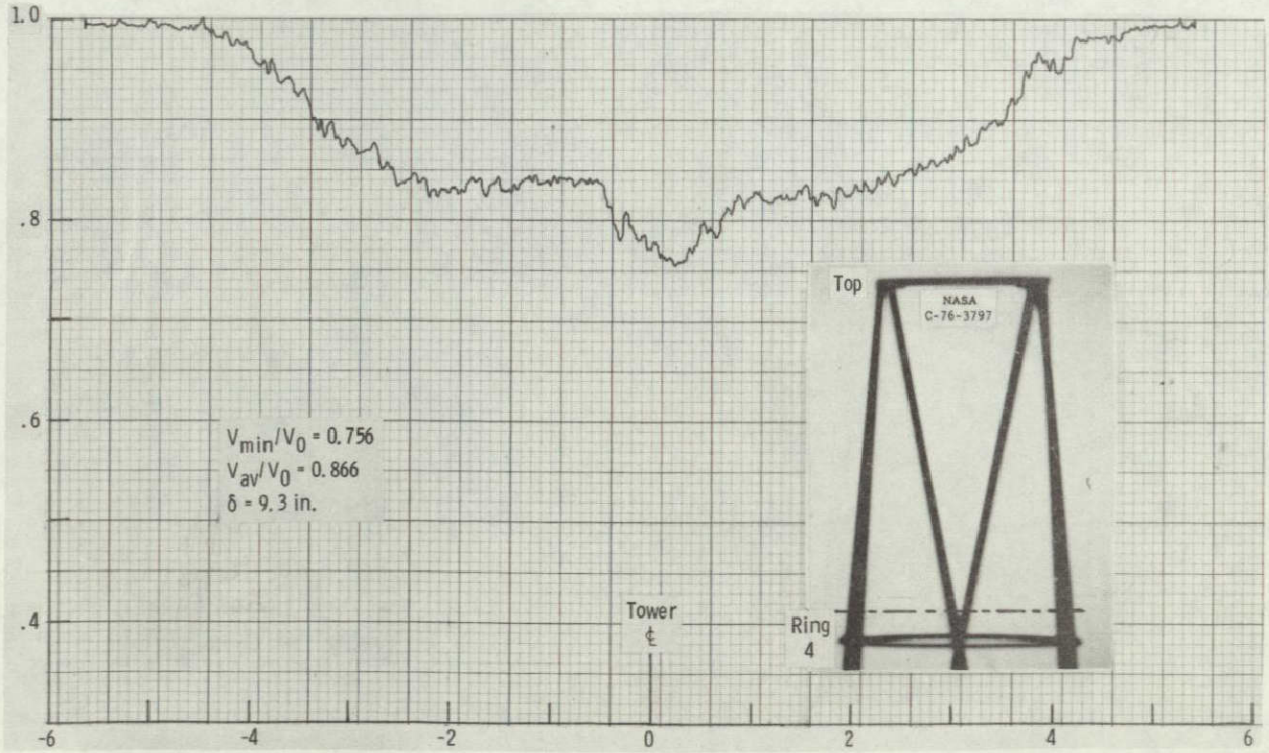

Velocity ratio, V/V_0

Horizontal position, in.

(d) Elevation, H = 36.5 in.

Figure 9. - Concluded.

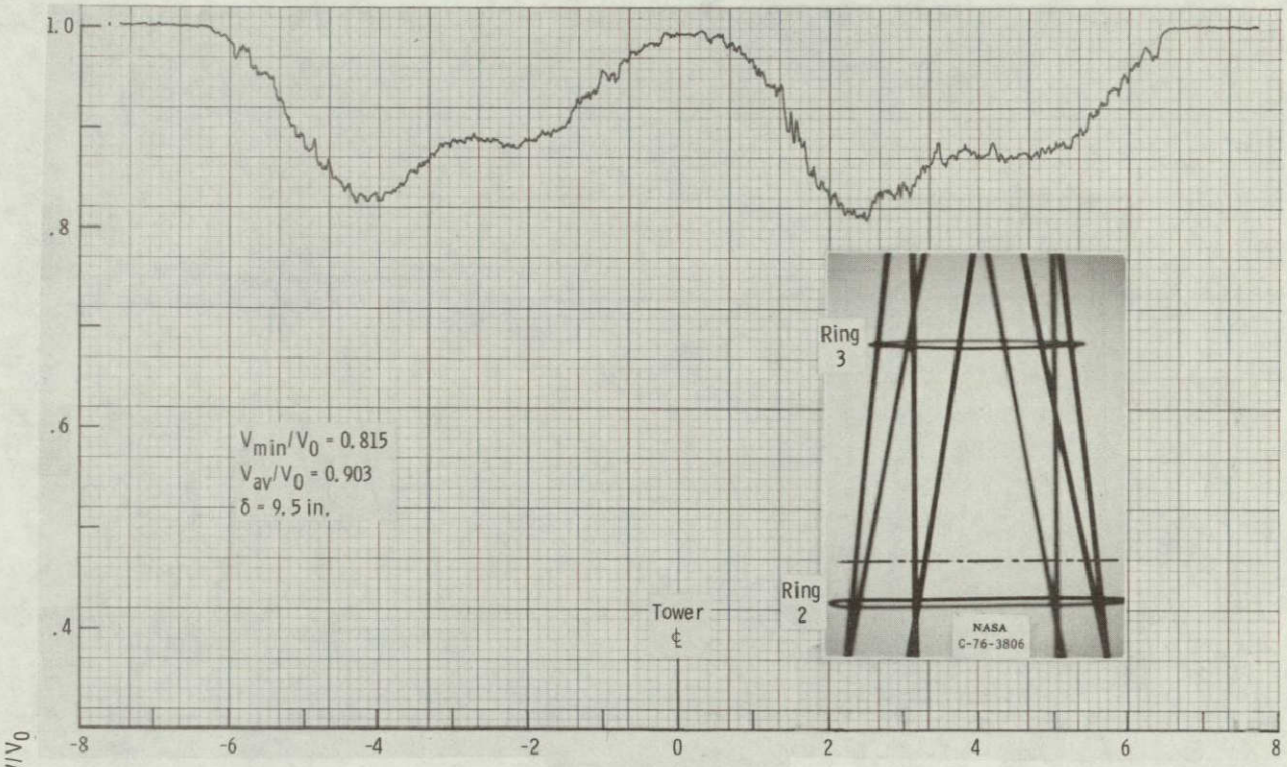

(a) Elevation, H = 19.5 in.

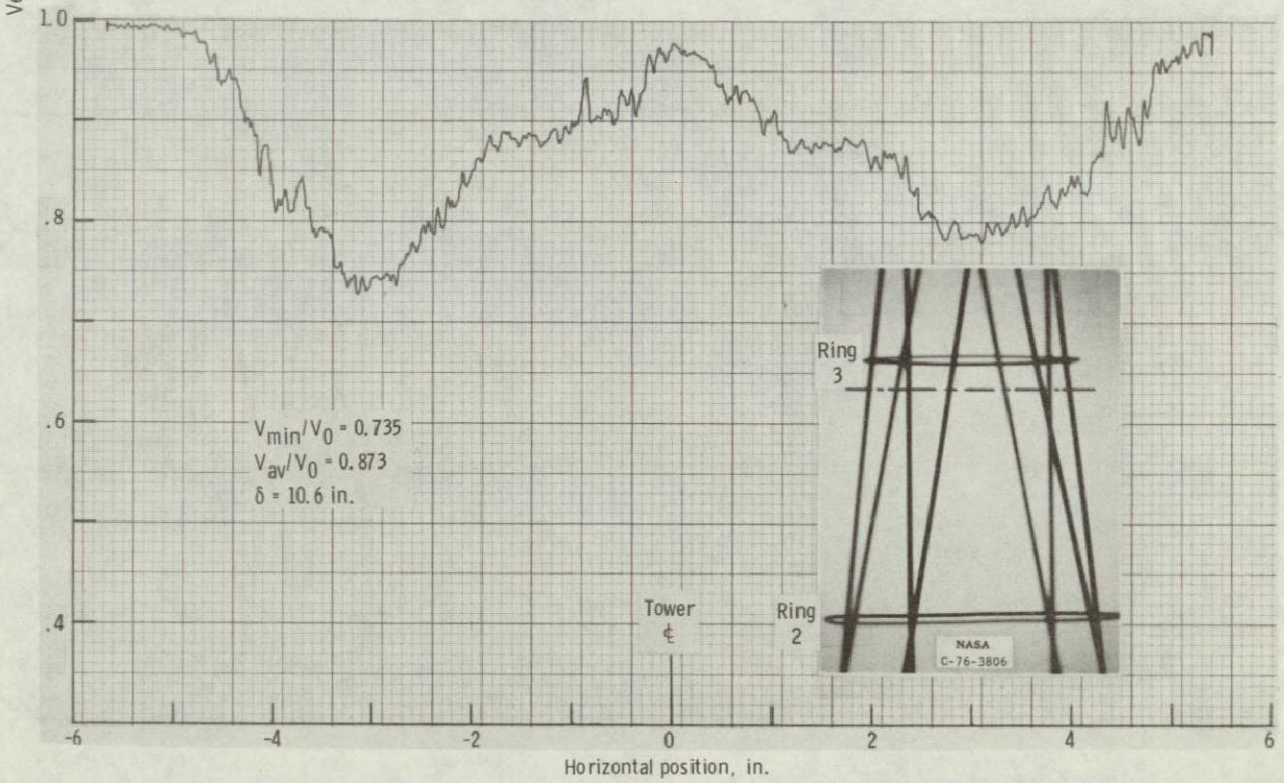

Velocity ratio, V/V_0

Horizontal position, in.

(b) Elevation, H = 26.0 in.

Figure 10. - Wind speed profiles in the wake of the 8-leg tower model at wind approach angle, $\theta = 15^0$.

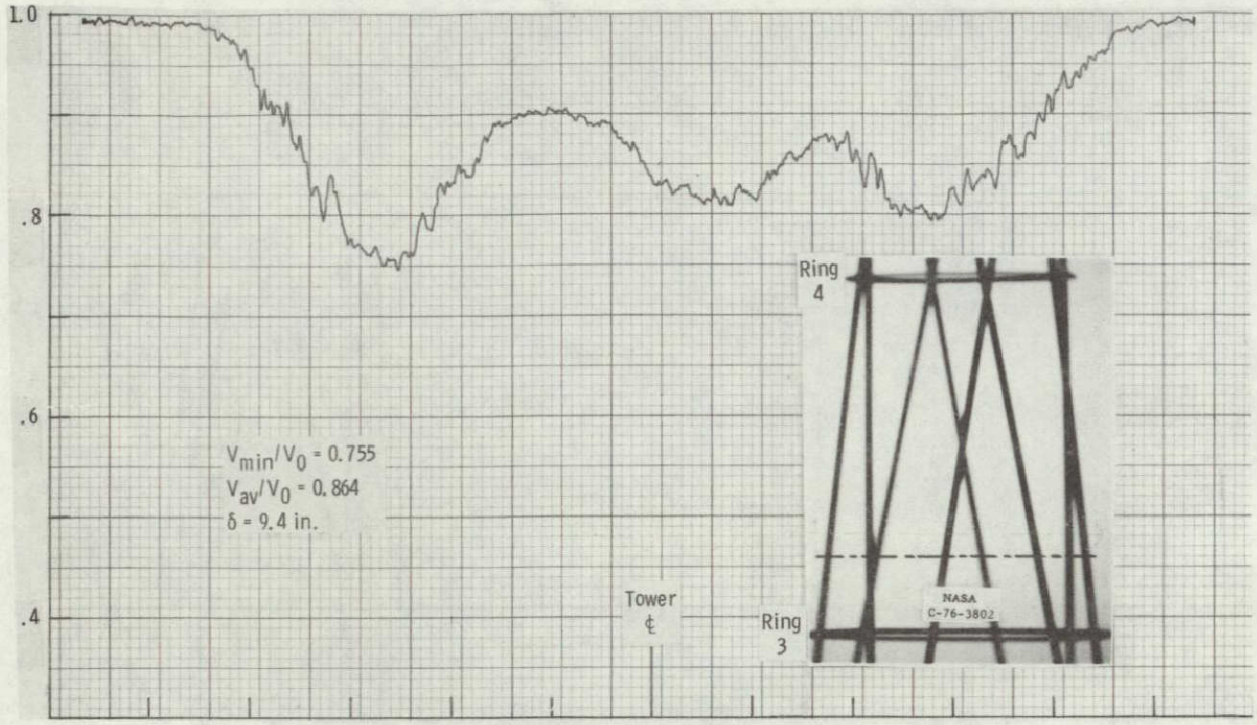

(c) Elevation, H = 29.0 in.

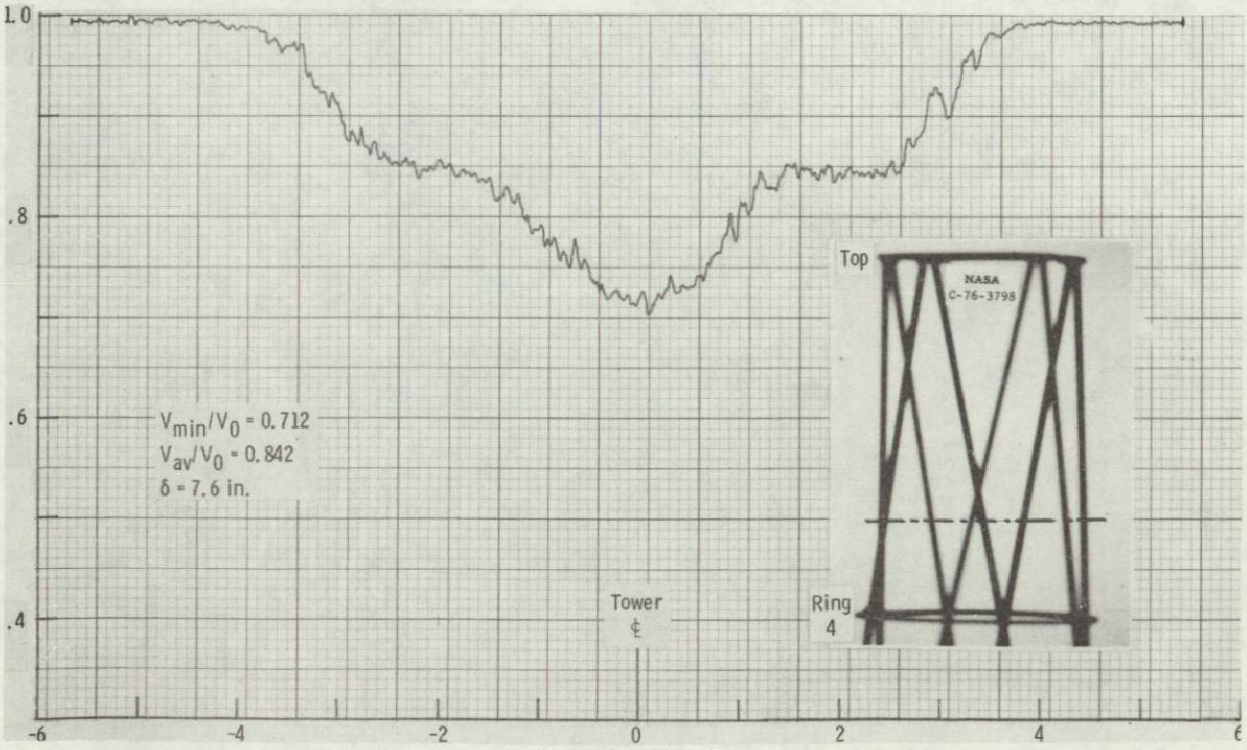

(d) Elevation, H = 38.0 in.

Figure 10. - Concluded.

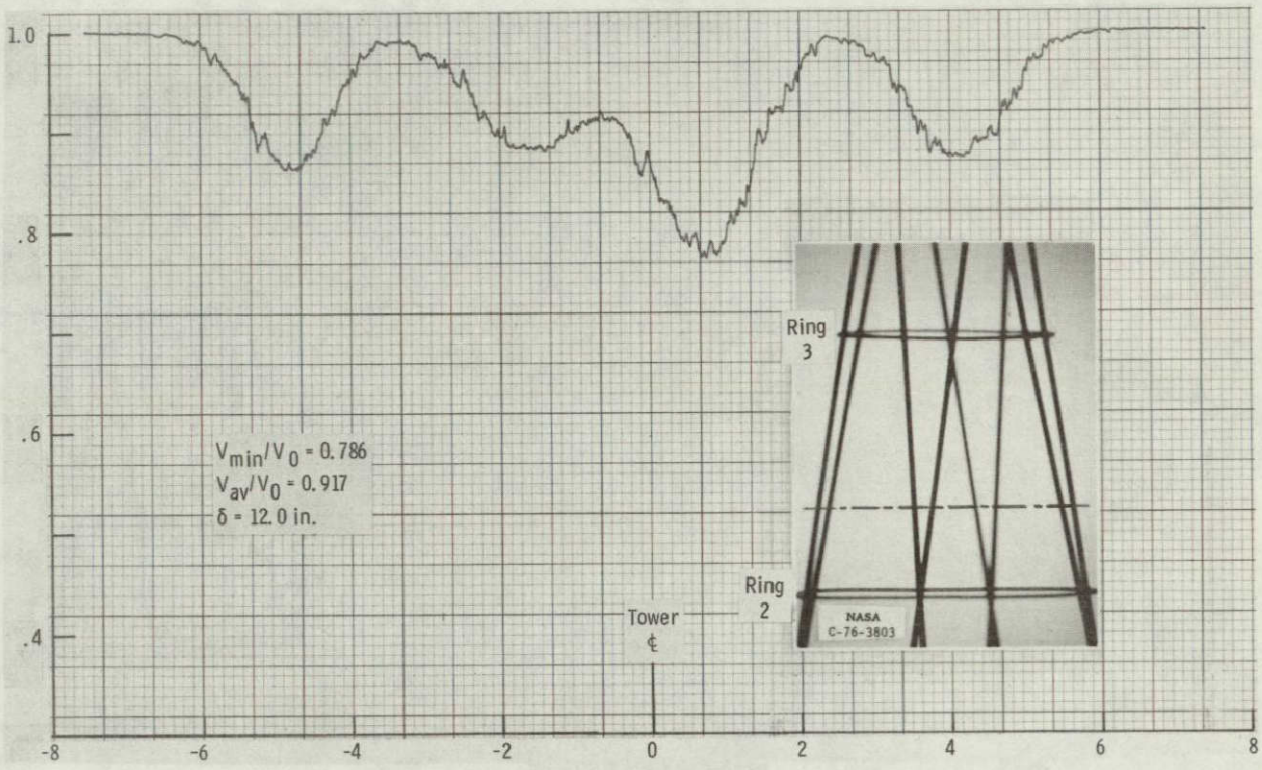

(a) Elevation, H = 21.0 in.

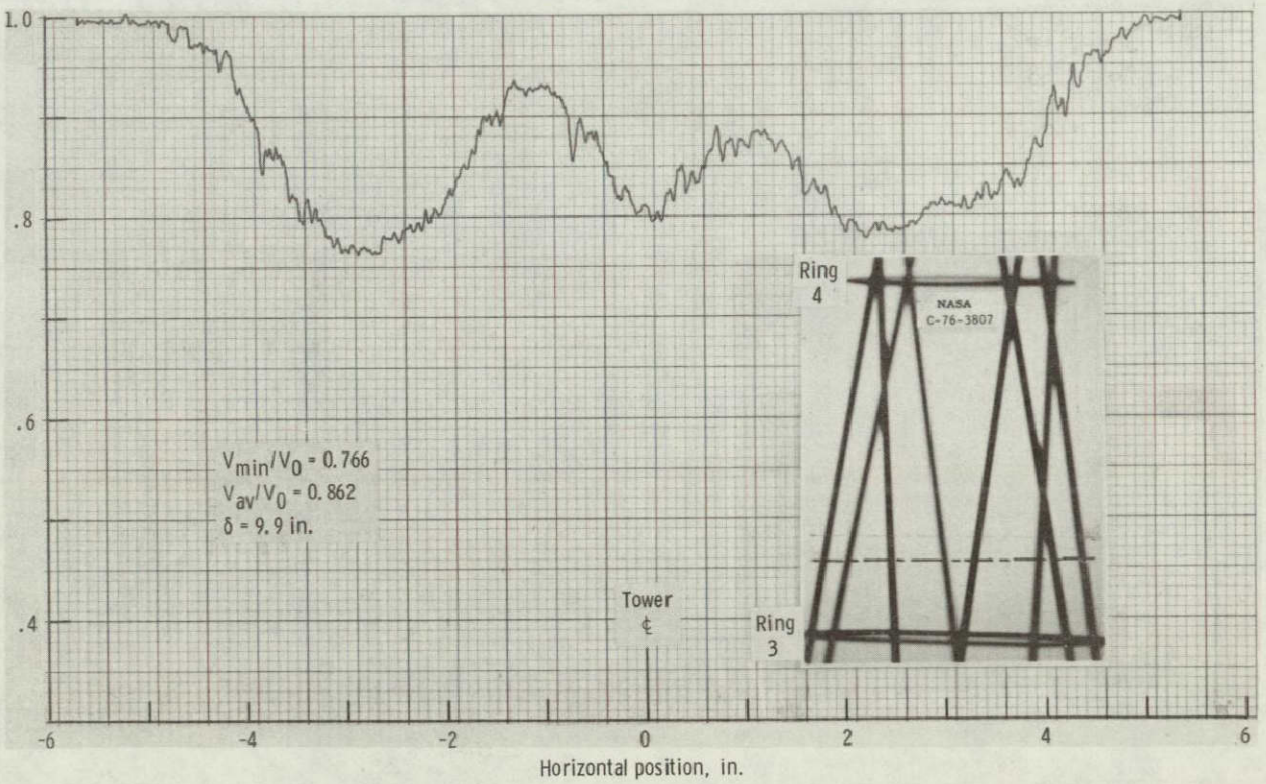

Velocity ratio, V/V_0

Horizontal position, in.

(b) Elevation, H = 29.0 in.

Figure 11. - Wind speed profiles in wake of the 8-leg tower model at wind approach angle, $\theta = 30^0$.

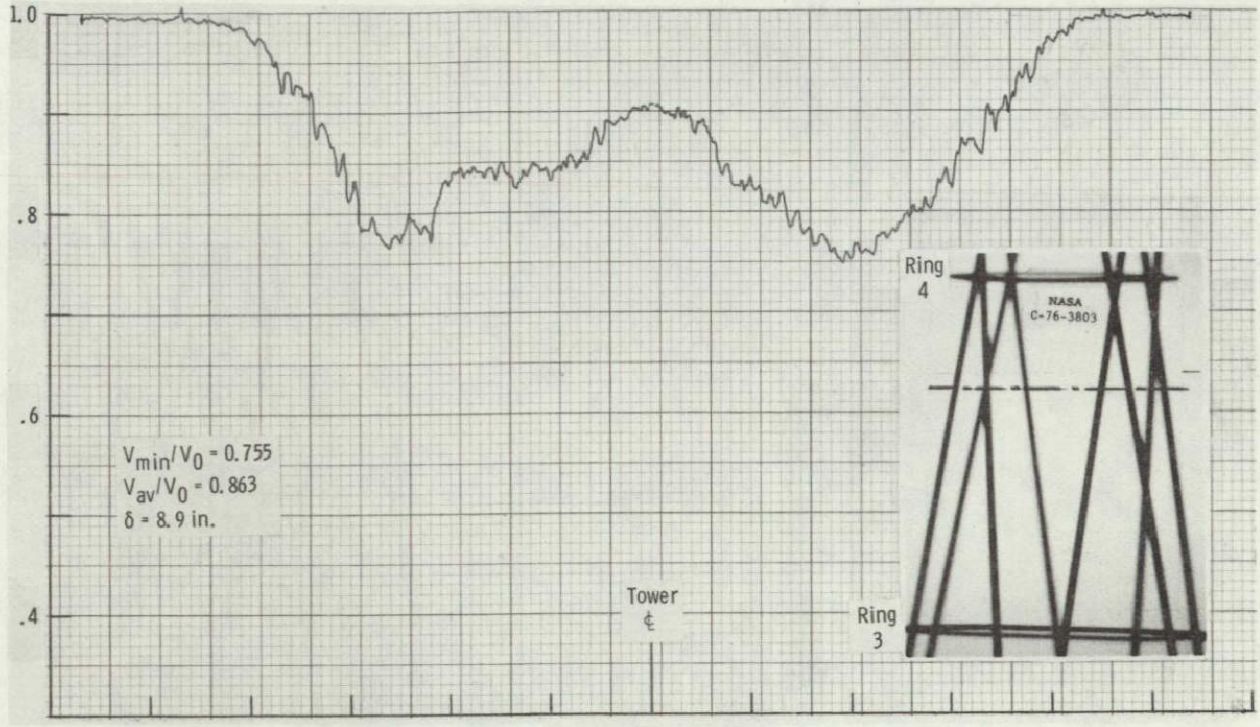

(c) Elevation, H = 33.0 in.

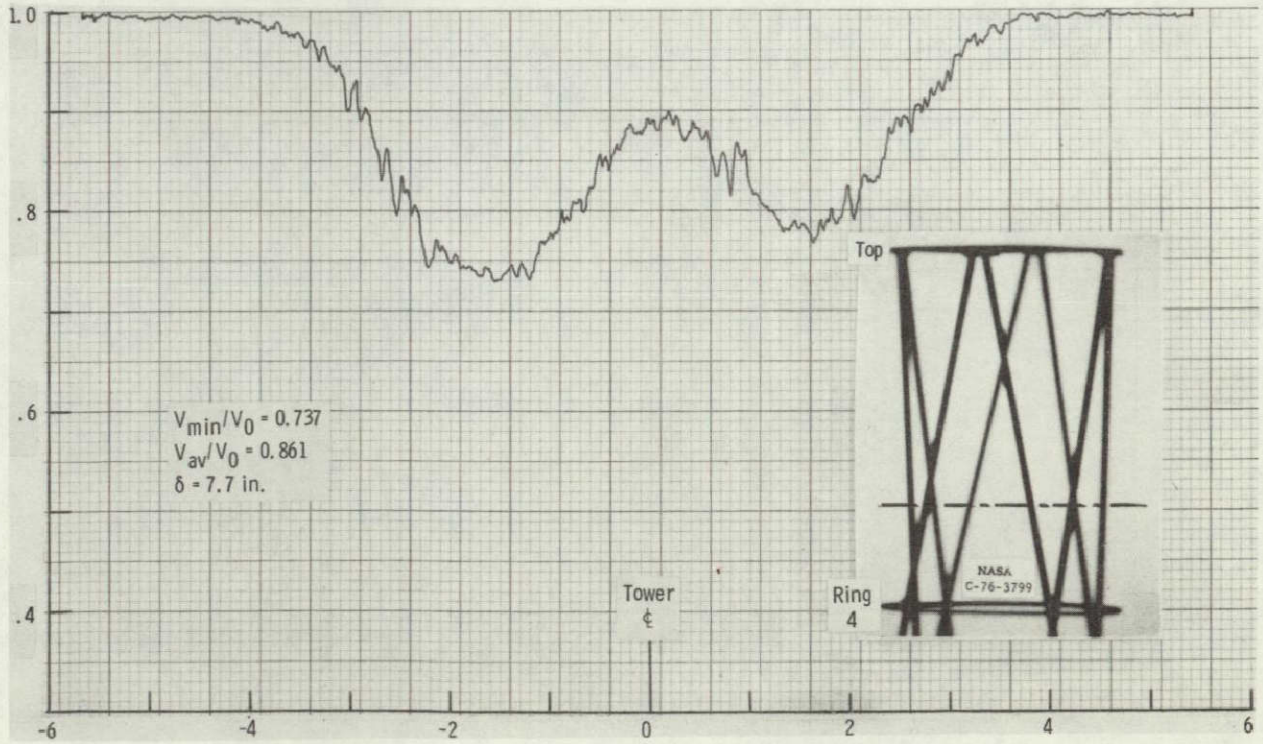

Velocity ratio, V/V_0

Horizontal position, in.

(d) Elevation, H = 38.0 in.

Figure 11. - Concluded.

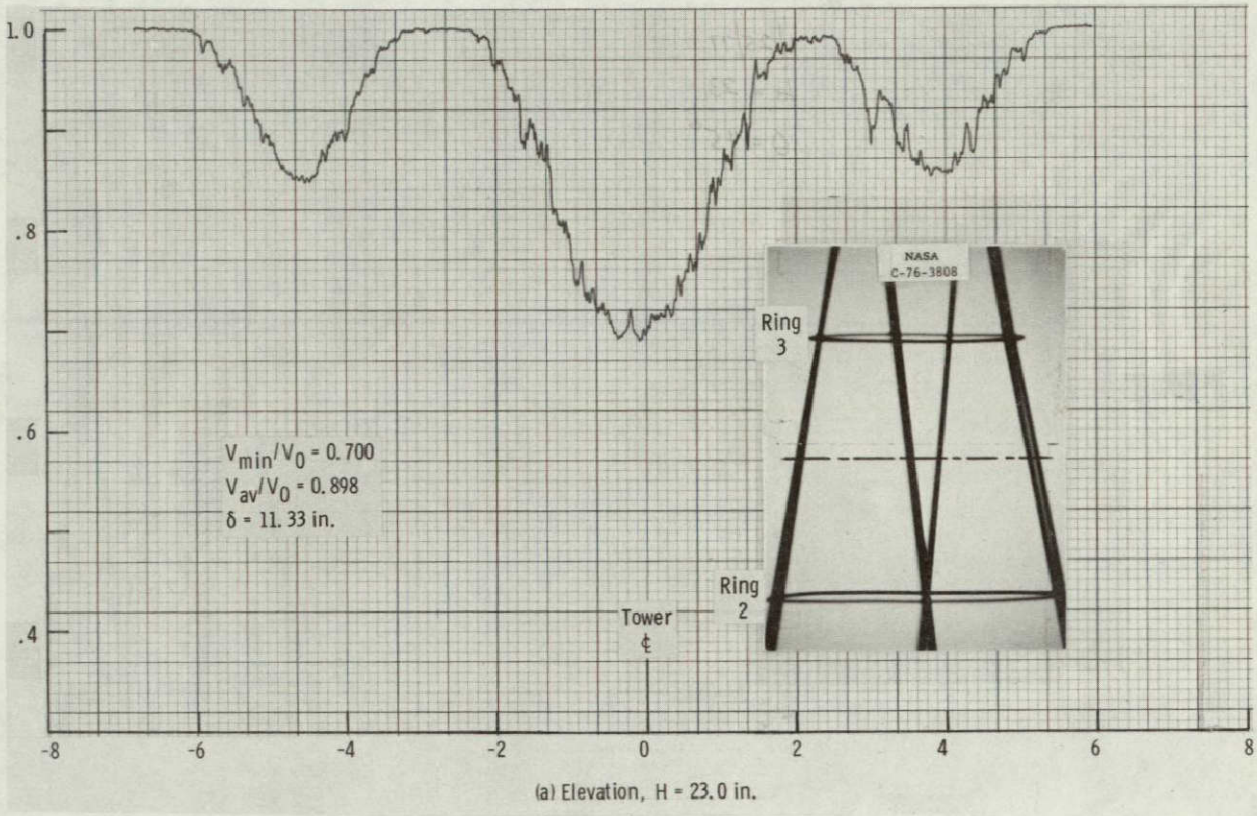

(a) Elevation, H = 23.0 in.

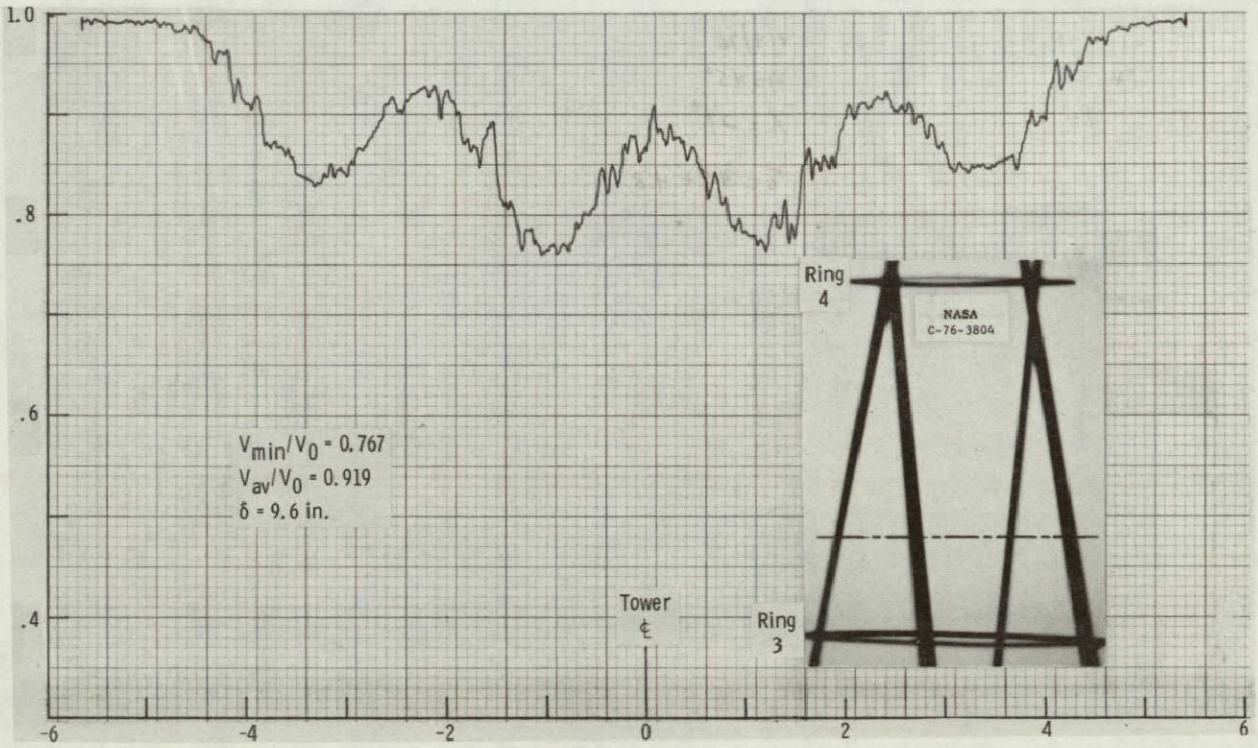

(b) Elevation, H = 29.0 in.

Figure 12. - Wind speed profiles in the wake of the 8-leg tower model at wind approach angle, $\theta = 45^{\circ}$.

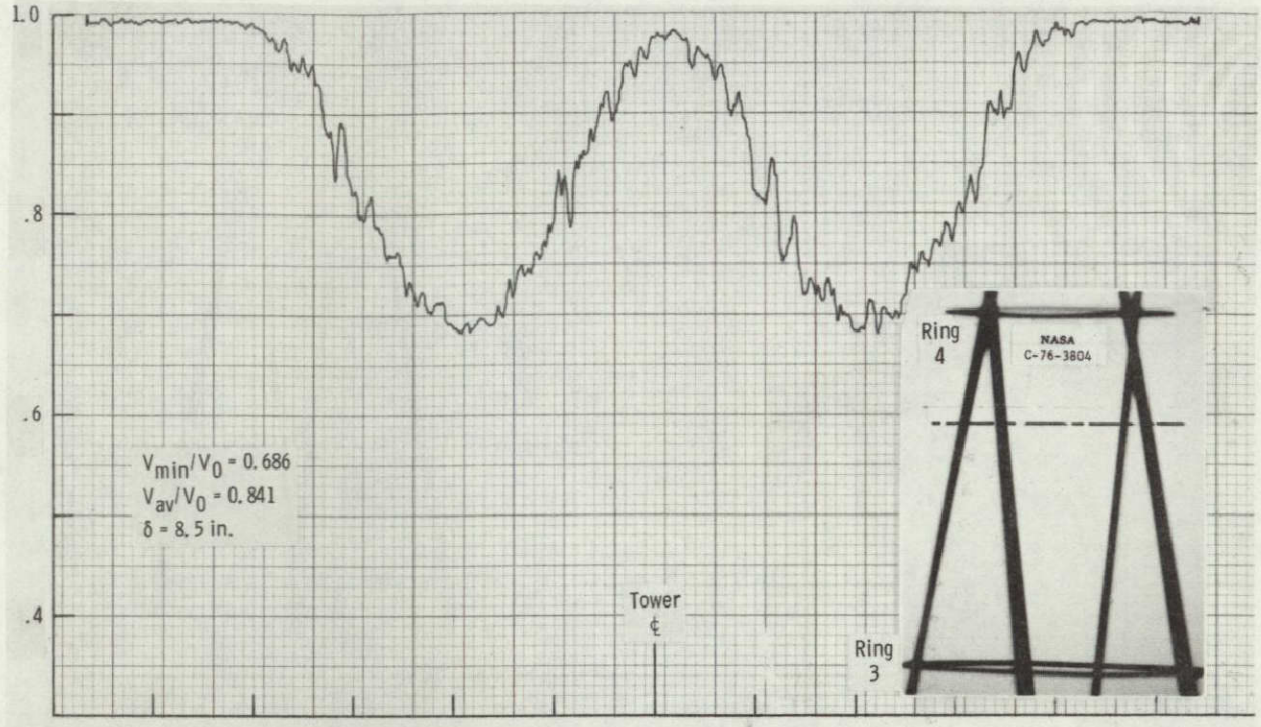

(c) Elevation, H = 33.0 in.

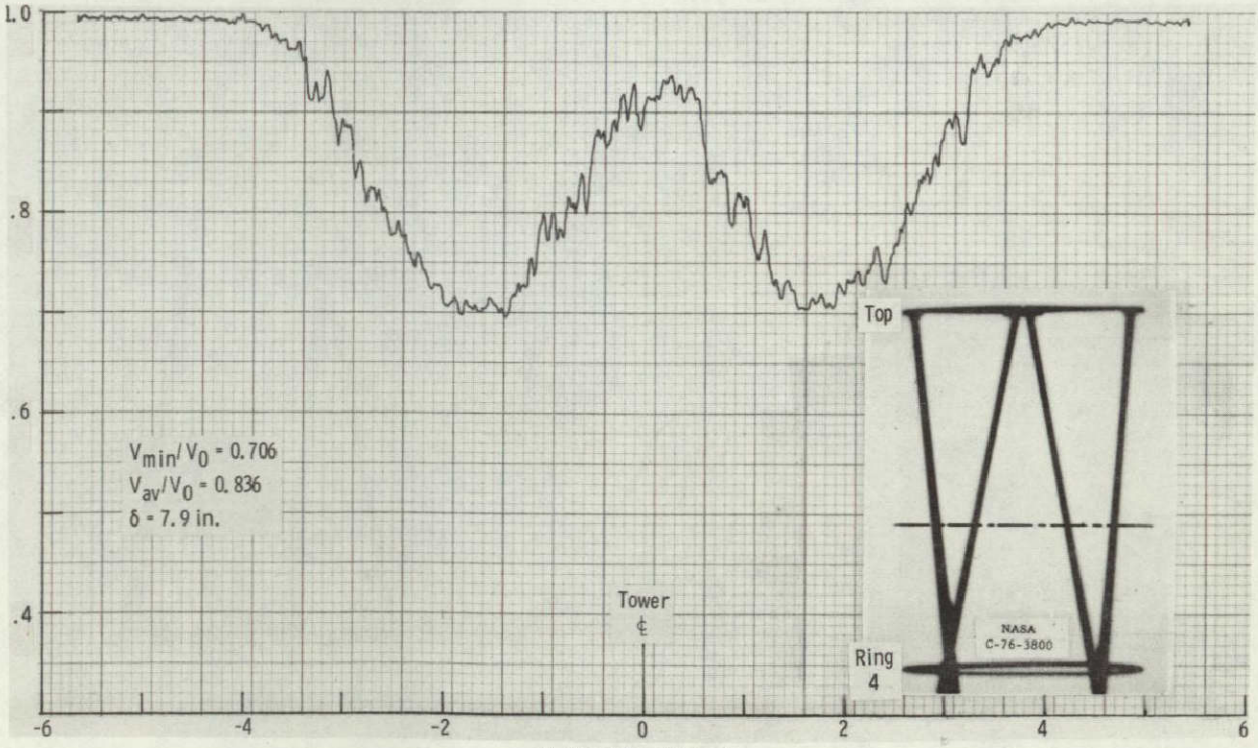

Velocity ratio, V/V_0

Horizontal position, in.

(d) Elevation, H = 39.0 in.

Figure 12. - Concluded.

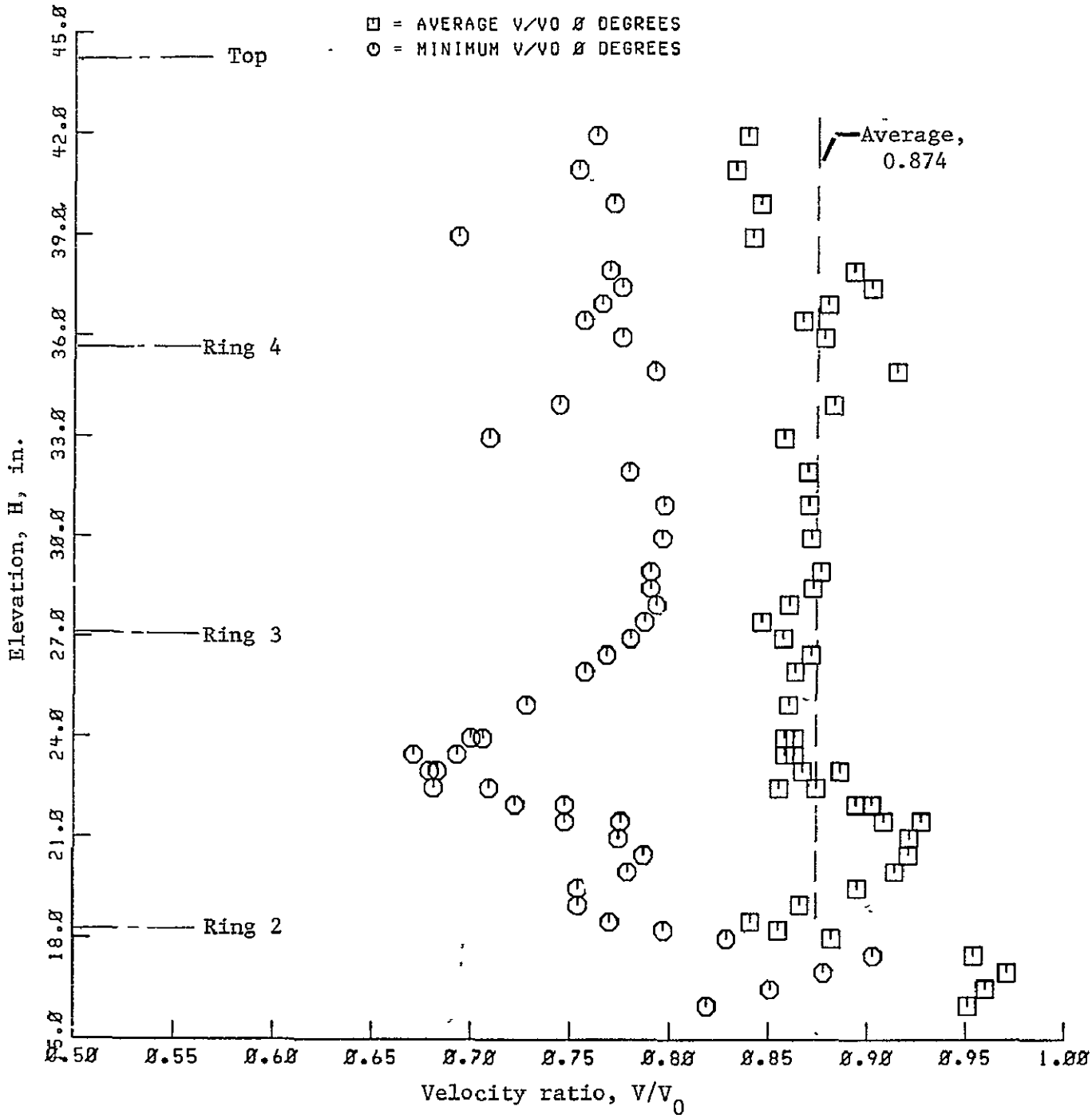

(a) Wind approach angle, $\theta = 0°$.

Figure 13. - Minimum and average velocity ratios in the wake of the 8-leg tower model.

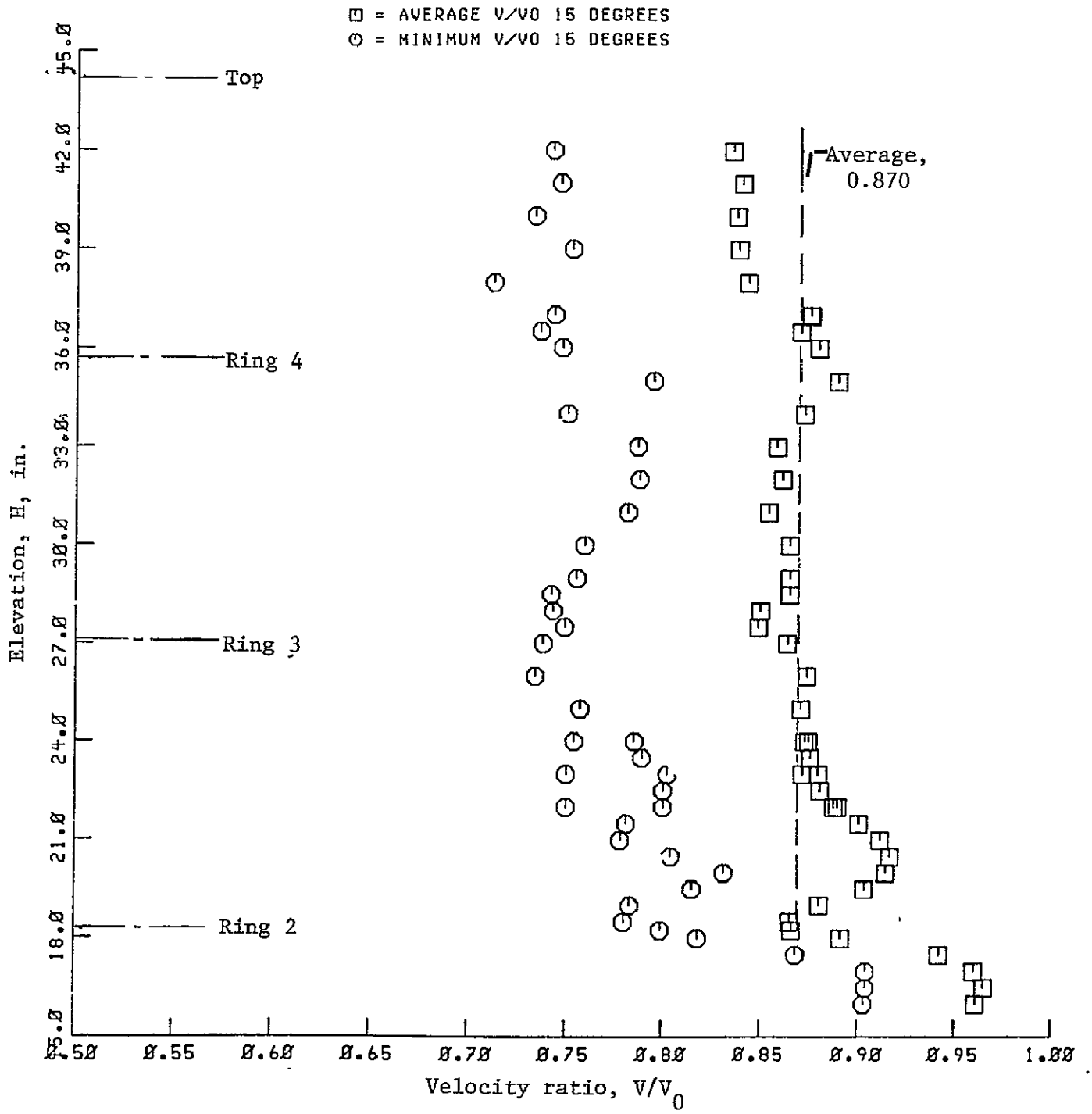

(b) Wind approach angle, $\theta = 15°$.

Figure 13. - Continued.

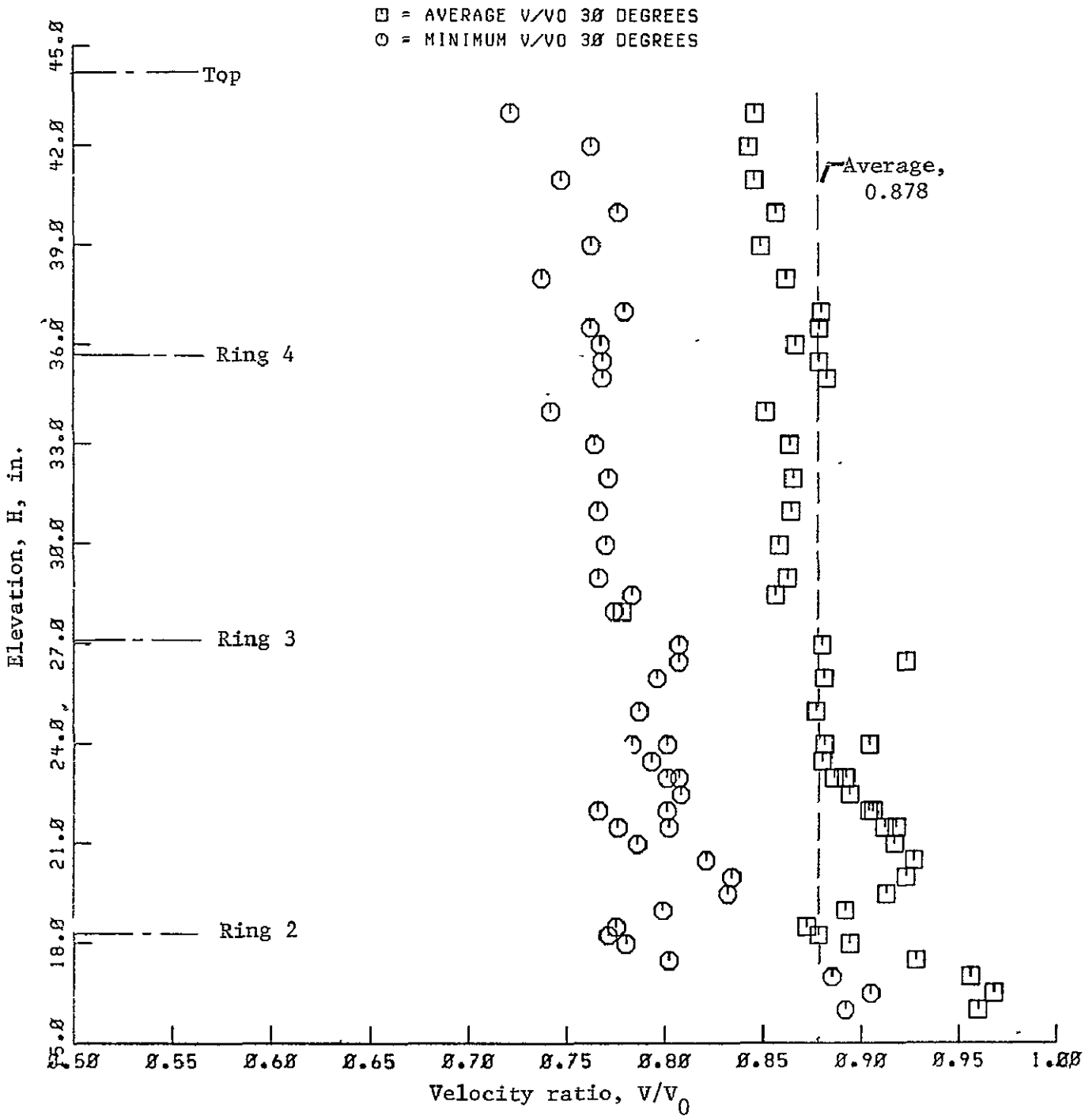

(c) Wind approach angle, θ = 30°.

Figure 13. - Continued.

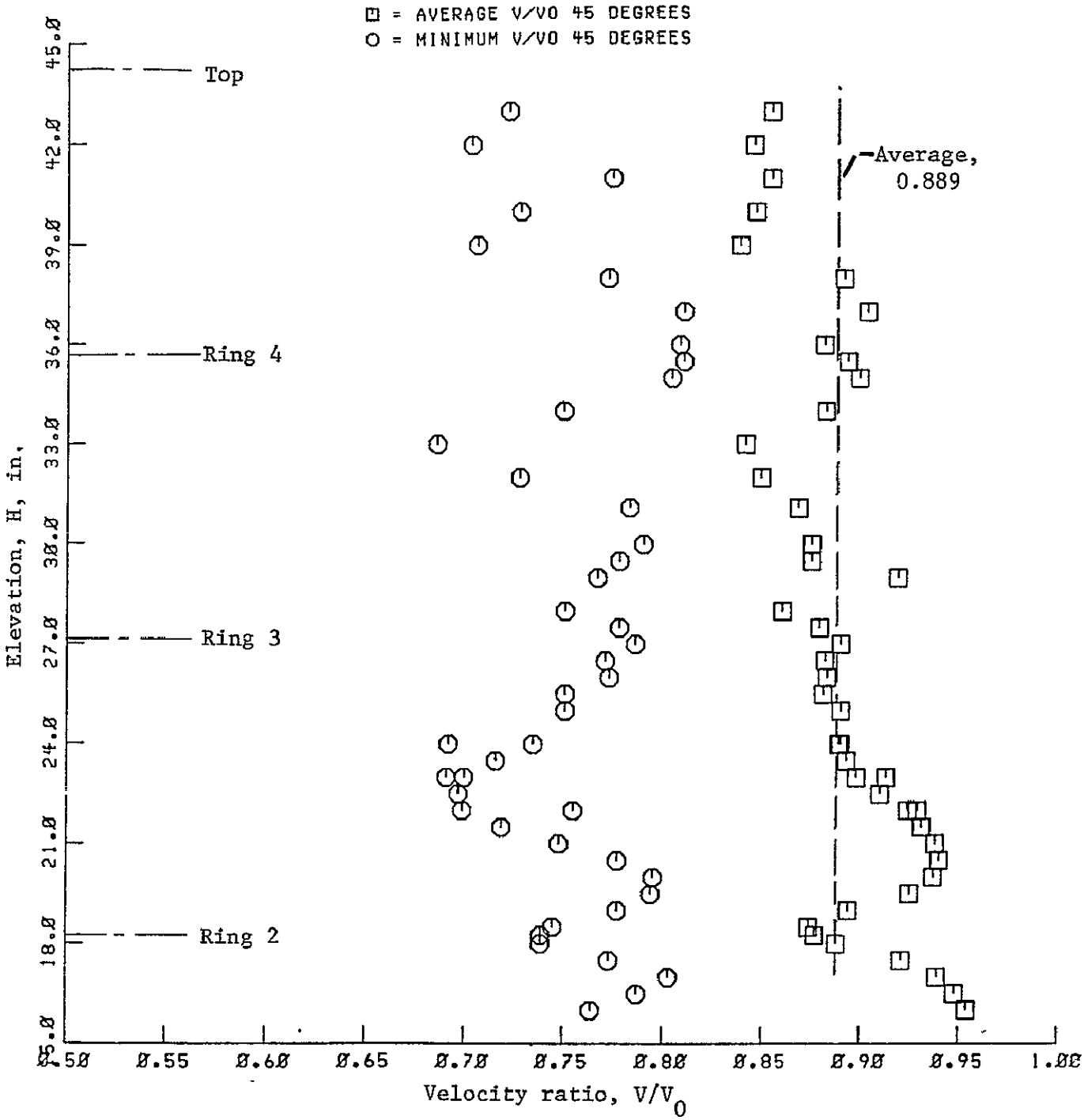

(d) Wind approach angle, $\theta = 45°$.

Figure 13. - Concluded.

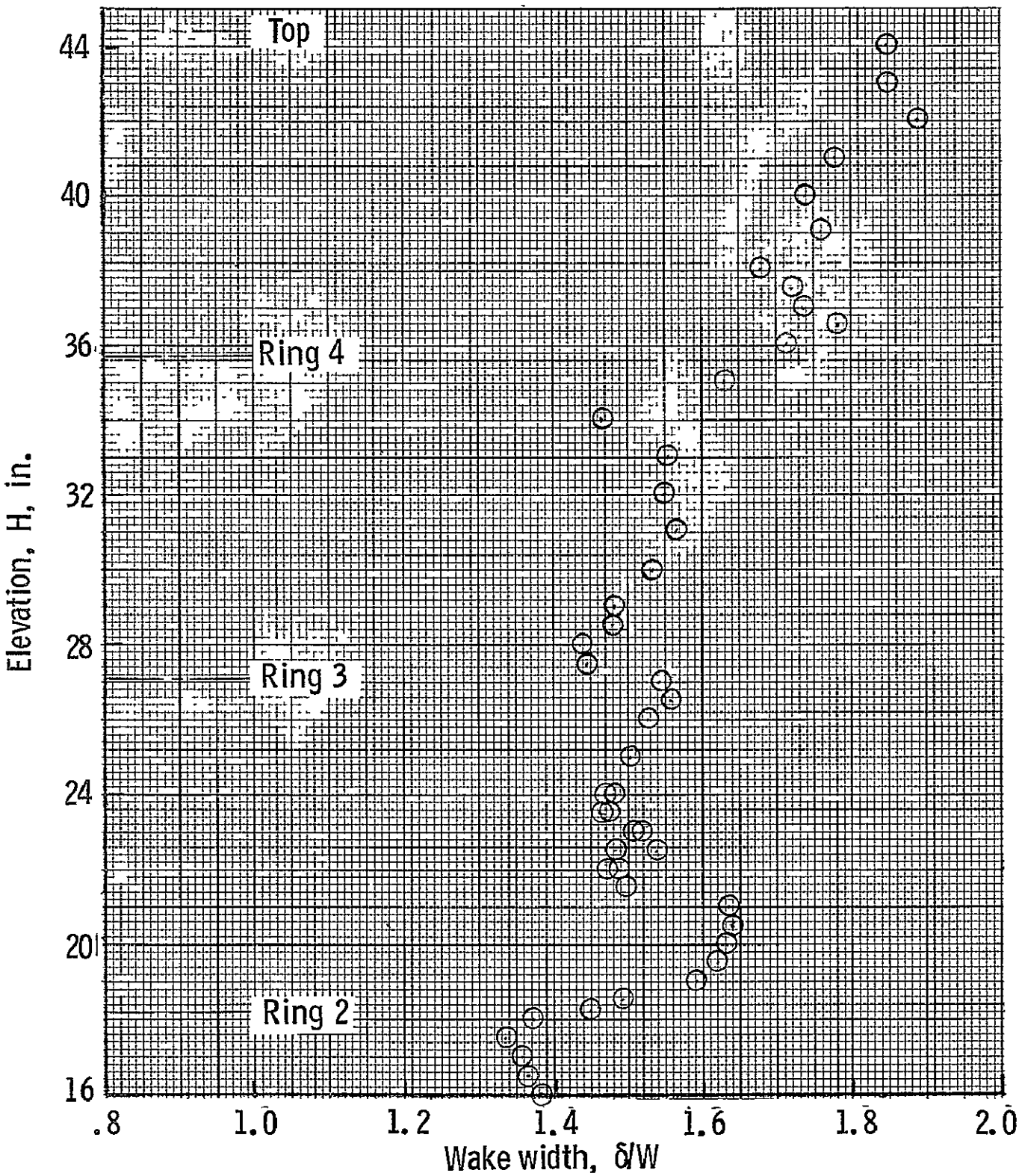

(a) Wind approach angle, θ = 0 deg.

Figure 14. - Ratio of wake width to projected tower width for 8-leg tower model.

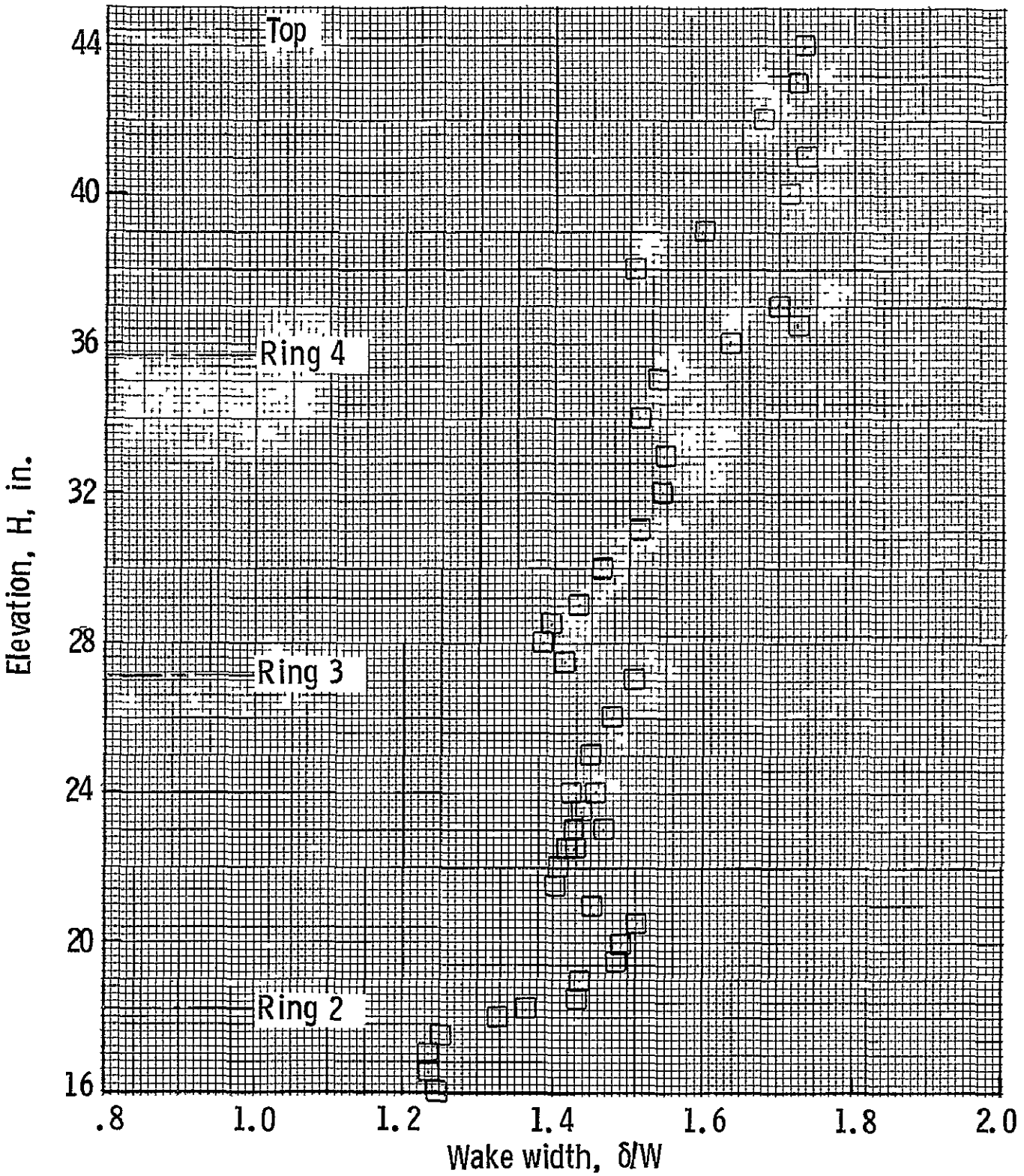

(b) Wind approach angle, $\theta = 15$ deg.

Figure 14. - Continued.

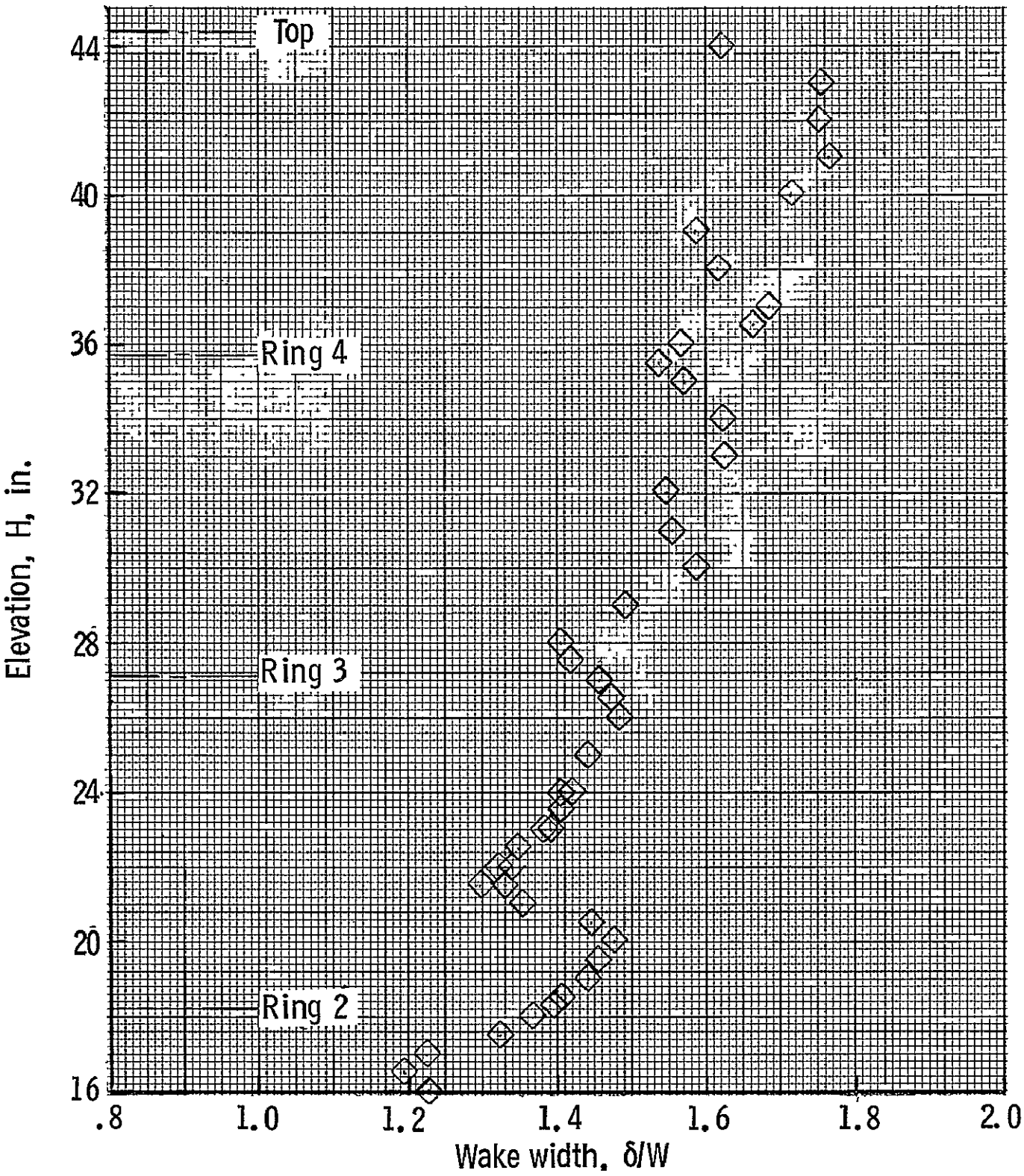

(c) Wind approach angle, θ = 30 deg.

Figure 14. - Continued.

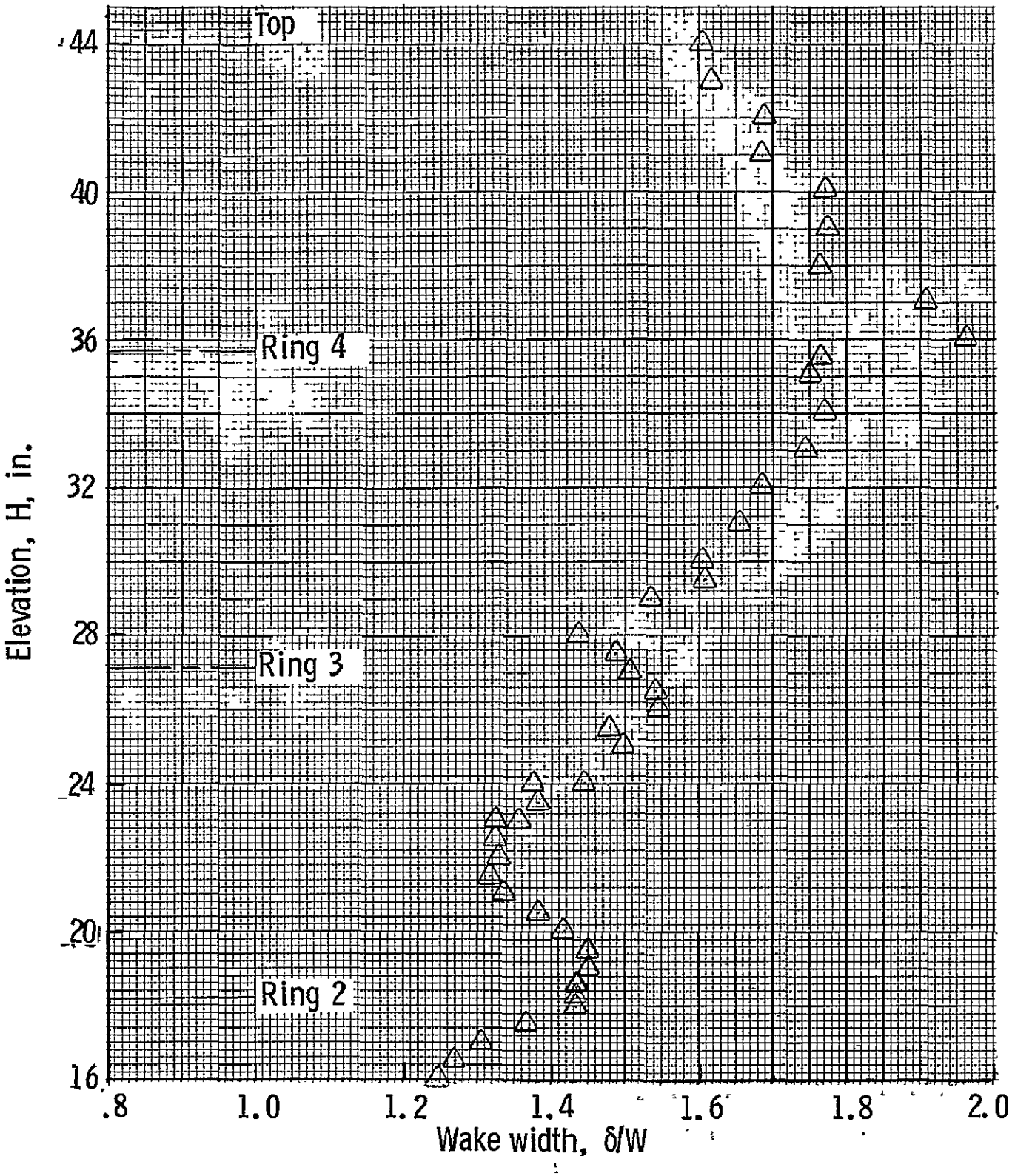

(d) Wind approach angle, $\theta = 45^0$ deg.

Figure 14. - Concluded.

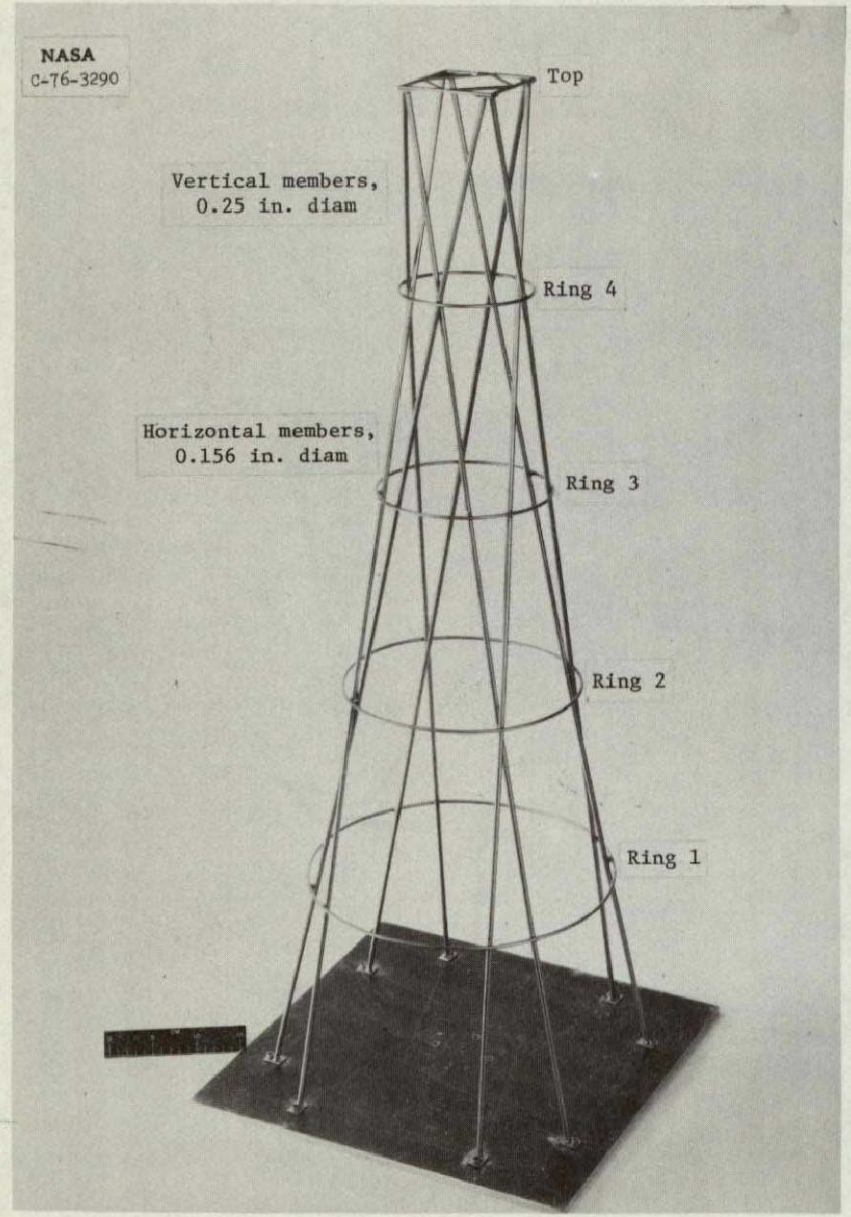

(a) 8-Leg tower model; 1/25th scale.

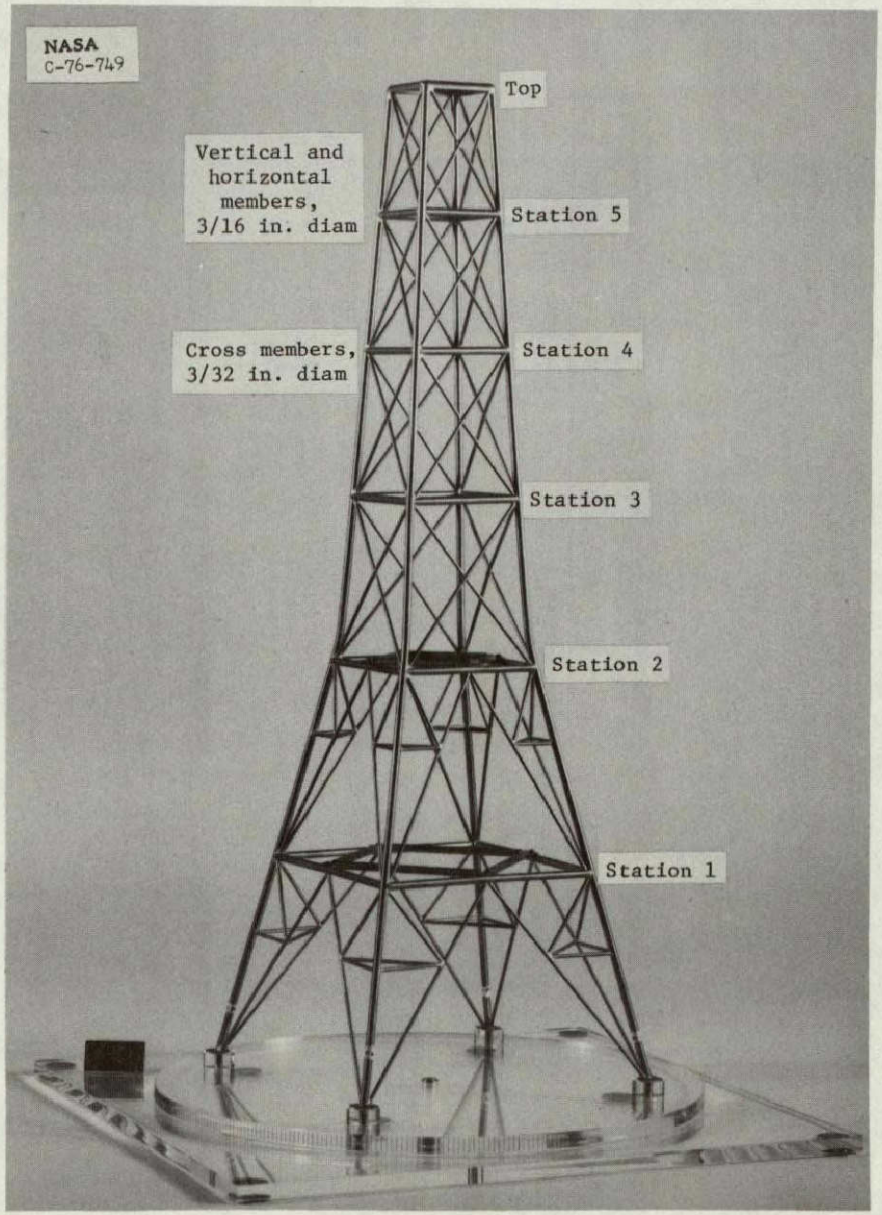

(b) 4-Leg tower model; 1/48th scale.

Figure 15. - Comparison of 8-leg and 4-leg tower models with tubular members.

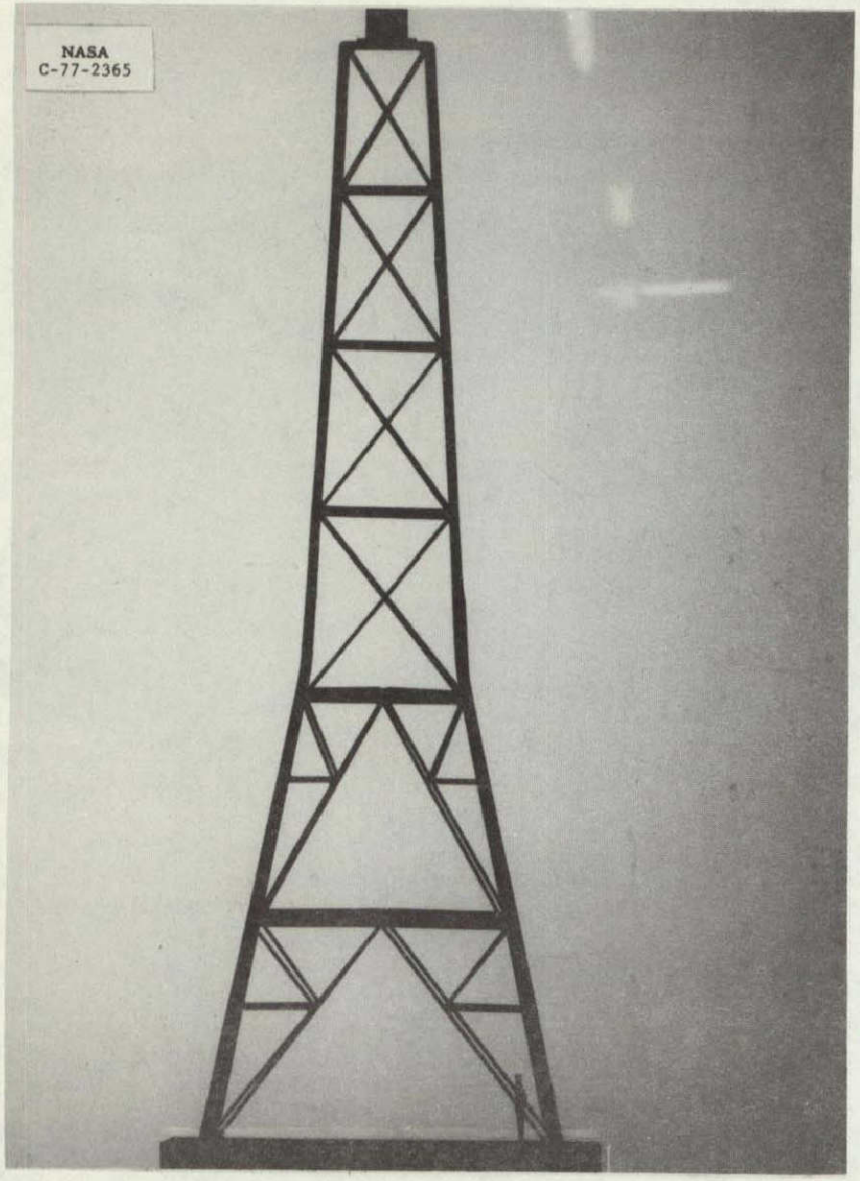

(a) Wind approach angle, $\theta = 0°$.

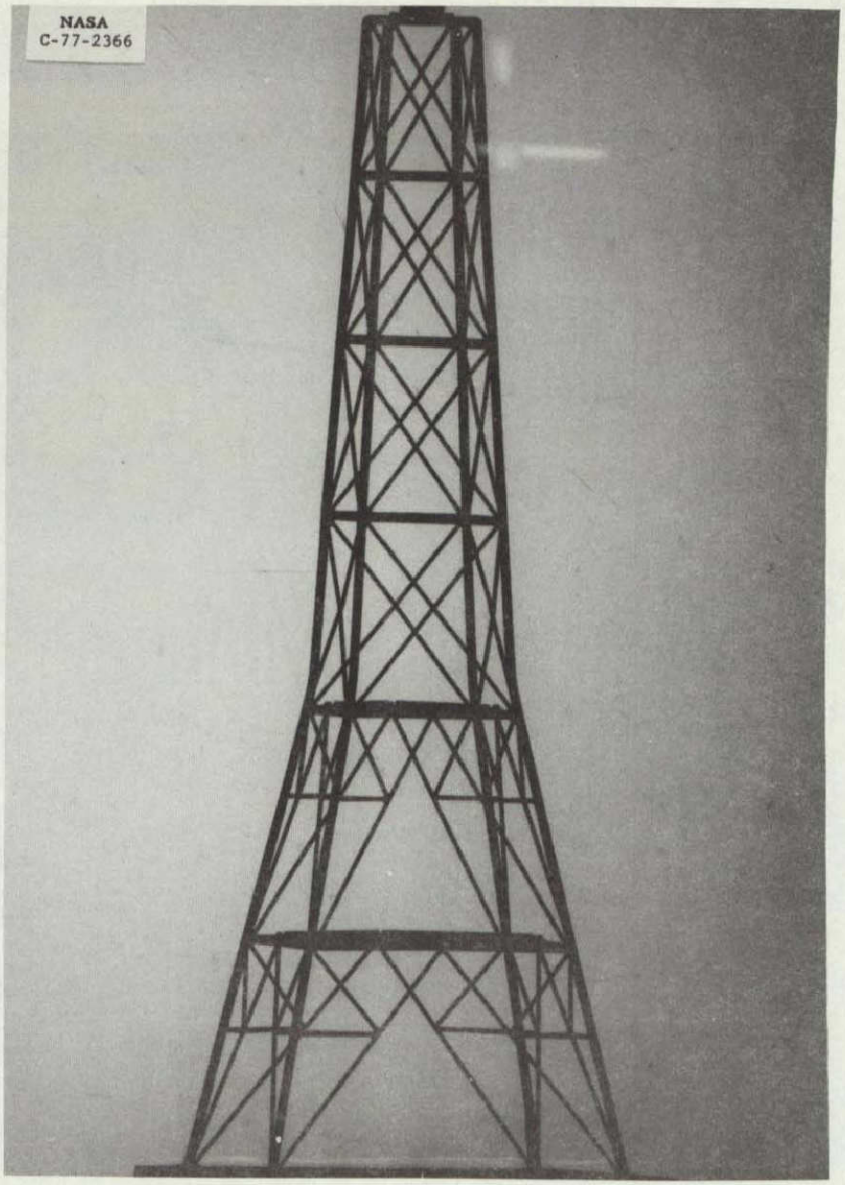

(b) Wind approach angle, $\theta = 15°$.

Figure 16. - Shadow photographs of 4-leg, tubular-element tower model of reference 5.

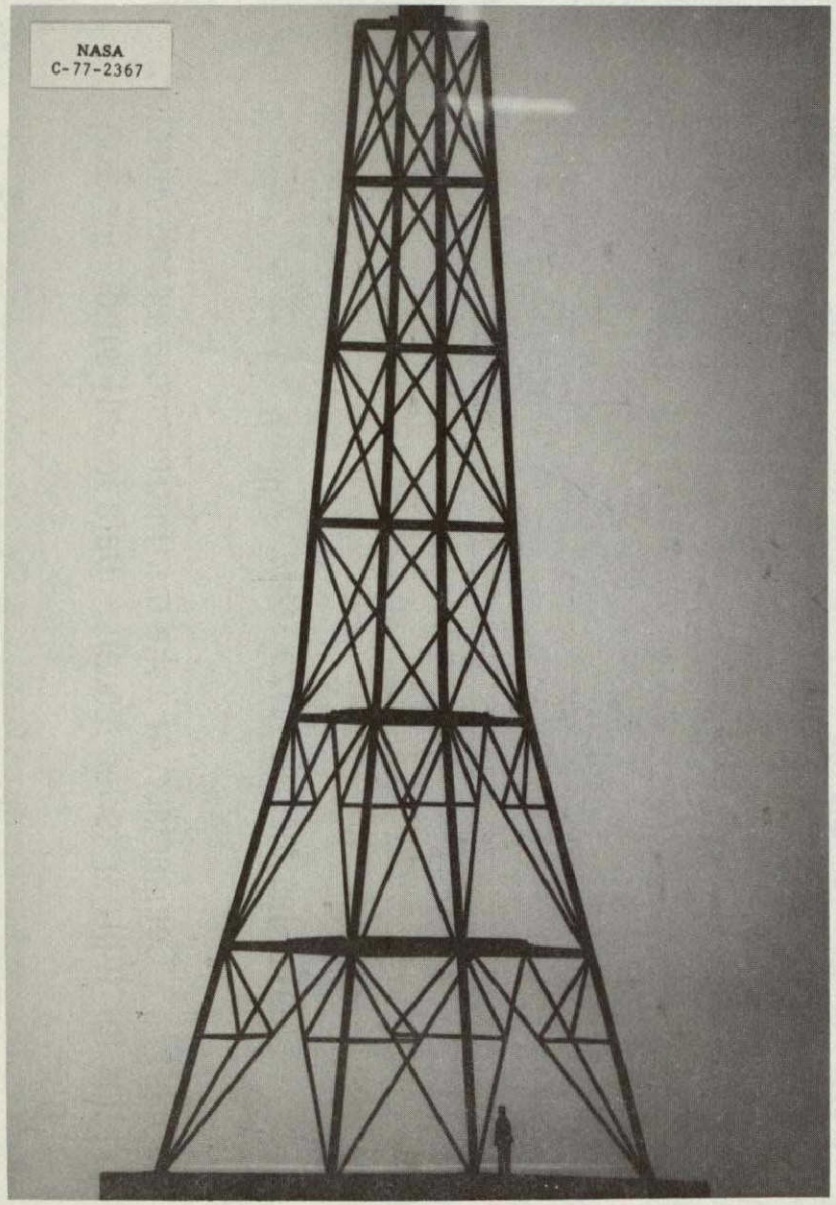

(c) Wind approach angle, $\theta = 30°$.

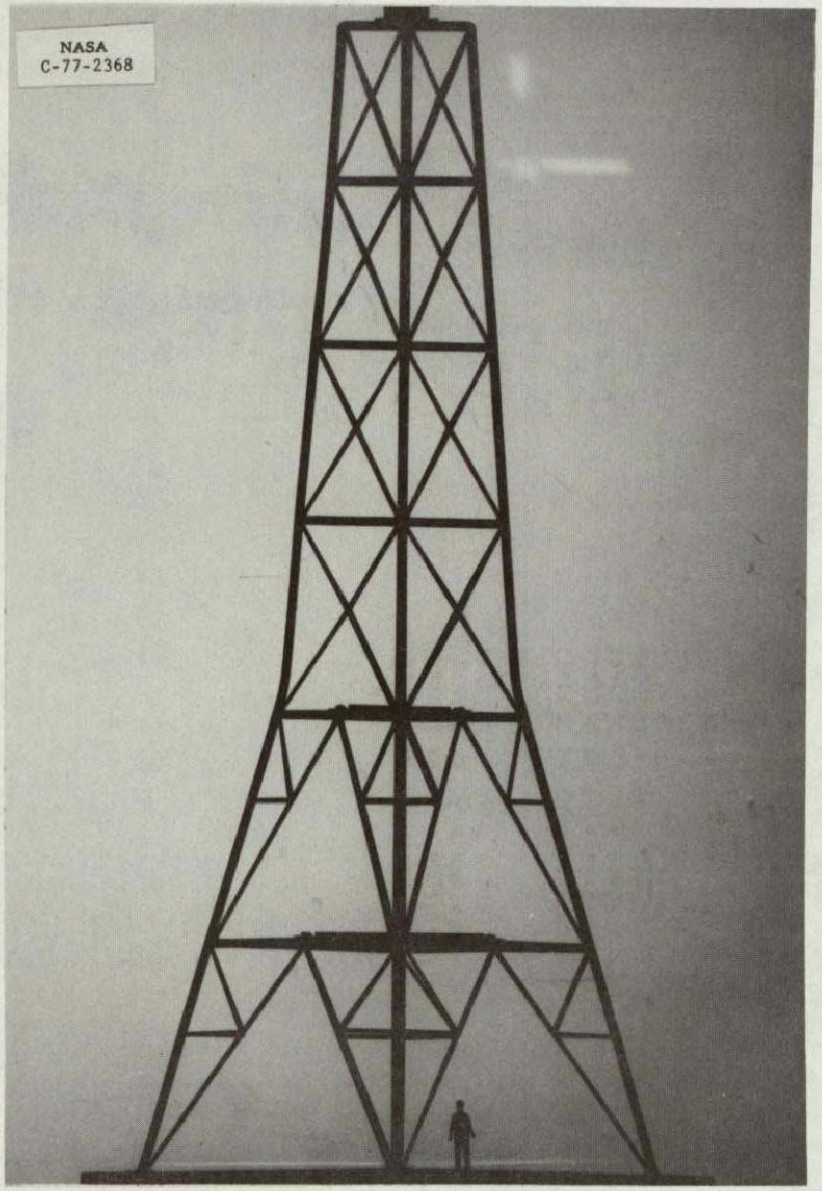

(d) Wind approach angle, $\theta = 45°$.

Figure 16. - Concluded.

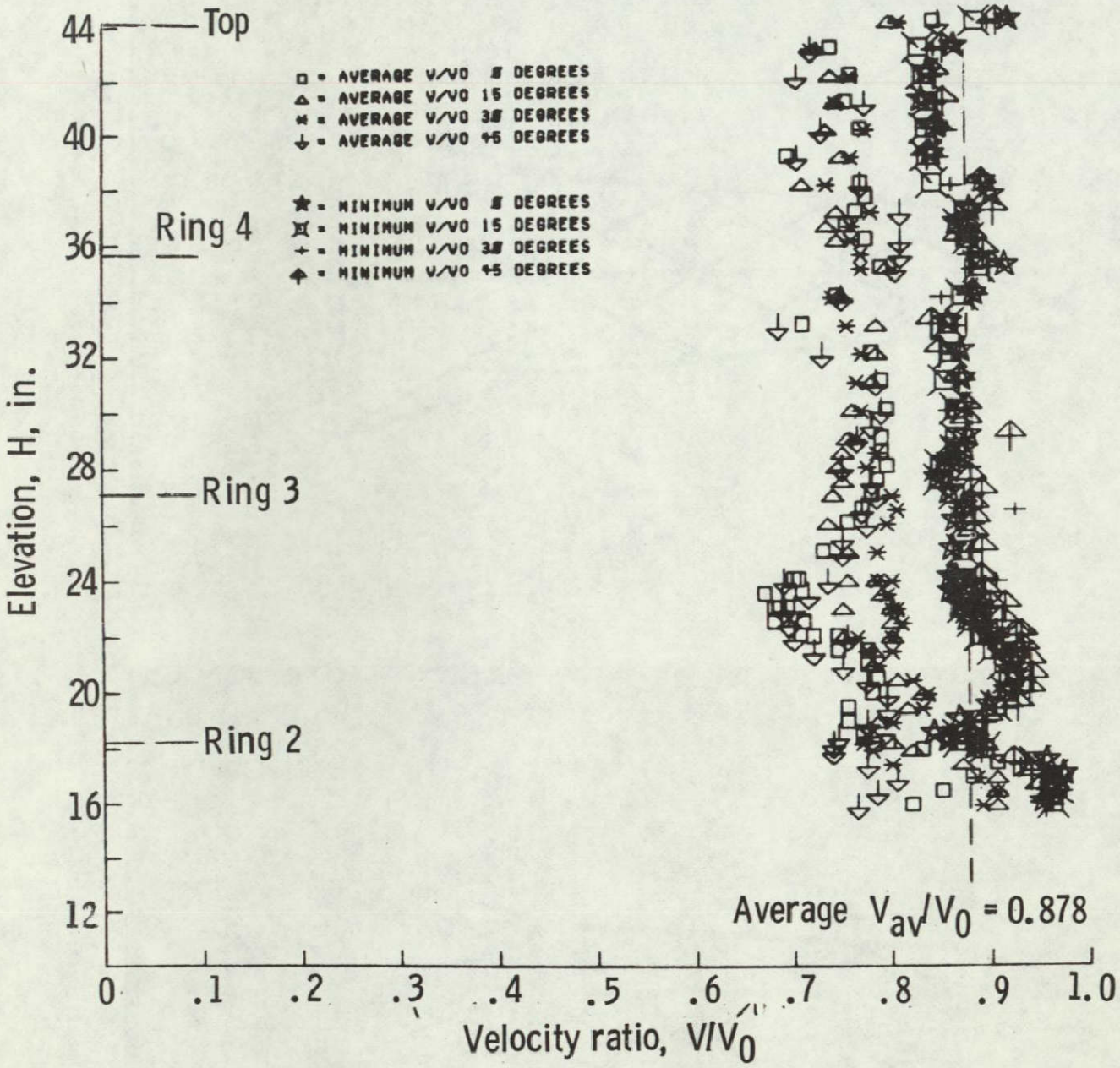

(a) 8-leg model. 1/25 scale, X_m/R_b = 0.519.

Figure 17. - Comparison of wake minimum and average velocity ratios for tubular tower models. Data for all wind approach angles.

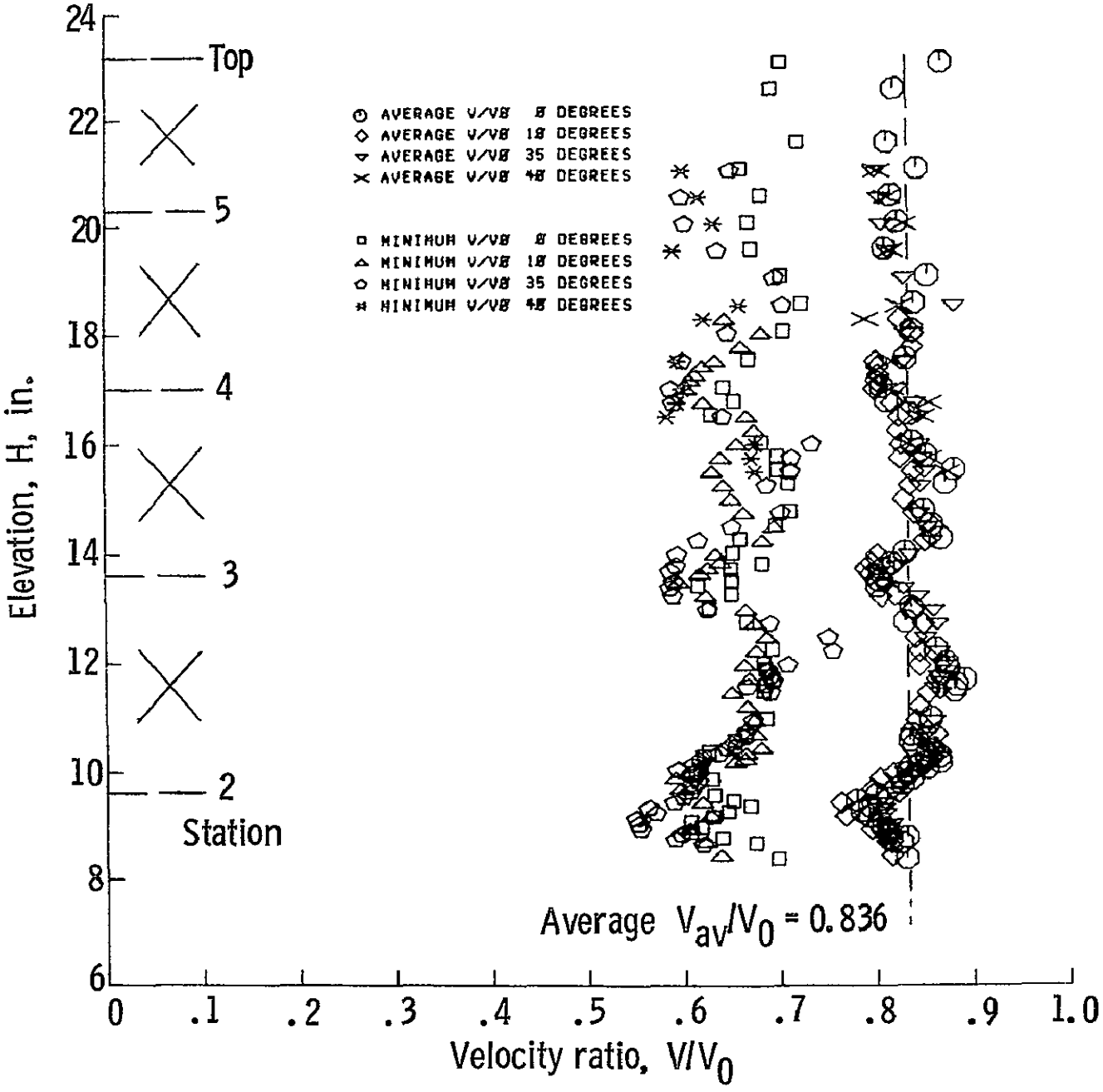

(b) 4-leg model. 1/48 scale, X_m/R_b = 0.36.

Figure 17. - Concluded.

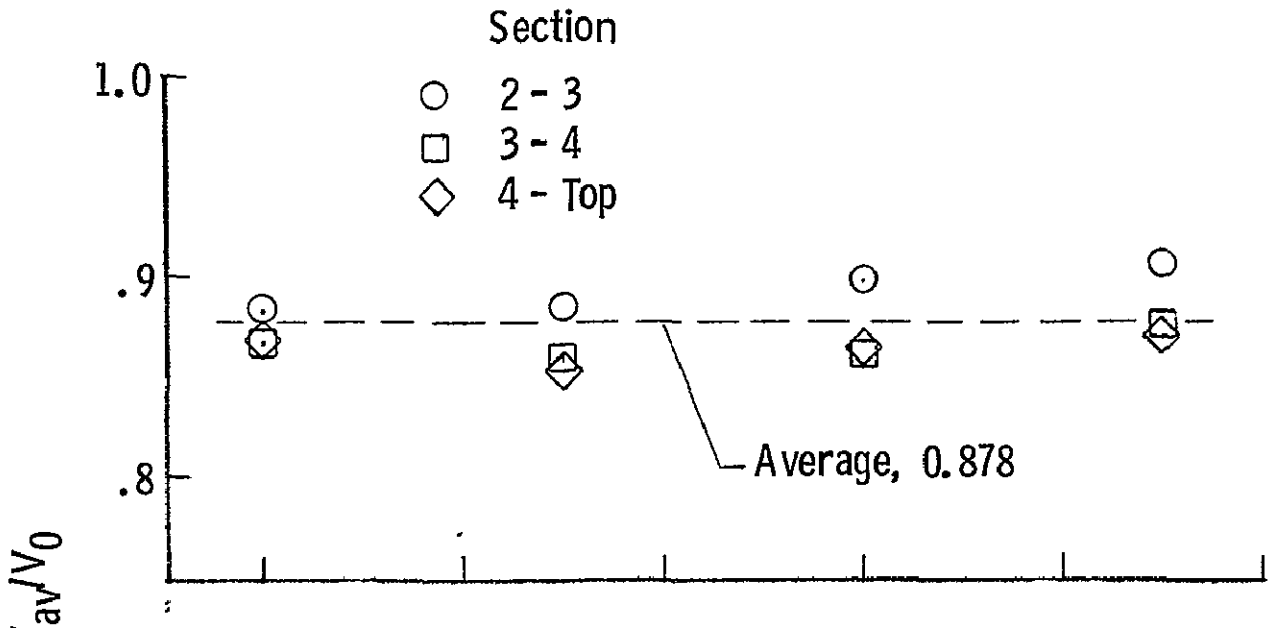

(a) 8-leg model, $X_m/R_b = 0.519$.

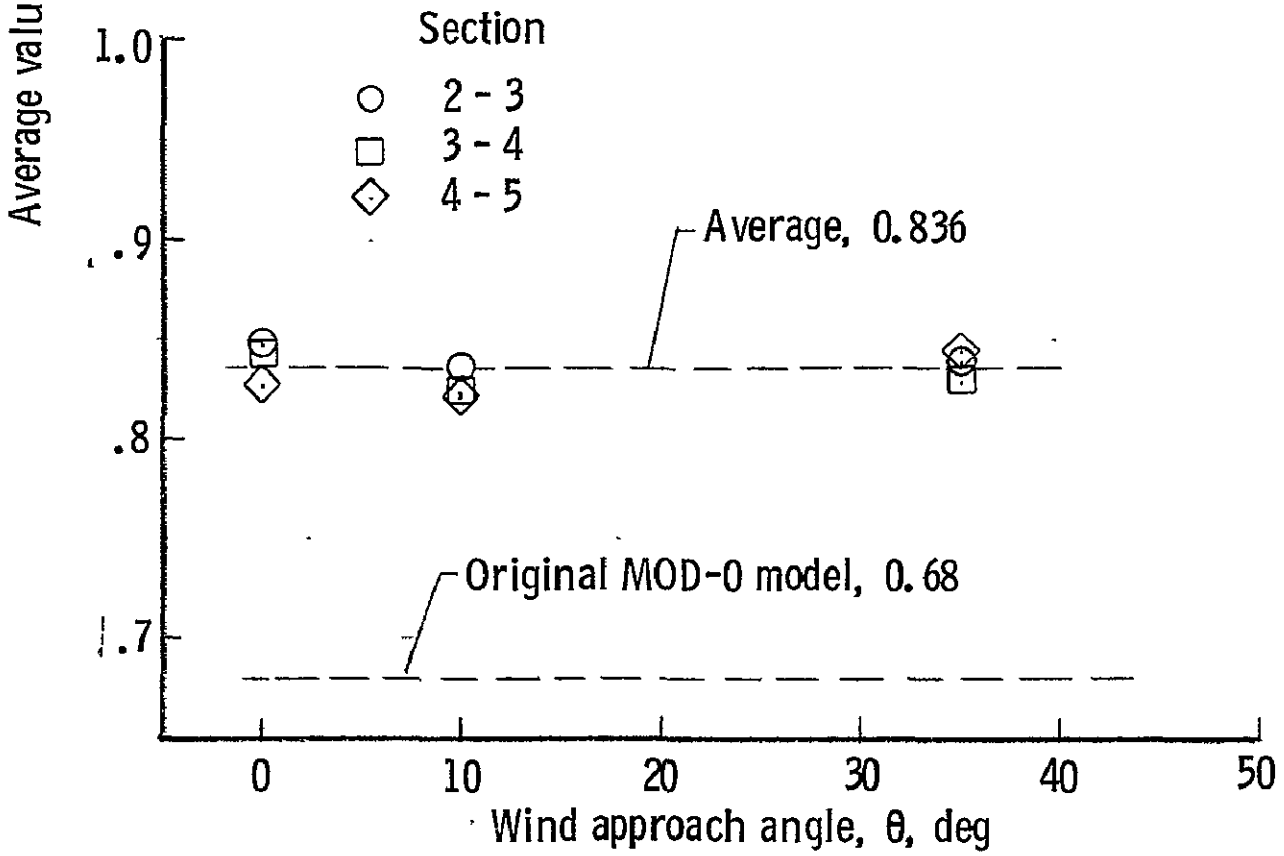

(b) 4-leg model, $X_m/R_b = 0.360$.

Figure 18. - Average values of wake average velocity ratio for upper sections of the 8-leg and 4-leg tower models. Data in measuring plane.

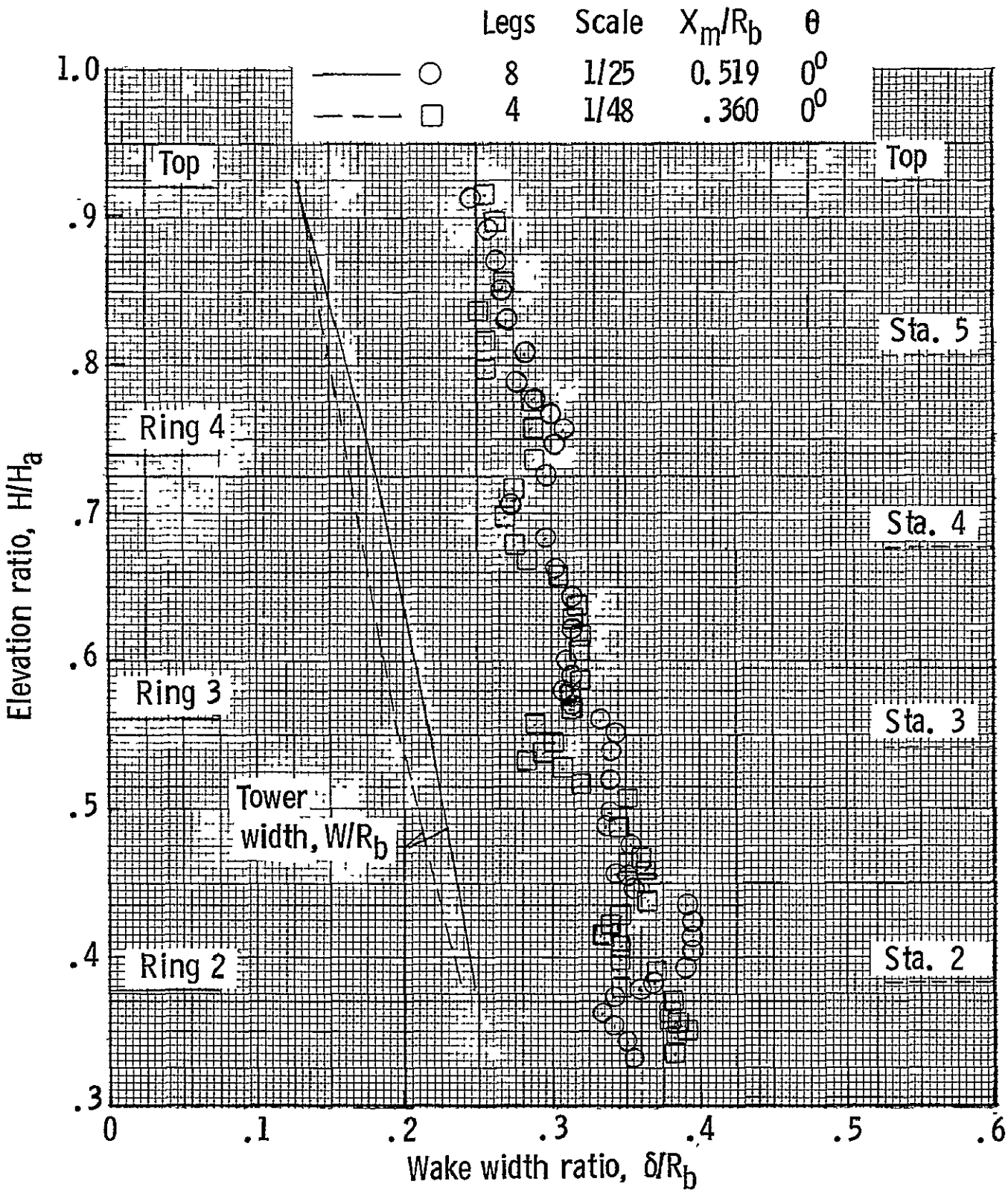

(a) Wind approach angle, θ = 0 deg.

Figure 19. - Comparison of vertical variation of wake width for 8-leg and 4-leg tower models.

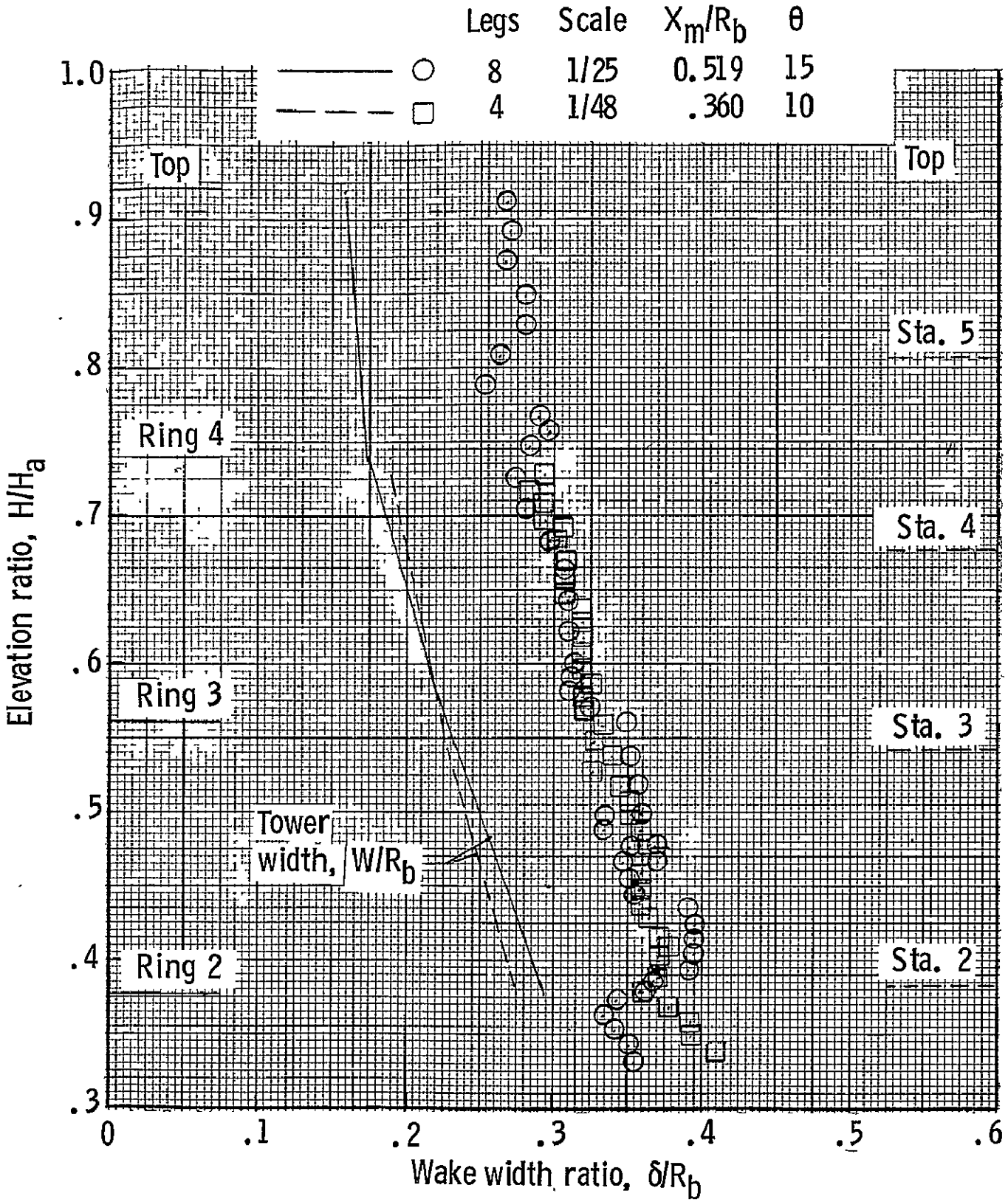

(b) Wind approach angle, θ = 10 - 15 deg.

Figure 19. - Continued.

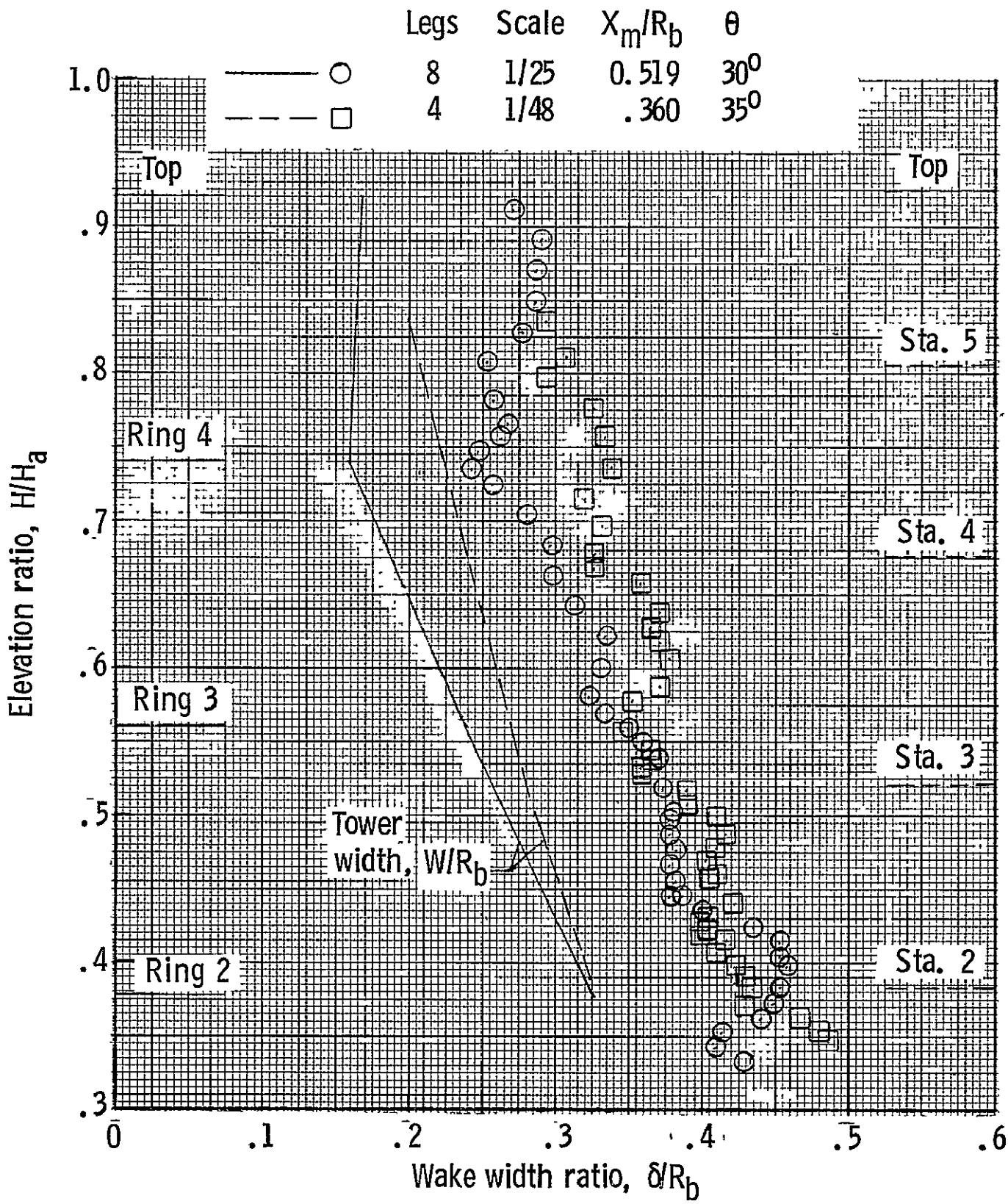

(c) Wind approach angle, θ = 30 - 35 deg.

Figure 19. - Continued.

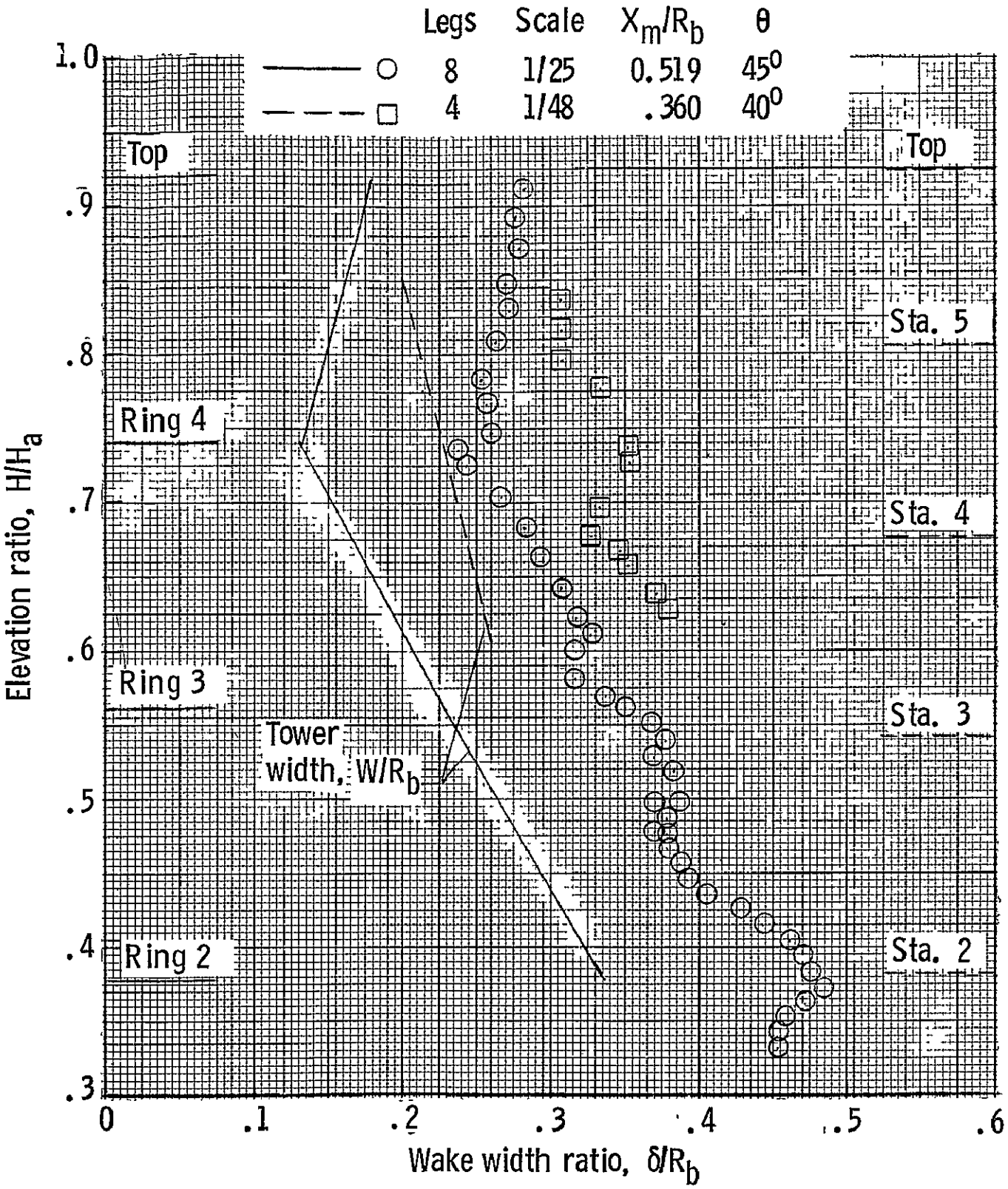

(d) Wind approach angle, θ = 40 - 45 deg.

Figure 19. - Concluded.

☆ U S GOVERNMENT PRINTING OFFICE 1978— 757-139/6326

NATIONAL AERONAUTICS AND SPACE ADMINISTRATION
WASHINGTON, D C. 20546

OFFICIAL BUSINESS
PENALTY FOR PRIVATE USE $300

SPECIAL FOURTH-CLASS RATE BOOK

POSTAGE AND FEES PAID
NATIONAL AERONAUTICS AND
SPACE ADMINISTRATION
451

U.S.MAIL

POSTMASTER

If Undeliverable (Section 158
Postal Manual) Do Not Return